UNIVERSITY OF SOUTHAMPTON

Towards the Combinatorial Synthesis of Azo-dyes

By

James Merrington

Doctor of Philosophy

Department of Chemistry

Faculty of Science

Submitted May 2003

UNIVERSITY OF SOUTHAMPTON

ABSTRACT

FACULTY OF SCIENCE
DEPARTMENT OF CHEMISTRY

Doctor of Philosophy

TOWARDS THE COMBINATORIAL SYNTHESIS OF AZO-DYES

By James Merrington

During this project a variety of novel techniques were investigated for the synthesis of azo-dyes, which could be adapted for use in a combinatorial manner.

Initially, this involved the generation and use of diazonium salts supported on ion-exchange resins, and was successfully applied to the synthesis of a 36-member azo-dye library.

Convergent synthesis of a selection of azo-dyes was achieved, using parallel synthetic techniques to prepare the triazine and azo-dye precursors. Microwave synthesis was utilised to produce the final dyes, which were purified by solid-phase extraction.

Solution- and solid-phase synthesis of azo-dyes was attempted using a safety-catch linker approach to immobilise the dye intermediates.

Finally, a digital image analysis system was developed to analyse images of resin beads. This system was used to analyse the size-distribution of bead samples and was compared standard size-analysis methods.

Preface

The research described in this thesis was carried out under the supervision of Prof. Mark Bradley at the University of Southampton between October 1999 and December 2002. No part of this thesis has been submitted to this or any other University.

Acknowledgements

Firstly, I would like to thank my Supervisor and mentor, Professor Mark Bradley, for all the advice and support he has given me over the last three years. I would also like to thank Mark James and Avecia, for their help, hospitality and funding without which this project would not have been possible. I would also like to thank GL and JH in the MS dept. and NW and JS in the NMR dept.

During my research here, the Bradley group has become like my family, always willing to listen to my problems, and without their help I would not be in the position I am now in. Although that comment applies to the entire group, I would like to thank especially a few people who I have grown very fond.

In the post-doc category comes, and in no special order, SM, JDD, MB and FB for helping me by proof-reading bits of my thesis; JK, JFT and MT for being smashing house-mates, putting up with my awful cooking and having the occasional drinkie with me.

In the PhD student category, although I hope you won't be that for too long, comes MM, KM, MD, LSW and JAJ for also proof-reading bits of my thesis, and the last two for advice on particle analysis; YL, HM, MM and BY for introducing me to food from the far-flung corners of the world; and IL for just being IL and teaching me how to deconstruct HPLCs; to my contemporaries, SL, KJ, LLS, CV and MM for support and not writing up too quickly (in most cases); past members who are gone but not forgotten, JB, AB, TZ and DO. Last, but not least, I would also like to thank Lynne, my family and friends for keeping me sane.

Here's to you all...

Sköl

Abbreviations

Ac_2O	acetic anhydride
AcOH	acetic acid
Amberlyst A-15	macroporous PS-*co*-DVB SCX, © Rohm-Haas
Amberlyst A-26	macroporous PS-*co*-DVB SAX, © Rohm-Haas
aq.	aqueous
ArgoPore	macroporous PS-*co*-DVB, © Argonaught Technologies
bs	broad singlet
C-18	octadecyl
CBS	carboxylic acid binding site
CCD	charge-couple device
$CHCl_3$-d_1	deuterated chloroform
conc.	concentrated
d	doublet
DCC	dicyclohexylcarbodiimide
DCM	dichloromethane
DCU	dicyclohexylurea
DIA	digital image analysis
DIC	diisopropylcarbodiimide
DIPEA	diisopropylethylamine
DMF	*N,N*-dimethylformamide
DMSO	dimethylsulphoxide
DMSO-d_6	deuterated DMSO
DNA	deoxyribonucleic acid
ELSD	evaporative light scattering detector
EM	electro-magnetic
ESI-MS	electrospray MS
FT-ICR-MS	fourier-transform ion cyclotron resonance MS
GFP	green-fluorescent-protein
H_2O-d_2	deuterated water
H-acid	5-amino-4-hydroxynaphthalene-2,7-disulphonic acid, sodium salt
HOBt	*N*-hydroxybenzotriazole

HPLC	high-pressure liquid chromatography
HRMS	high-resolution MS
HTS	high through-put screening
IPP	Image Pro Plus, © Mediacybernetics
^{i}PrOH	isopropanol
IR	infra-red
LC/MS	liquid chromatography/mass spectrometry
m	multiplet
m/z	ratio of mass to charge
MALDI-TOF-MS	matrix-assisted laser desorption ionisation time-of-flight MS
MAS	magic angle spinning
MBHA	methylbenzhydrylamine
m-CPBA	meta-chloroperbenzoic acid
mg	milligrams
MHz	megahertz
Mpt.	melting point
MS	mass spectrometry
MSD	mass spectrometer detector
MWD	multiple wavelength detector
PAM	phenylacetamidomethyl
PEG	polyethylene glycol
PEGA	polyacrylamide-*co*-polyethylene glycol
pH	$\log_{10}[H^{+}]$
ppm	parts per million
PS	PS-*co*-DVB
PS-*co*-DVB	polystyrene-*co*-divinylbenzene
PSR	polymer-supported reagent(s)
pst	psudo-triplet
q	quartet
qt	quintet
R_f	retention factor
RGB	red/green/blue
RP-HPLC	reverse-phase HPLC
R_t	retention time
s	singlet
SASRIN	super-acid sensitive resin
SAX	strong anion exchanger

SCX	strong cation exchanger
SEM	scanning electron microscopy
SPE	solid-phase extraction
SPOS	solid-phase organic synthesis
SPPS	solid-phase peptide synthesis
t	triplet
TEA	triethylamine
TentaGel	PEG-grafted PS-*co*-DVB
TFA	trifluoroacetic acid
TFMSA	trifluoromethanesulphonic acid
THF	tetrahydrofuran
TLC	thin-layer chromatography
TMSCl	chlorotrimethylsilane
VWD	variable wavelength detector

Chapter 1: Introduction

1.1 Printing Processes

1.1.1 Brief History of Printing

In 1271 Marco Polo left Venice to travel the width of Asia and make contact with the Emperor of Mongolia and China, Kublai Khan. Although his prime purpose was to introduce Christianity into Mongolia and hence strike an alliance between the Mongols and Christendom, this well documented expedition achieved more. While there he noted the use of wood blocks to print a basic form of currency.[1]

This was the first documented account of impact printing to reach Europe, but it took over a century before it was reproduced effectively, notably by Johann Gutenberg (Figure 1.1).

Figure 1.1: Johann Gutenberg; his text [3] and portrait.[4]

He adapted the methodology, fashioning each letter as an individual metal block. The blocks were then held together in racks, coated with ink and pressed onto paper to produce an image, a technique which would become known as letter-press. Whereas previously to print a page of text the printer needed to carve a new printing surface each time, with Gutenberg's technique any page of text could be generated by simple rearrangement of the letter blocks in the rack. Although it cannot be claimed he invented printing, he did develop it from little more than an art, and set it upon a road to being a powerful reprographic technique.

The effect this apparently simple technique had on Western Europe was monumental. The emergence of printing was one of the major factors attributed to the advent of the Renaissance in the fifteenth century.[5] At the time Europe was awakening to new technologies, rediscovering forgotten ones, and becoming more aware of the world around it. All of these events resulted in a proliferation of knowledge, and the new printing techniques allowed this information not only to be recorded, but also to be spread rapidly

across the continent. It had a comparable effect on Europeans at the time to the introduction of the Internet in the 1990's.[5]

Gutenberg cast the letter blocks with the image surface higher than the non-image surface. This method of printing is known as relief printing (Figure 1.2a).[6]

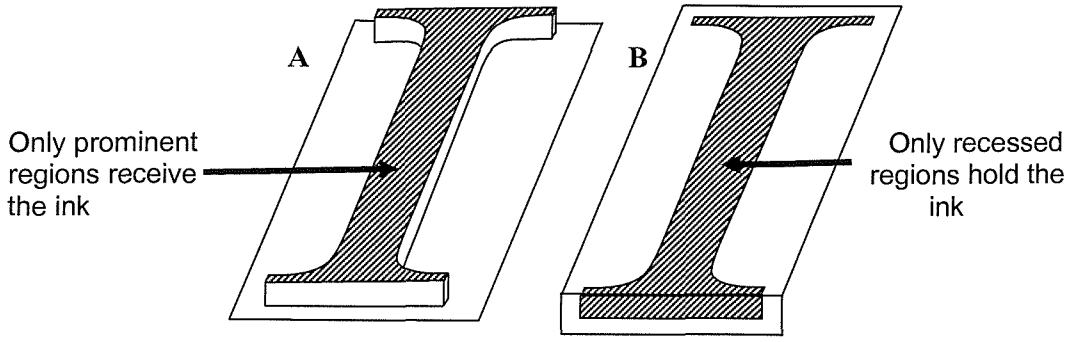

Figure 1.2: a) Relief printing; b) intaglio printing (image-surface marked in black).

The printing of text, dominated by Gutenberg's letterpress-based techniques, remained essentially unchanged for over three hundred years. Intaglio printing was also developed at the same time for printing illustrations (Figure 1.2b).[7] This method of printing, also known as gravure, involved the printer scraping the image into a soft copper plate. Ink applied to the surface of the plate was held in the recessed holes, and an image could be obtained by pressing the plate onto a sheet of paper. The deeper the indent, the more ink was held, the darker the image at that point.

Lithography, the first planographic technique, was developed by Johann Senefelder at the end of the eighteenth century.[8] During planographic printing techniques the image and non-image surfaces of the printing-plate are in the same plane.

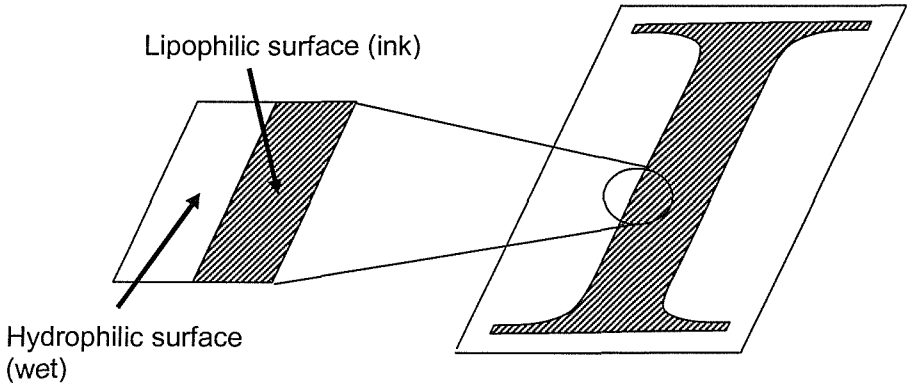

Figure 1.3: Lithographic printing; image-surface marked in black.

He discovered that if he created an image of wax onto stone and the stone was dampened the water would quickly run to the unwaxed regions (the non-image surfaces).

A hydrophobic ink was then applied to the dry image-surfaces, and the stone was pressed onto a sheet of paper to obtain an image (Figure 1.3).

At the end of the nineteenth century another important printing technique emerged. The image was cut into a rubber sheet so that the image-surfaces were raised above the non-images surfaces (in relief), a printing technique later to become known as flexography.[9]

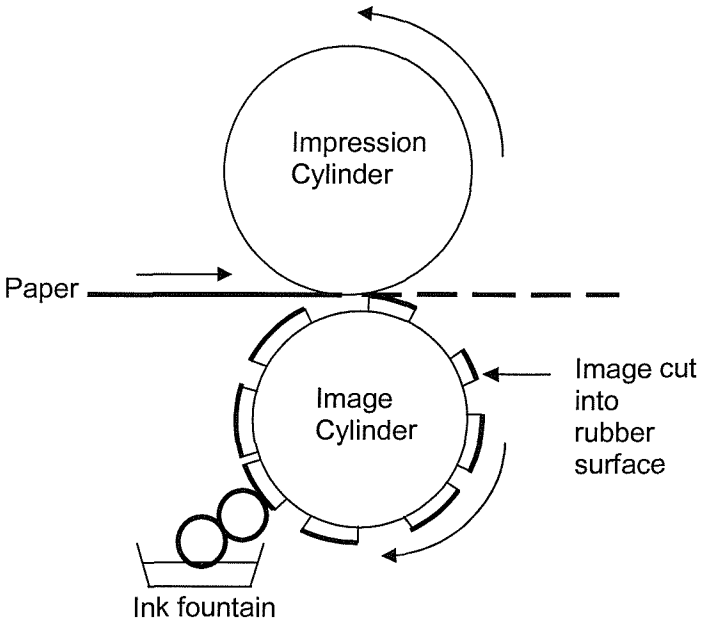

Figure 1.4: Rotary flexography.

To speed up to the printing process the rubber sheets could be attached to a metal cylinder and the printing media was passed between the image cylinder and a second impression cylinder (Figure 1.4). The paper was then fed in-between the cylinders continuously. The attachment of image surfaces to printing cylinders in this fashion is known as rotary printing, and was used in conjunction with intaglio, relief and lithographic printing methods in order to increase their output.[10]

The black ink Gutenberg would was probably a mixture of linseed oil as solvent, phenolic resin as the binder, with ground carbon as the colourant. Once the ink was applied to the paper the phenolic resin oxidised to form a tough layer and ensure the black pigment remained well attached to the surface.[11]

As printing techniques developed so novel inks were developed to suit the new requirements. However, the combination of colourant, binder and solvent remained a constant theme. The modern equivalents include aromatic hydrocarbons, alcohols and ketones for the solvent, and nitrocellulose, polyamide resins, methacrylates for the binder.[12] Further materials are sometimes added, to optimise the performance of the ink.

These might be to ensure the stability of a pigment or to further control the ink transport thorough the printing rollers.

1.1.2 Early Colourants

During the nineteenth century the dye industry was also changing. In 1856 Perkin discovered the first synthetic dye, Mauvine, which he synthesized on a large scale.[13] This was a milestone in the development of colourants, because before Perkin all commercially available dyes were from natural sources. These had remained largely unchanged for hundreds of years, and were time-consuming and therefore expensive to prepare.

The most important yellow dyes available were flavones, chalcones and polyenes, obtained from vegetable sources. The most significant of these was Weld (**1**) due to it's relatively high light-fastness (Figure 1.5).[14] This was obtained from *Reseda Luteola L*, a plant more commonly known as Dyers Rocket.

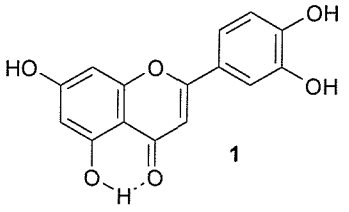

Figure 1.5: Weld (Luteolin).

The important red dyes were all of the anthraquinone class, the most significant being Madder (Alizarin) (**2**) which was obtained from the roots of *Rubia Tinctorum* (Figure 1.6).[15] Synthetic anthraquinones dyes are still used today, due to their good light-fastness and bright colour.

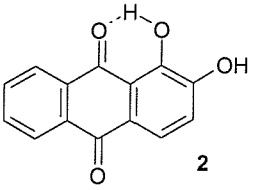

Figure 1.6: Madder (Alizarin).

The only naturally occurring blue dye available was Indigo (Woad) (**3**), which was usually obtained from *Indigofera Tinctoria L*, otherwise known as the indigo plant (Figure 1.7).[16] It was combined with Weld (see above) to produce Lincoln Green, made famous by the fictional character Robin Hood.[17]

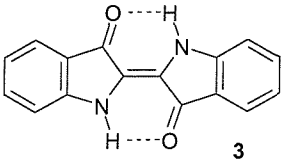

3

Figure 1.7: Indigo (Woad).

The remaining significant dyes were Tyrian purple and Logwood. The former was obtained from *Murex Brandaris*, a mollusc found in the Mediterrainean sea, and was strucurally very similar to indigo (6,6'-dibromoindigo). Logwood was found in the heartwood of *Haematoxylon Campechiancum L*, and was red.[18] However it was discovered that when combined with chromium it turned black (Figure 1.8). The dye complex (**4**) is still used today, for the dying of silk and leather. It absorbs over the entire visible light range, a property normally only accomplished by dye mixtures.

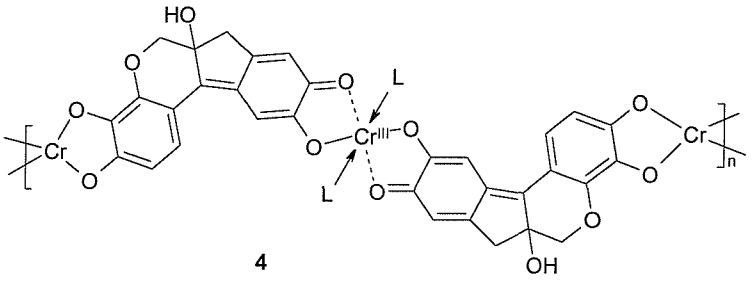

4

Figure 1.8: The assumed complex of Logwood and chromium III.

Although Perkin is generally acknowledged as the 'father of the modern dyestuffs industry', his discovery came at a time where many innovations were emerging in the chemical world. From 1845 onwards, Hoffman had been working on extracting and working with the aromatic components of coal tar.[19] Perkin, one of his students, first synthesed Mauvine (**5**) (Figure 1.9), by mistake while trying to find a route to quinine.[13]

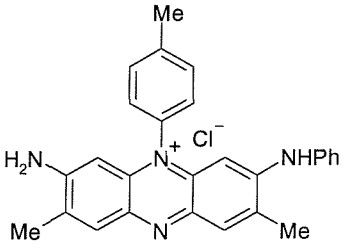

5

Figure 1.9: Mauvine or Mauve Dye.

After Perkin, there came a rush of dye related discovery. Only two years afterwards, Griess first performed the diazotisation reaction, by oxidising anilines with

HONO (see section 1.2.1).[20] In 1859, a new class of dyes, the triphenylmethanes, were discovered by Verguin.[21] Tin(IV) chloride was reacted with crude aniline, to form a dye he called Magenta (**14**) (Scheme 1.1).

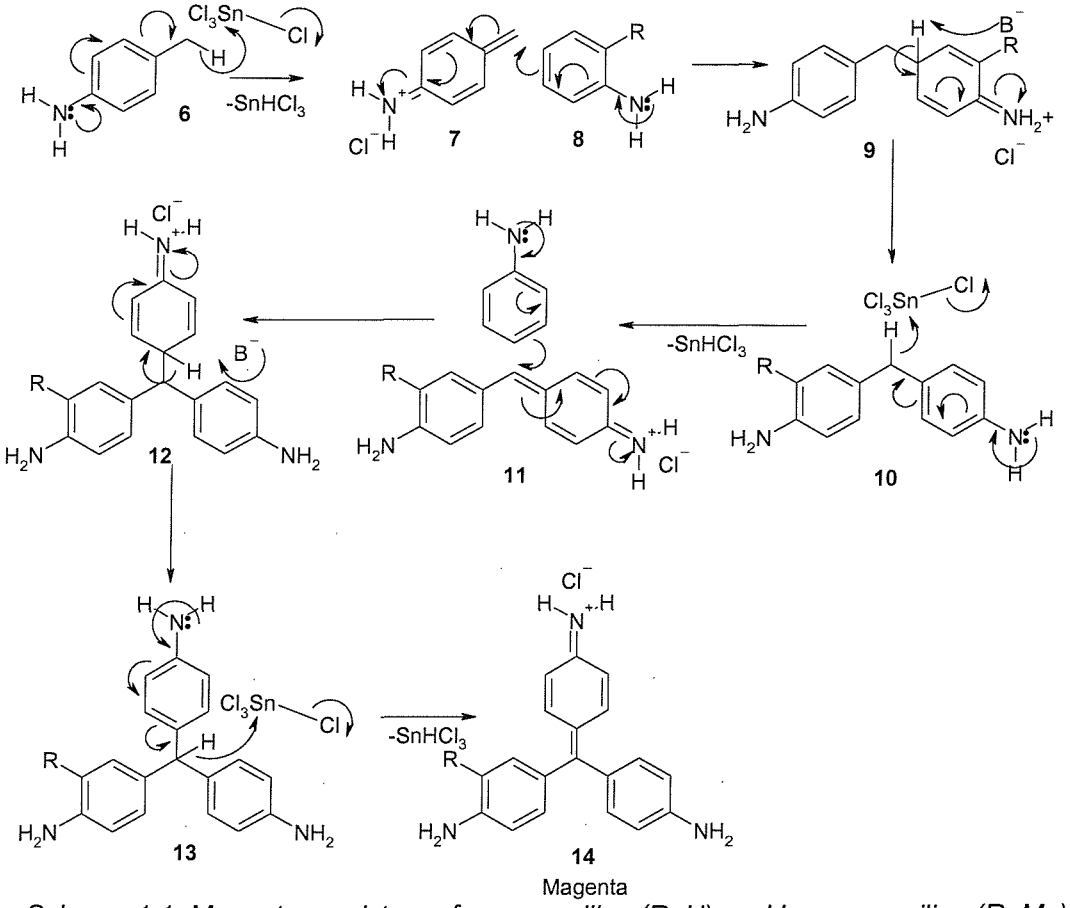

Scheme 1.1: Magenta; a mixture of parasoaniline (R=H) and homorosaniline (R=Me).

Due to the impurities of *ortho*- and *para*-toluidine present in the reaction mixture, a mixture of two dyes was in fact present; *parasoaniline* and *homorosaniline*. However, not all the new synthetic dyes were stumbled upon by chance. The characterisation and synthesis of natural dyes was made possible with new theories on the nature of organic compounds. In 1857-8 Kekulé hypothesised on the valency of carbon, and the nature of the C-C and C-H bond, and the structure of aromatic compounds.[22] With his new ideas of six-membered ring-systems in mind, and after many painstaking experiments, in 1860 Graebe and Lieberman were able to elucidate the structure of Alizarin.[23] Unfortunately, the synthetic route they proposed was not commercially viable, but it was not long before a suitable synthetic route was found by Perkin.

1.1.3 Inkjet Printers

Inkjet is a non-impact printing technology during which droplets of ink are pushed from small apertures directly to a specified position on a surface to create an image.[24] Modern micro-fabrication techniques allow many of these apertures to be formed in a tiny print head (Figure 1.10), allowing high-resolution images to be obtained.

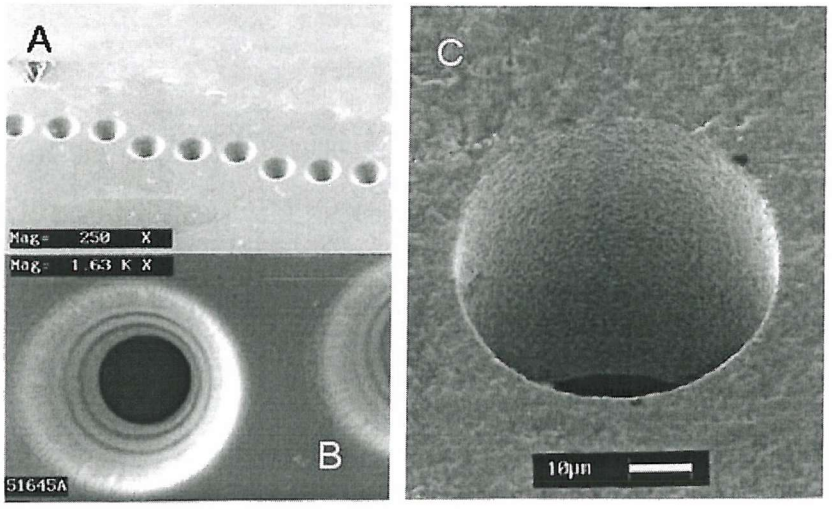

Figure 1.10: Micro-fabricated inkjet apertures; SEM photographs of apertures etched into polymer (A & B) and steel (C).[24]

Although inkjet printing is used for many printing applications, the largest market by far is in the office and home and will be the main focus of this chapter. Inkjet technology, summarised in Figure 1.11, can be split into the early 'continuous' flow inkjet systems and the more recent 'drop-on-demand' systems.

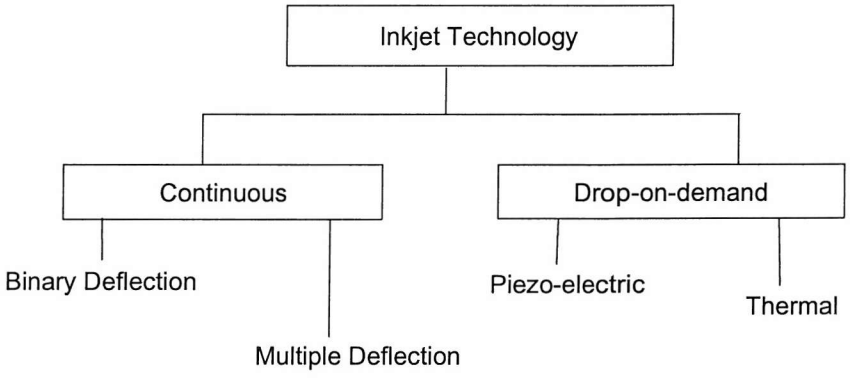

Figure 1.11: Technology Map for Inkjet Printing.

Rayleigh first described the mechanism by which a liquid stream breaks up into droplets in 1878.[25] However, it was not until 1965 that Sweet developed a method to

further manipulate the droplet stream.[26] This was achieved by applying a charge to the surface of the droplets, by passing them between charging electrodes. The drops were then passed through an electric field, which deflected the charged drops towards the paper to form an image. The uncharged drops remained undeflected, and were channelled into a gutter for recirculation (Figure 1.12).

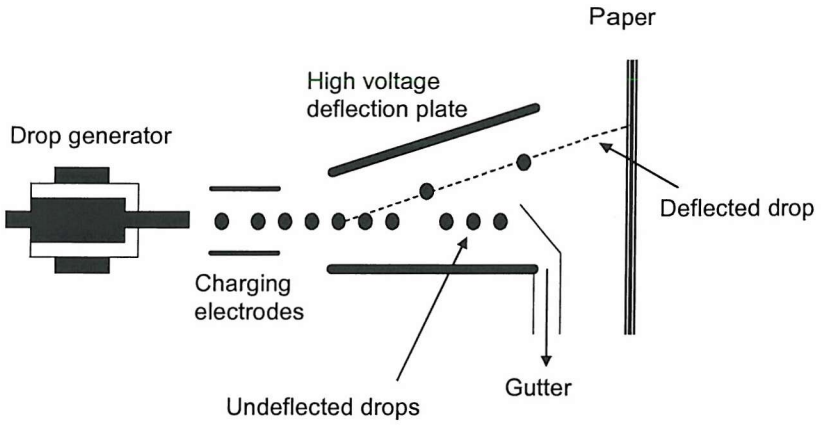

Figure 1.12: Multiple deflection continuous inkjet system.

The charge on each droplet could also be regulated, resulting in a range of deflection trajectories. This method of continuous inkjet became known as multiple deflection. While the development of continuous inkjet systems was strong, the development of "drop-on-demand" inkjet methods were also popularised. Zoltan, Kyser and Sears were among the pioneers of these systems, which came to market during the mid 1970's.[27] A drop-on-demand device ejects ink droplets only when they are needed to produce an image on the surface. This approach eliminates the complexity of droplet charging and deflection hardware, as well as the inherent unreliability of the ink recirculation systems required for the continuous inkjet technology. The ejection of the ink droplets from these new printing systems relied on pressure waves, generated by the flexing of a piezoelectric crystal (Figure 1.13).

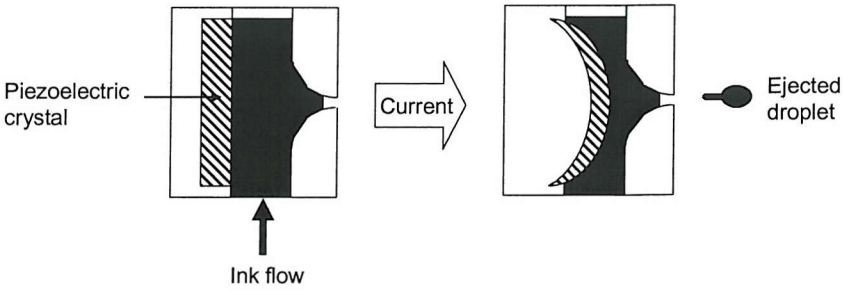

Figure 1.13: Piezoelectric print head design.

At the beginning of the 80's there was a competitor to the piezoelectric approach to inkjet printing. Endo and Hara invented a new drop-on-demand method where ink droplets were ejected from the aperture by the growth of a vapour bubble, generated by a small heater located opposite the nozzle (Figure 1.14), a technique they called 'Bubble-jet'.[28] The simple design of the bubble-jet print head allowed print heads to be built at an even lower cost, and with more apertures compressed into the same size print head.

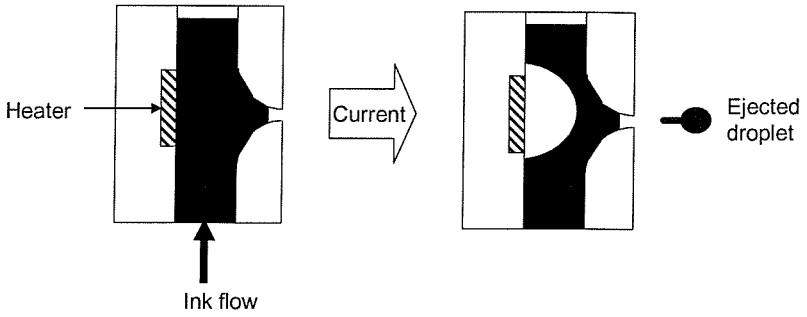

Figure 1.14: Thermal 'Bubble jet' print head.

The major drawback in thermal Inkjet technology was the unreliability associated with the heating of a complex ink-mixtures, which could result in clogging of the aperture. At the present time the home/office printer market is spilt between piezoelectric and thermal Inkjet approaches.

1.1.4 Inkjet Ink

The other important factor in the success of an inkjet printer, besides the print head, is the constitution of the ink propelled through it. The formulation of the ink not only determines the droplet ejection characteristics and the reliability of the printing system, but also the quality and longevity of the printed image. Many different types of inks have been developed and used in inkjet applications. Figure 1.15 illustrates a technology map of different inkjet inks.[24]

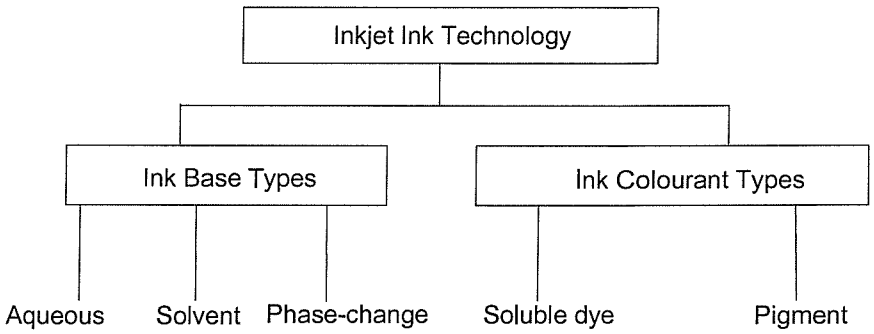

Figure 1.15: Inkjet ink technologies map.

1.1.4.1 Ink-Base Types

Aqueous Inks:

Water is the most commonly used solvent in home and office inkjet printers. In the case of thermal inkjet printers, water is the preferred material of choice due to its suitability towards the bubble-formation process. Although drying times are generally longer than with non-aqueous inks, there are no risks associated with environmental problems, fire or solvent inhalation. Aqueous inks are generally complex mixtures, containing many components to ensure reliable printing. Water evaporation around the print head can cause crystallisation of these components, which can lead to blocking of the aperture. This evaporation is controlled, to a degree, by the addition of co-solvents, such as diethylene glycol or pyrrolidinones, which act as humectants. Co-solvents can also be used to control the viscosity, surface tension and stability of the ink to ensure reproducibility in the printing system.[29]

A biocide must also be introduced to prevent bacterial and fungal growth during storage and use. Alcohols and glycols are often added for this purpose. in order to minimise corrosion and coagulation the inks used must be of high purity. A typical composition of a water-based ink for inkjet printing is shown in Table 1.1.[24]

Table 1.1: Composition of water based inks for inkjet printing.

Component	**Function**	**% w/w**
Deionised Water	Aqueous carrier medium	60-90
Colourant	Provides colour	1-10
Surfactant	Wetting, penetration	0.1-10
Biocide	Prevents biological growth	0.05-1
Buffer	Controls the pH of the ink	0.1-0.5
Other additives	Chelating agent, defoamer etc	> 1

Solvent Inks:

The use of nonpolar oil-based media allows the use of many more water-insoluble dyes. The use of solvent-based inks is predominantly found in industry, where the fast solvent drying times are crucial for high production rates, and where hydrophobic surfaces are often encountered.[30] Traditionally, ketonic solvents were used, such as methylethylketone. However, these organic solvent present both environmental and toxicity hazards, and due to these factors their use is decreasing. Alternative alcoholic solvents are replacing them.

Phase-change Inks:

Phase-change, also called hot-melt, inks are solids at room temperature, and only becomes liquid during the printing process. Upon hitting a cool surface, the molten ink droplet solidifies immediately, thus preventing the ink from spreading or penetrating the printed media.[31] Long chain fatty acids (C_{18}-C_{24}), alcohols or sulphonamides are mostly used for this application, having the desired melting point between 60-125°C. This gives phase-change inks an unprecedented image quality and good water fastness since the inks used are hydrophobic in nature.

1.1.4.2 Ink-Colourant Types

Pigments, or dispersed colourants, are so called as they consist of fine colourant particles dispersed in the ink-base.[32] They have several major advantages over their soluble counterparts. Due to their insolubility they excel on waterfastness, and also tend to display high lightfastness. However, they are inherently difficult to apply to inkjet systems, due to a propensity to clog the apertures.

Of the remaining soluble colourants, azo-dyes are the most commonly used. In the infancy of office inkjet printing off-the-shelf impure textile azo-dyes were used that were unsuitable due to impurities which could cause crystallisation and clogging. The first suitable dye that was found to overcome this issue was the highly soluble dye CI Food Black 2 (**15**) (Figure 1.16).[33]

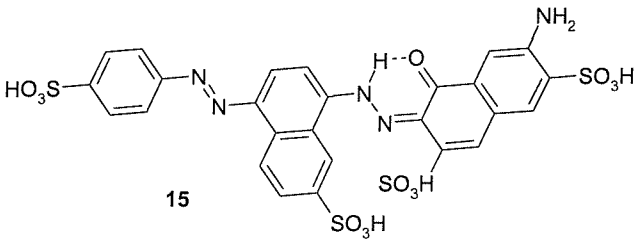

15

Figure 1.16: CI Food Black 2.

However, its major failing was that it was too soluble and failed waterfastness tests. In the continuing search for better dyes for inkjet inks, candidates are chosen carefully so that a balance of solubility vs. waterfastness is maintained.

Early colour inkjet printing used dye-sets, or trichlomats, borrowed from other areas of the printing industry, such as magazine and photographic reproduction.[34] A typical example of an inkjet trichlomat is CI Acid Yellow 23 (**16**), CI Acid 24 (**17**), and phthalocyanine CI Direct Blue 199 (**18**) (Figure 1.17).

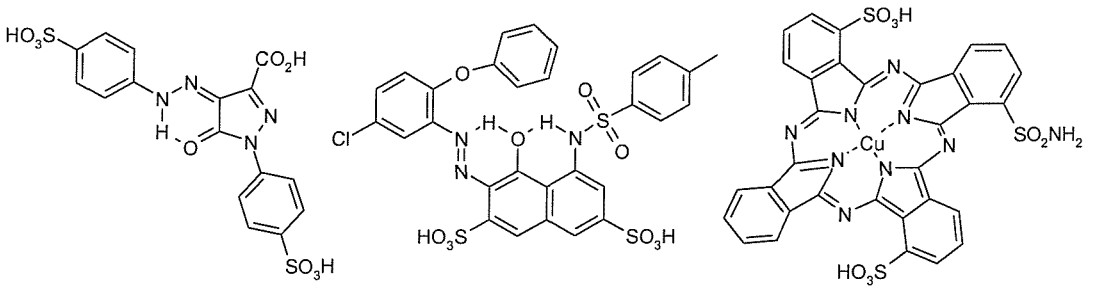

16 17 18

Figure 1.17: Typical inkjet trichlomat.

Azo phase-change colourants can also be found. Since they must dissolve in the wax carrier fluid, they are lipophilic in nature, such as CI Pigment Yellow 12 (**19**) shown in Figure 1.18.[35]

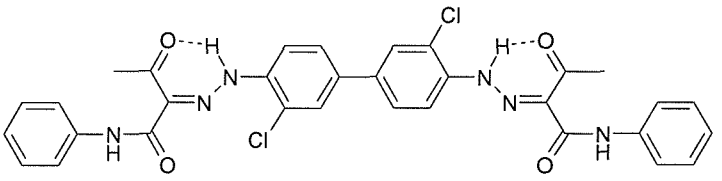

19

Figure 1.18: Phase-change colourant; CI Pigment Yellow 12.

1.2 Azo-Dye Chemistry

1.2.1 Synthesis

Peter Griess first performed the diazotisation reaction, essential for azo dye formation, in 1858.[20] This is accredited as the most important reaction in the synthetic dye industry, as over half of the dyes made in the world use this process.[36] Their continued success is due to several factors. They are tinctorially very strong dyes that mean they strongly absorb light over a broad region of the visible spectrum. They can be modified in many ways to cover a large shade range and have excellent light fastness properties. They can also be prepared from cheap starting materials in a standard multipurpose chemical plant.

The diazotisation reaction involves the nitrosation of an aromatic amine (**20**), usually in aqueous solution, followed by dehydration.[37] The coupling reaction between the diazonium salt (**21**) and a suitable aromatic nucleophile (**22**) yields an azo-dye (**23**) (Scheme 1.2).

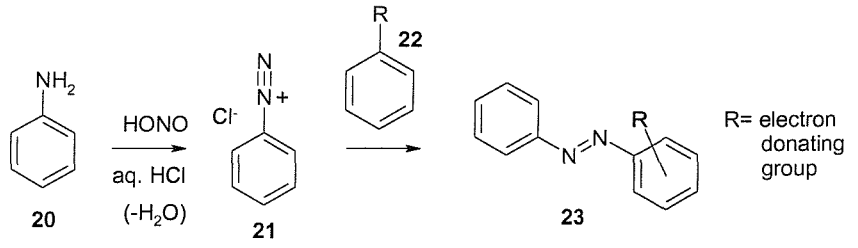

Scheme 1.2: The diazotisation and diazonium coupling reactions.

These reactions are complicated by strong sensitivity to pH, which affects the mechanism, intermediate stability and regioselectivity of the product.[38] The reagent of choice for the diazotisation is usually sodium nitrite, due to its low cost and high solubility in aqueous media. If the reaction is performed in organic solvent alternative reagents are used, such as pentyl nitrite.[39]

When nitrous acid (**24**) is dissolved into acidic solution it reacts to form a variety of nitrosating species, all of which are capable of reacting with aromatic amines. Possible forms are nitrous anhydride (**26**), nitrous acidium ion (**25**), nitrosonium ion (**27**), or nitrosyl halide (**28**). They all exist in equilibrium depending on the pH of the solution (Scheme 1.3).[40]

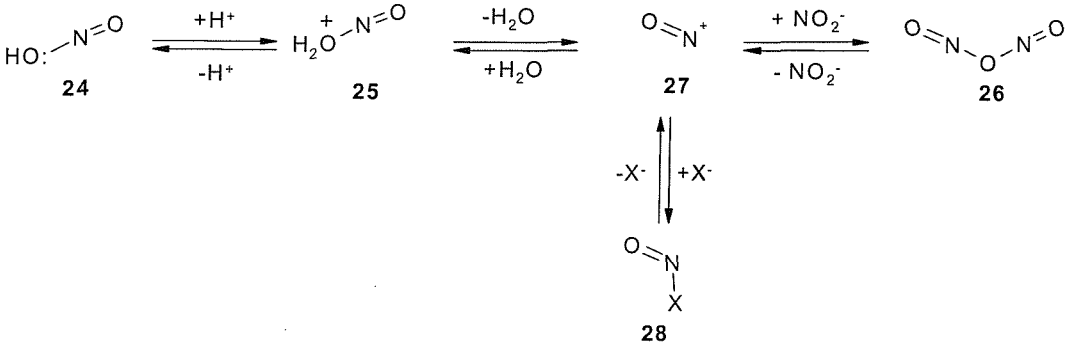

Scheme 1.3: Nitrosating agent interconversion.

At low acid concentrations the available nitrosating agent is nitrous anhydride (**26**) and the rate-limiting step of the reaction is its formation from nitrous acid. At slightly higher concentrations of acid (0.1 to 6.5 M, pH 1 to -0.8) the nitrous acidium ion (**27**) is present in significant amounts, a nitrosating agent which is more reactive than nitrous anhydride. At concentrations higher than 6.5 M (pH< -0.8) the highly reactive nitrosonium ion (**27**) is present. When the diazotisation is performed in the presence of halide ions then a rate increase is observed, suggesting a forth possible nitrosating agent at high acid concentrations, the nitrosyl halide (**28**).

However, the active species also depends on the amine present and its pK_b. Soft nucleophiles react faster with nitrous anhydride, whereas more reactive (hard) nucleophiles react preferentially with the nitrous acidium ion or nitrosonium ion. Hence,

the nitrosation of soft nucleophiles will not proceed more rapidly if the pH of the solution is increased. Whatever the nitrosating agent, reaction with an aromatic amine results in the same sequence of intermediates (Scheme 1.4).[41]

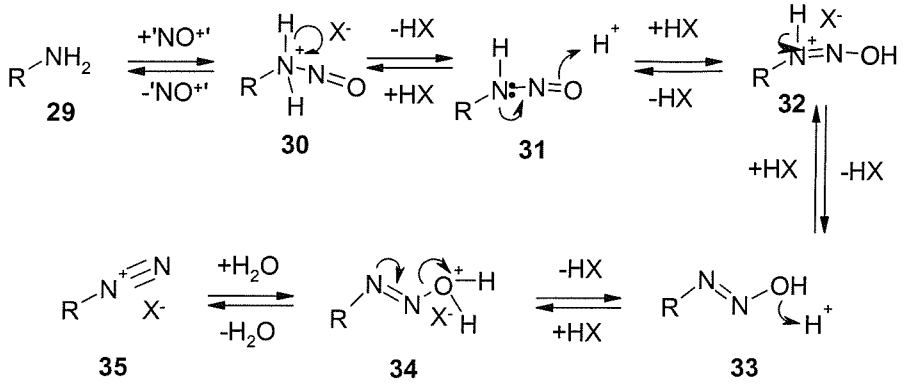

Scheme 1.4: Reaction of aniline with 'NO$^+$'.

At high acid concentration (>6.5 M, pH -0.8) the rate is determined by the deprotonation of intermediate **30** and the rate decreases with increasing acid concentration. In aqueous solutions, the diazonium ion (**36**) exists in equilibrium with its diazohydroxide (**37**) and diazotate (**38**) forms (Scheme 1.5).[39]

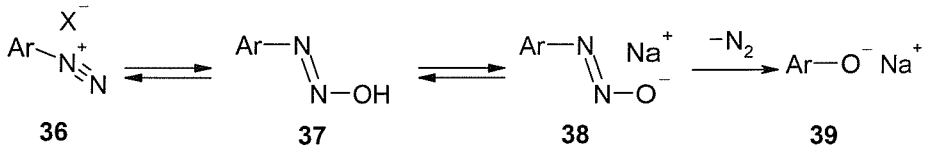

Scheme 1.5: The diazonium equilibrium, with pH increasing from left to right.

This equilibrium is partly controlled by the pH of the solution; the left-hand side favoured at low pH and the right-hand side at higher pH. The different forms exhibit different reactivities towards nucleophiles. The diazonium form is the most reactive, the diazotate form much less so. At very high pH (>10) diazonium decomposition to the phenol **39** becomes a significant factor.[39]

The stability of the diazonium salt increases with electron donation into the aromatic system.[42] This is due to increased stabilisation of the positively charged nitrogen. This trend is also seen in the reactivity of diazonium salts towards nucleophilic reagents (Scheme 1.6). In general, 4-nitrobenzene diazonium salts react approximately 10^5 times faster than *p*-methoxybenzene diazonium salts. 2,4,6-Trinitrobenzene diazonium salts are so reactive they will even react with trimethylbenzene.

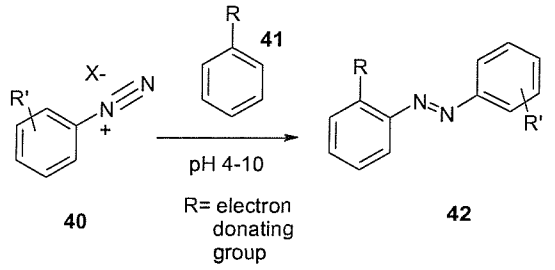

*Scheme 1.6: Diazonium coupling reaction to form azo-dye **42**.*

The pH of the diazonium coupling reaction is usually between 4 and 10, but must be chosen with care (Scheme 1.6). There is always a trade-off between the stability of the diazonium salt, (**40**) and reactivity of the nucleophilic reagent (**41**). Very reactive nucleophiles can be reacted at relatively high pH, as the coupling rate will be much higher than that of decomposition. If a less reactive nucleophile is used the pH must be low, to ensure stability of the diazonium salts over the extended reaction time. Reaction with aromatic amines is generally undertaken at pH >4, as this allows for availability of the free amine (**44**) (pK_b = 3-5) (Scheme 1.7).[43]

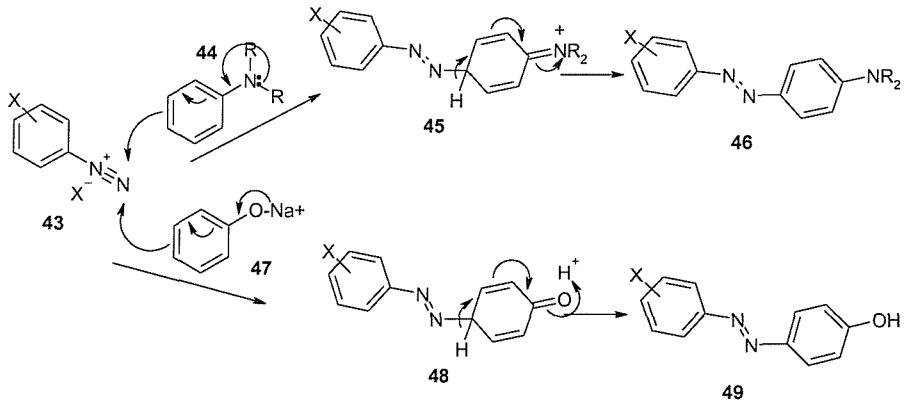

Scheme 1.7: Reaction between diazonium salts and nucleophilic coupling reagents.

If a phenol nucleophile is used a pH greater than 7 is required to ensure significant amounts of phenolate ion (**47**). Phenols and anilines generally couple at the 4-position and 1-naphthols couple at the 2- and 4-positions.[39] The situation becomes more complicated with species which contain more than one nucleophilic site, as more factors come into play. This is the case with 5-amino-4-hydroxynaphthalene-2,7-disulphonic acid (**50**), or H-acid for short (Figure 1.19).[44]

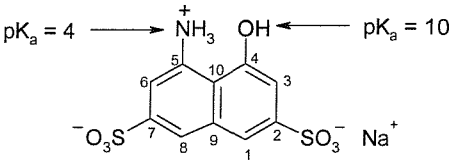

50

Figure 1.19: H-acid.

This multifunctional reagent can be selectively coupled through the 3- or 6-position. The selectivity between these two sites is pH dependant. At pH 2-7 coupling takes place slowly at the 6-position. As the highly reactive naphtholate group is not available the reaction takes place with the electrons directed from the less reactive free amino group. At higher pH both the free amine and naphtholate group are available, but as the naphtholate reacts much faster than the neutral amine, only the 3-coupled product is recovered. Reaction of this reagent with diazonium salts is also unusual because diazonium coupling only occurs at the 3- and 6-positions, and not at the 1- and 8-positions, accredited to the steric congestion from the sulphonate groups (Figure 1.20).

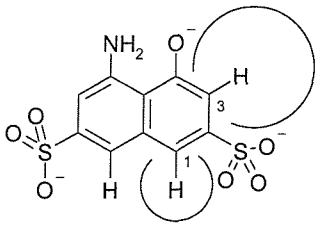

50

Figure 1.20: Steric congestion around H-acid.

1.2.2 Structure

Azo-dyes can exist in either the *cis*- (**51**) or the *trans*- (**52**) forms, although only the *trans* isomer is normally observed (Scheme 1.8).[45]

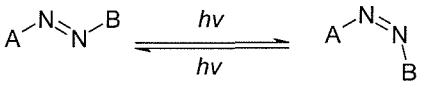

51 **52**

Scheme 1.8: Cis-trans isomerism in azo-dyes.

The groups A and B are normally carbocycles, although recently heterocycles increasingly have been used.[46] Scheme 1.9 shows an azo dye containing an *ortho* hydroxy group. The presence of the conjugated phenol results in tautomerism between the azo (**53**) and hydrazo (**54**) forms. This tautomerism is affected by many factors, such

as solvent and aromatic substituents, and will affect the shade, stability and tinctorial strength of the dye.[47]

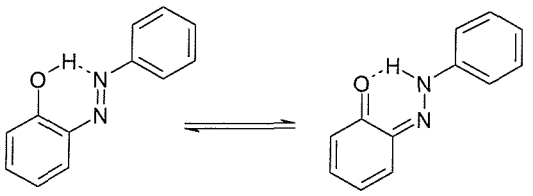

53 54

Scheme 1.9: Azo-hydrazo tautomerism of azophenol dyes.

The tautomeric balance depends on the thermodynamic stability of the two isomers. In this case, the difference in bond energies between the two forms is 108 kJ mol^{-1} in favour of the hydrazo-form. However the hydrazo-form has only one aromatic ring, and therefore contains approximately 134 kJ mol^{-1} less resonance stabilisation energy. As a result, the azophenol-form is predominantly observed.[47]

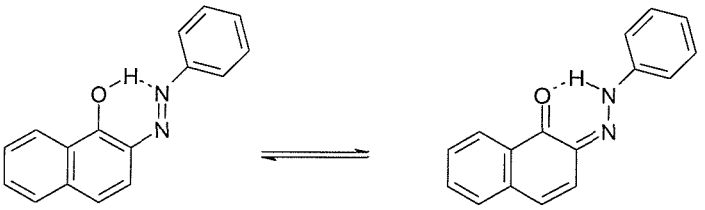

Azo, **55**. Hydrazo, **56**.

Scheme 1.10: Azo-hydrazo tautomerism in azonaphthol dyes.

In the case of azonaphthol dyes (Scheme 1.10) the loss due to resonance stabilisation energy is much less (approximately 90 kJ mol^{-1}), and a negligible thermodynamic difference between the two forms, and consequently both are observed. The tautomeric balance can be easily offset either way, through carbocycle functionalisation.

1.2.3 Azo-Dye Testing

For an ink to be a commercial success in any application it must be long-lasting once attached to the substrate. The consumer expects a product to be the same shade when purchased and discarded. In the case of tissues or wrapping paper this is not an excessively long time, and cheap colourants are used. In the case of books or posters, a high quality ink must be used to ensure the image does not fade.[48]

The most popular inkjet inks contain azo-dyes, because they are cheap to produce, are tinctorially strong and are also highly adaptable to suit many substrates and environments.[49]

The properties of new dyes are thoroughly tested, critically with ink colourants for waterfastness and lightfastness. The former investigates the dyes affinity for paper in the presence of water. This affinity will be affected by the dyes solubility in water, and attractive forces between it and the substrate. These include ionic, Van der Waal's and hydrogen bonding interactions.[50] Lightfastness tests measure the rate of photochemical reaction under strong light. When a dye molecule absorbs a quanta of light, several processes can occur (Figure 1.21).[51]

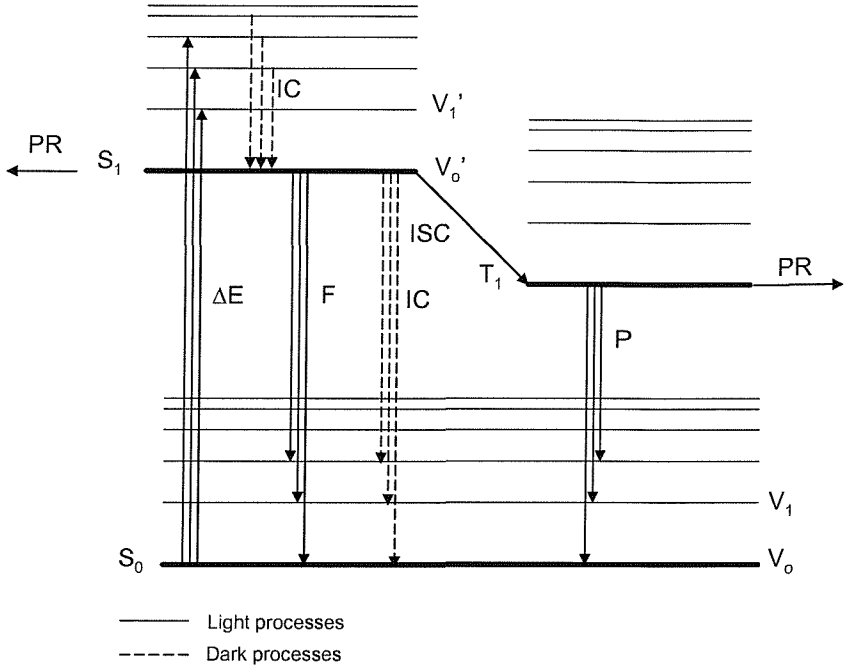

Figure 1.21: Photochemical processes: S_o = electronic ground state; V_o = ground vibrational state; V_1 = first excited vibrational state; S_1 = first electronic excited state; ΔE = excitation; IC = internal conversion; F = fluorescence; ISC = inter system crossing; P = phosphorescence; PR = photochemical reaction.

At room temperature the molecule is likely to be in the lowest vibrational level (v_o) of the ground electronic state (S_o). When a photon is absorbed an electron is excited to a higher electronic and vibrational energy level (ΔE, Figure 1.21) where the energy difference is equal to the energy of the incoming photon (Eq. 1.1).

$$\Delta E = E_{excited} - E_{ground} \qquad \text{Eq. 1.1}$$

This process is very fast, taking only 10^{-15} seconds. The dye molecule is now at the first excited energy level (S_1) but it has also gained vibrational energy and can therefore be at

any of the vibrational energy levels of the excited state, labelled V_0', V_1'. The exact energy of excitation is statistically governed and is the cause of broadened bands seen in absorption spectrum. The molecule can remain in the single excited state for a relatively long length of time (10^{-9} s), and can undergo one of several processes. A general relaxation process that can occur from any energy level, electronic or vibrational, is internal conversion (IC, Figure 1.21). This happens when energy is transferred to the surrounding environment as heat, and results in no emitted light (a 'dark' process).

The electronic energy can also be released by a 'light' process, which results in fluorescence (F, Figure 1.21), and the molecule returning to the ground electronic state, S_0. Like the excitation energy, the exact emission energy is also statistically governed as this transition can be to a number of ground electronic state vibrational levels, which results in a broadening of the emission peak.

Another possible relaxation pathway is intersystem crossing (ISC, Figure 1.21). This is described as the transition between the excited singlet state (S_1) across to the excited triplet state (T_1). The triplet state has a longer lifetime than the singlet state (10^{-3} s) and will relax slowly back to the ground electronic state – an emission known as phosphorescence (P, Figure 1.21).

From either the S_1 or T_1 states, the molecule contains enough energy to react with itself or a second molecule in a photochemical reaction (PR, Figure 1.21). The quantum yield of photochemical reaction can be expressed as:

$$\Phi_{PR} = \text{number of molecules reacted / number of quanta absorbed} \qquad \text{Eq. 1.2}$$

and is dependant on many variables. These include the nature of the incoming light, the adsorption of the dye and the lifetime of states S_1 and T_1. It is also dependant of other chemical species present, including solvent, printing substrate, oxygen, moisture, and impurities present in the dye-mixture. A typical fading mechanism of azo-dyes which exist partly in the hydroazo tautomer is through reaction with singlet oxygen (Scheme 1.11).[52] This mechanism requires the presence of the hydrazo form (**58**) of the dye, and hence dyes which preferentially exist in the azo tautomer (**57**) form exhibit good lightfastness qualities.

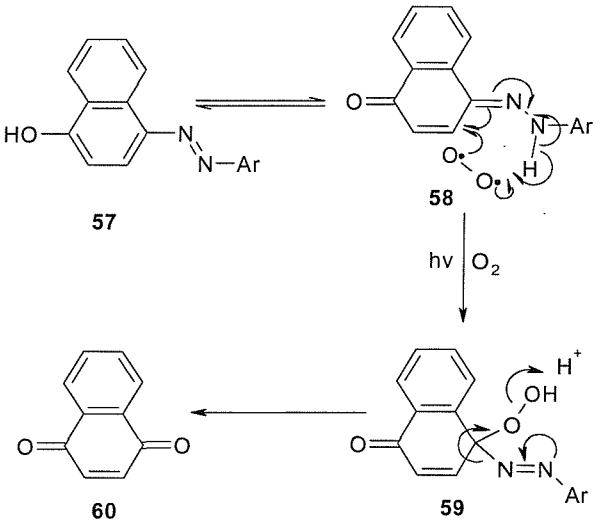

Scheme 1.11: Photochemical fading mechanism.

1.3 Combinatorial Chemistry

1.3.1 Background of Field

In the 1980's the field of biological *in vitro* screening was pushing forward in leaps and bounds. The powerful combination of robotics and sensitive assay techniques led to the development of *high-throughput screening* (HTS).[53] Using this process small amounts of potential drug candidates are rapidly assayed using robotics, and their binding with biological receptors studied. This technique allowed the rate at which pharmaceutical companies could perform biological assays to increase exponentially in a matter of years.[54]

A repercussion of this development was that the bottleneck of pre-clinical pharmaceutical research shifted from the screening step to the production of sufficient numbers of new materials to be assayed (Figure 1.22). This was the founding stone of a new field of organic synthesis - *Combinatorial Chemistry.*

Combinatorial chemistry is used at two important points in the drug discovery process. Once the biological receptor has been identified, it is screened against compounds from a wide range of sources, including diverse combinatorial libraries, in order to find potential drug candidates. This process is known as *lead discovery.* Any 'hits' are then developed by an iterative process, involving the synthesis and screening of libraries of structurally related compounds, until the best variation is identified. This process is known as *lead optimisation*, and the successful candidates it generates can then progress to clinical development.

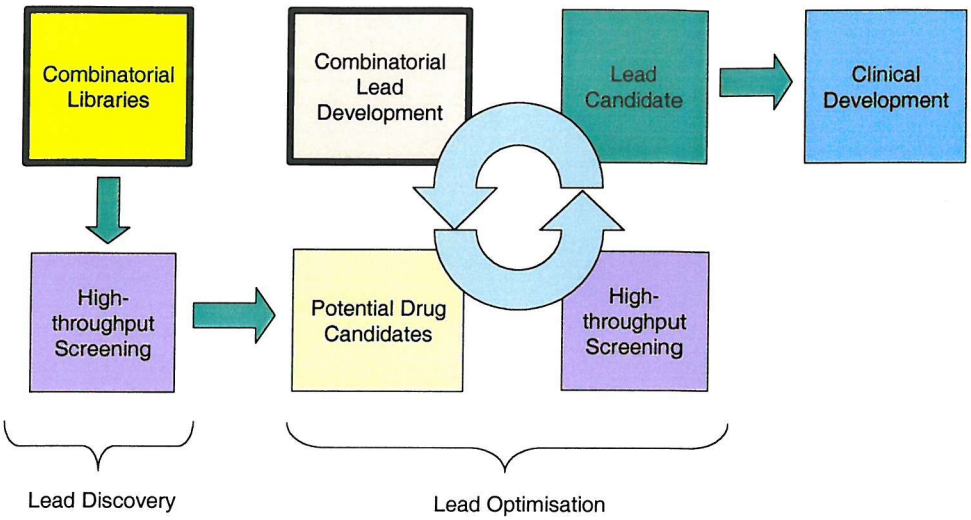

Figure 1.22: Combinatorial chemistry in the drug development process.

1.3.2 Principles of Combinatorial Chemistry

Traditional chemical synthesis involves chemists producing one compound at a time. Following this approach, a chemist can not be expected to produce more than a few novel materials per week. The aim of combinatorial synthesis is to produce many structurally related substances simultaneously.[55] Instead of linking together material A and B to make the novel compound AB, a set of reagents A with n components is reacted with a second set of reagents B with m components to give a final set of materials with n*m components (A_nB_m). The chemical reactions between sets can be performed in separate compartments, or simultaneously in the same vessel. The former of these approaches is called 'parallel synthesis', currently the most popular method, while the latter will result in a mixture of products being formed.

1.3.3 Solution vs. Solid-Phase Synthesis

The synthetic combinatorial chemist has a choice of synthetic methodologies when preparing a library. The first will probably be whether to work in solution or on solid-phase. Solid-phase chemistry involves the immobilisation of compounds onto inert, insoluble support particles, which allow facile compound handling during the reaction (it is discussed in greater detail in section 1.4).[56] As summarised in Table 1.2, solid-phase methodology gives great advantages, but it is still relatively undeveloped.

Table 1.2: Comparison between solution and solid-phase methodology.[57]

Solid-phase Synthesis	Solution Phase Synthesis
Advantages 1. Reactions can be 'pushed' to completion with high concentrations of excess reagent. 2. Rapid purification of product by washing the support. 3. Facile automation of reactions possible. 4. Split synthesis possible, for synthesis of very large libraries.	1. All known organic reactions can be used. 2. No additional cleavage/linkage steps from support required. 3. Process is easily scaled-up. 4. Facile reaction monitoring.
Disadvantages 1. Longer development time required for new chemistries on the solid-phase. 2. Additional reaction steps involved with attachment and cleavage of substrate. 3. Reaction monitoring techniques limited.	1. Purification required after each step. 2. Automation of reaction steps less efficient.

1.3.4 Parallel vs. Mixture Synthesis

Another choice to be made when devising a combinatorial approach is whether to produce compounds by parallel synthesis, or by the synthesis of compound mixtures.

In the early days of combinatorial chemistry, mixture synthesis was commonplace, as the synthetic emphasis was on creating large libraries.[58] This was sometimes undertaken by the solid-phase 'split and mix' technique.[59] However, by the mid 90's the emphasis had shifted towards smaller, more focused libraries.[60] This resulted in a decrease in the production of libraries of mixtures, and the further development of parallel methodology.[61]

During parallel synthesis each product is formed in a separate reaction chamber.[62] This can be either performed using a conventional parallel approach, or a split-parallel approach (Scheme 1.12). The 96-well plate is perfectly suited for parallel synthesis, as it is compact, can be heated or cooled, and is in a format which is compatible with automated analytical systems.

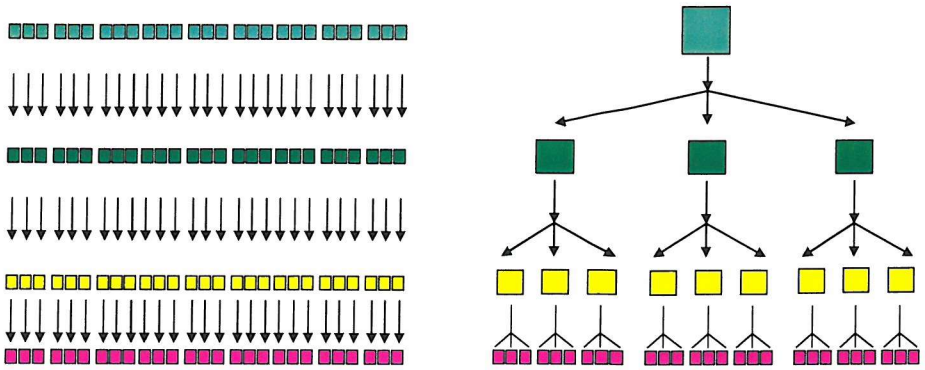

Scheme 1.12: Conventional parallel synthetic methodology (left hand side), split-parallel methodology (right hand side).

1.3.5 Library Design

For a successful library synthesis, there are many aspects to consider,[63] including;

1. Do the reactions introduce diversity into the molecule?
2. Is the process of compound production amenable to automation?
3. Should the product-set be structurally similar or diverse, and what structural features will denote diversity?

In the production of non-oligomeric libraries, most synthetic sequences will consist of 3 or 4 reaction steps, each one introducing a new point of diversity. This means that the number of reactions, and hence the time spent on purification, is kept to a minimum.

The second point is very important, as parallel-based approaches to medium sized libraries rely on robotic reagent handling and reaction monitoring to achieve a high-throughput. With the advent of preparative-LC/MS, automated parallel purification of complicated mixtures has become feasible.[64]

The concept of diversity, addressed in point 3, is not as obvious as it seems. Early in the development of combinatorial chemistry, it was common to exploit the technique to its full, and construct massive libraries using many structural motifs. This approach is still used today, generally in the early stages of an investigation, where little known about the desired product. During lead development more is understood about the necessary features of a successful material and the library size is reduced.

The experienced combinatorial chemist will recognise that not all the motifs will significantly affect the properties of the resulting material, and will be a waste of time to synthesise. A methyl, ethyl, propyl, butyl variation in a series of liquid-crystals may denote diversity in the properties of that material, but the same variation in drug candidates may result in little change in response towards the target receptor. Diversity should therefore be seen as only relative to the application of the material being developed.

1.4 Polymer-Assisted Synthesis

1.4.1 Solid-Phase Peptide Synthesis

In 1963 R.B. Merrifield published the synthesis of a tetrapeptide using a curious new technique, soon to become known as 'solid-phase' peptide synthesis (SPPS).[65] At that time the synthesis of peptides was undertaken exclusively in solution.[66] The synthesis of peptides in solution was problematic, due to the need for purification of the product after each reaction step. Merrifield's new technique involved the attachment of the growing peptide into an inert insoluble polymer, allowing facile separation of the immobilised peptide from the dissolved reagent by filtration (Scheme 1.13).[67] This technique allowed quantitative yields to be achieved through the use of high reagent concentrations and trivial purifications.

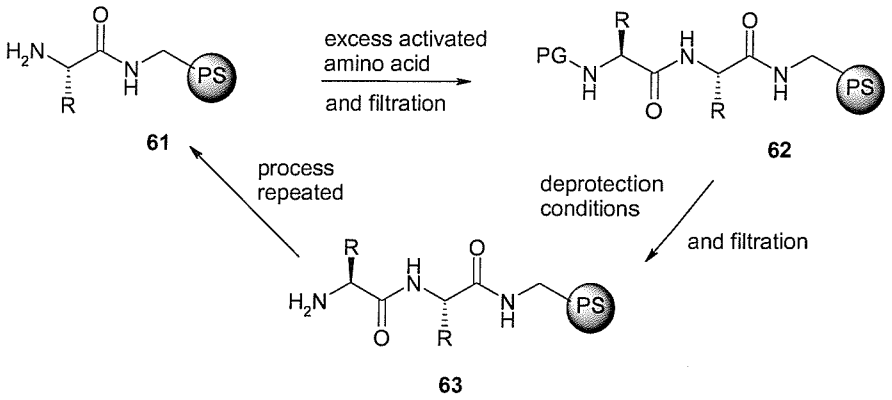

Scheme 1.13: Solid-phase peptide synthesis.

A few years after the initial work, solid-phase peptide synthesis was adapted for the production of other bio-polymers, notably by Letsinger [68] and Frechet.[69]

1.4.2 Support Polymers

To be an effective support for solid-phase synthesis, the polymer must be both insoluble and inert. Support insolubility was achieved using a low proportion of cross-linking agent in the polymerisation mixture. This resulted in a flexible lattice that allowed the solvent to enter into the interior of the polymer particle. This increased reagent accessibility to the majority of reactive sites deep inside the bead, as well as maintaining the bead structure (Scheme 1.14).

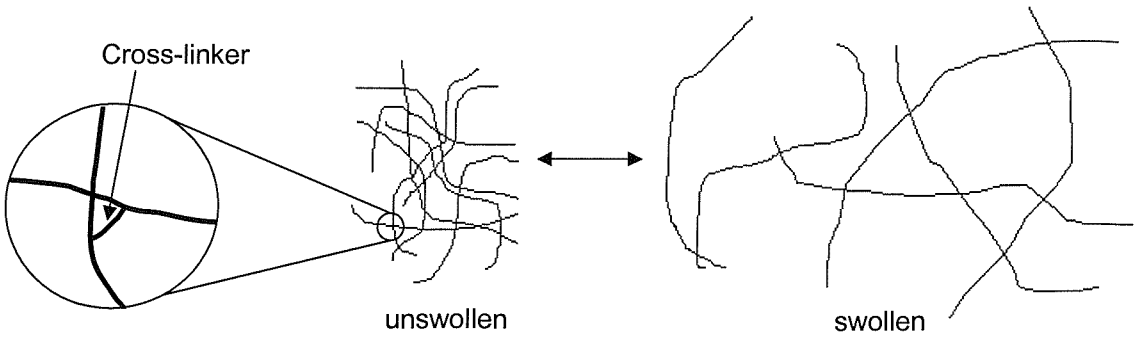

Scheme 1.14: Dry resin (middle) becomes solvated (right).

Merrifield used chloromethyl polystyrene-*co*-divinylbenzene (**66**) (PS-*co*-DVB) for some of his early work in solid-phase peptide synthesis.[70] This co-polymer was made *via* suspension polymerisation of two components; the monomer (**63**) (styrene) and cross-linker (**64**) (divinylbenzene).[71] Once the polymer beads were formed, a proportion of the polystyrene aromatic rings were functionalised with chloromethyl groups to give reactive sites to which the growing peptide was attached (Scheme 1.15).

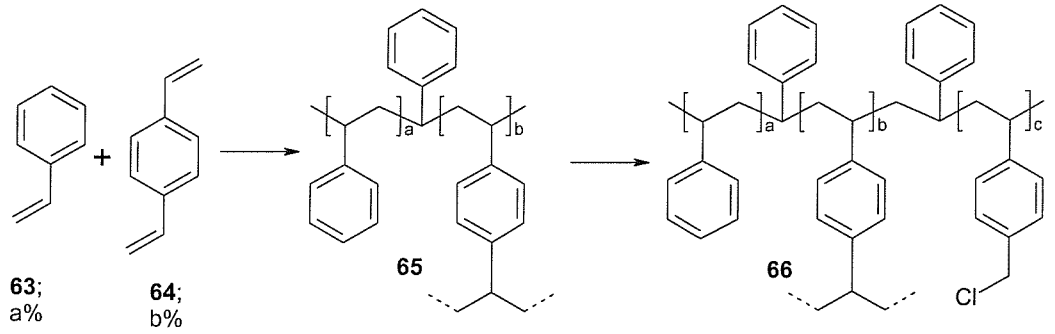

Scheme 1.15: Components in a suspension polymerisation.

Suspension polymerisation involves dissolving all of the components, and a radical initiator into an organic solvent and rapidly mixing it into a suspension with water.[72] Once a suspension has been created, radical polymerisation is initiated. When polymerization is complete, the polymer beads are the same size and shape as the organic droplets in which they were formed. The beads are then washed and sieved to obtain the desired particle size. The swelling characteristics of a polymer can be controlled by changing the percentage of cross-linking agent in the polymerisation mixture. Studies have shown how the swelling of polystyrene-*co*-divinylbenzene in common solvents can be affected by cross-linker levels.[73] Thus 2% cross-linked PS-*co*-DVB was mixed with ethanol a swelling volume of 2 mL/g was observed, but on treatment with chloroform the bead volume increased by a factor of 2.

The term 'macroporous' applies to rigid resins containing large pores. They are prepared using high levels of cross-linker and a suitable 'porogenic' solvent to help form large cavities inside the bead during the polymerisation.[74] These resins were developed to be compatible with polar solvents, such as methanol or water. They have also been used in flow-reactor systems, where bead were held inside reactor-tubes of a fixed size and reagents passed through them. Due to the fixed reactor volume, a resin was required which did not shrink or swell when the polarity of the solvent passing through the reactor changed.[75]

The mechanical stability of resin beads can be affected by many factors. It has long been recognised that the grinding effect associated with mechanical stirring causes damage to the beads. The degree of degradation is also affected by the amount of cross-linker used. If the percentage of cross-linker is too low, then the bead is very weak and its mechanical stability is reduced. If the percentage is too high, then the bead can be brittle, can degrade in abrasive environments. A compromise of 1-2% cross-linking is commonly used for gel-type PS resins.

The synthesis of highly polar materials, like DNA, on PS resin can result in poor yields due to the inherent incompatibly of the polar substrate and the apolar support matrix.[76] Popular polar resins available on the market incorporate polyethylene glycol (PEG) and polyacrylamide co-polymers. The polar functionality has been introduced into the beads structure *via*:

- Grafting polar chains onto the backbone, after polymerisation,
- Using a polar cross-linking component during polymerisation.

TentaGel is a PS-*co*-DVB-based polymer with PEG chains grafted to the polystyrene backbone.[77] The polymer can swell in a wide range of solvents, from water to DCM. PEGA resin also contains PEG chains, but introduced as the cross-linking component during polymerisation.[78] The dimethylacrylamide backbone of this resin is also more polar than polystyrene, resulting in unparalleled swelling in water and methanol. The large cavities which form within the swollen bead allow large macromolecules, such as enzymes, into the interior.[79]

The successful marriage of solid-phase chemistry with oligomer synthesis soon tempted the medicinal chemistry community to examine its application towards non-oligomeric substances.[80] Early trials involved peptide-like materials, like diketopiperazines,[81] but as research progressed it was shown that the solid-phase approach was suitable for the synthesis of many types of chemical compound.[82] This move opened up the field of solid-phase peptide synthesis to a much larger range of chemical transformations, resulting in the development of a wider range of supports and linkers which were compatible with these new conditions.[83]

1.4.3 Linker Groups

When considering a novel solid-phase approach, many technical aspects must be considered, like, for example, the choice of resin support. Also critical is the mechanism required to remove the substrate from the support on completion of synthesis. This is accomplished using a 'device' called a 'linker', which attaches the substrate to the support during the synthesis, but under certain 'cleavage' conditions will release the compound into solution.[84] Due to historical consequences in the development of solid-phase synthesis, many linker groups have been developed for the immobilisation of carboxylic acids.

Scheme 1.16 shows a carboxylic acid cleaving from Merrifield resin (**67**) under strongly acidic conditions.[70]

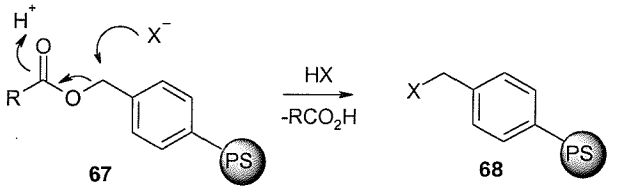

Scheme 1.16: Acid cleavage mechanism of Merrifield resin.

Merrifield first used this resin in conjunction with benzyloxycarbonyl-protected amino acids. This protecting group was removed with HBr in AcOH, and to prevent cleavage of the peptide during this highly acidic step the polystyrene resin was either nitrated or bromonated. If the substrate is not stable to strongly acidic conditions, then there are many mild-acid cleavable linkers available. The PS supported Wang linker (**69**) is shown in Scheme 1.17.[85]

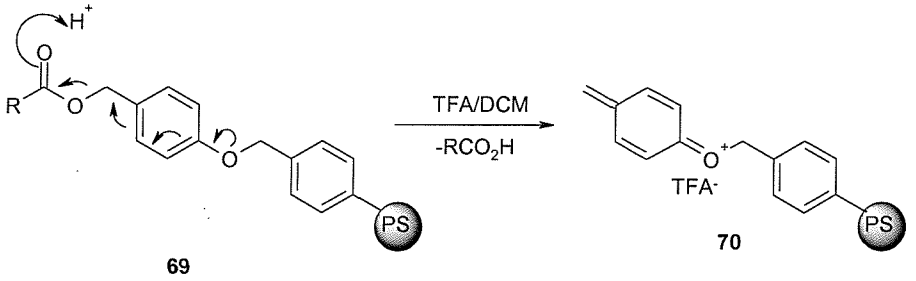

*Scheme 1.17: Carboxylic acid on the Wang linker (**69**) cleaving in TFA/DCM.*

Carboxylic acids can be cleaved from this linker under the relatively mild acid conditions, of 50% TFA in DCM, due to stabilisation of the benzylic cation by the ether group. First described in 1973, the Wang linker has become one of the most widely used linkers in solid-phase synthesis. It has successfully been converted to the chloro,[86-88]

trichloroacetimidate,[89] bromo, [93] iodo,[93] mesyl,[93] tosyl,[93] and nosyl [93] derivatives and has been applied to the synthesis of peptidic acids [85] and amines [94] as well as non-peptidic acids,[88] alcohols,[89,96] thiols,[95] phosphonates,[90-92] and amines (Scheme 1.18).[93] Use of the aldehyde version of this linker allows the loading of an amine scaffold by reductive amination.[94]

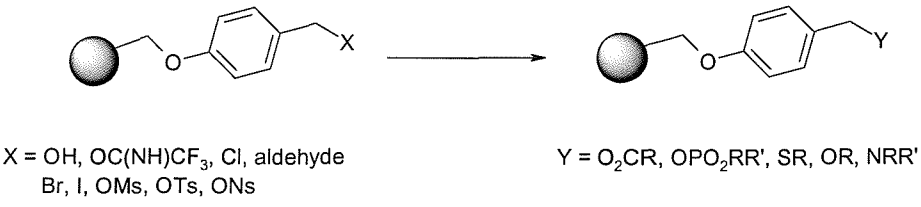

X = OH, $OC(NH)CF_3$, Cl, aldehyde
Br, I, OMs, OTs, ONs

Y = O_2CR, OPO_2RR', SR, OR, NRR'

Scheme 1.18: The Wang linker in its various forms, loaded with a variety of functional groups.

With further electron-donation into the aromatic system, the acid sensitivity of this type of linker can be further increased. The SASRIN (super-acid sensitive resin) linker (**71**) allows just this, by further stabilizing the benzylic cation with electron density from the *ortho*-methoxy group (Scheme 1.19).[97] Carboxylic acids have been cleaved from the SASRIN linker with as little as 1% TFA in DCM.

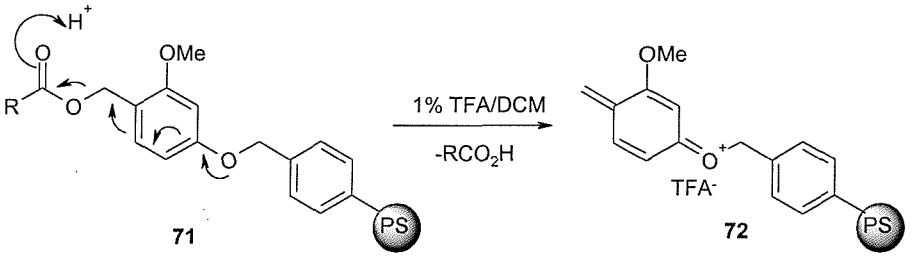

Scheme 1.19: Carboxylic acid cleaved from the SASRIN linker.

All of the linkers examined so far have relied on stabilisation of a cation, with varying degrees of +M effect from adjacent groups. This is usually the case for linkers cleaved with acidic conditions, other examples of which are shown in Table 1.3.

Table 1.3: Example acid-cleavable linkers.

		ref.
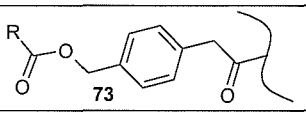 73	PAM anchor cleaved with HF or TFMSA	98
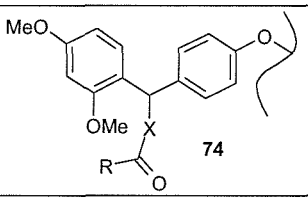 74	Rink acid (X=O)cleaved with AcOH/DCM Rink amide (X=NH) cleaved with TFA/DCM	99
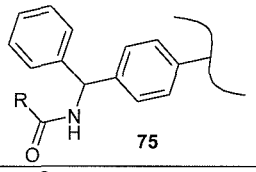 75	MBHA cleaved with TFMSA	100
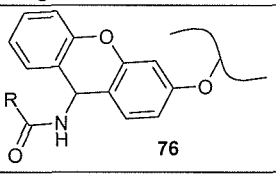 76	Sieber amide cleaved with TFA/DCM	101

There are also many linkers which are cleaved with non-acidic conditions. These include linkers that are cleaved under basic conditions, fluorination, hydrazinolysis or photolysis (Table 1.4).

Table 1.4: Example linkers cleaved by non-acidic conditions.

		ref.
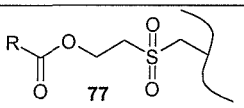 77	Cleaved with NaOH, *via* beta-elimination	102
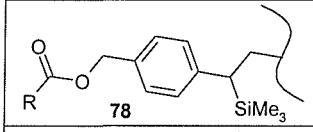 78	Cleaved with Bu_4NF	103
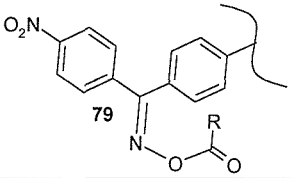 79	Cleaved with hydrazine hydrate; hydrazinolysis. Stable to 25% TFA	104
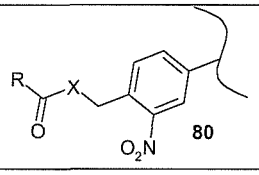 80	Cleaved by photolysis ($h\nu$ = 350 nm) X = O or NH	105

In order to assert a greater control over the cleavage conditions, the concept of safety-catch linkers was developed. These linkers cleave under two sequential reaction conditions. The first activates the linker, and the second cleaves the substrate.

The concept is demonstrated using the Kenner safety-catch linker (**81**) shown in Scheme 1.20.[106]

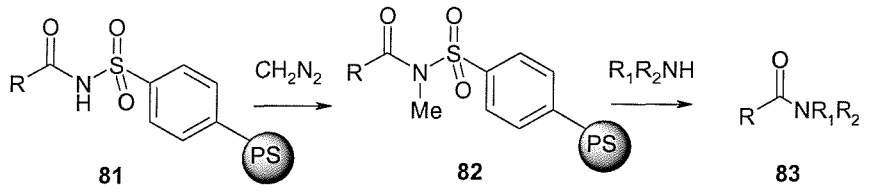

Scheme 1.20: The Kenner Safety-Catch linker.

Acylsulfonamide groups are stable to nucleophilic attack, due to ionisation of the NH groups (pK_a 2.4). However, once the nitrogen is alkylated with diazomethane to form the *N*-alkyl-acylsufonamide resin (**82**) the amide bond is activated towards nuclephilic attack to release the resulting amide **83** into solution.

1.4.4 Analysis of Resin-Bound Materials

One of the major drawbacks of solid-phase synthesis is that most modern analytical techniques are not suitable for resin supported substrates. Reaction progress can be monitoried by cleaving the substrate from an aliquot of resin, but this adds an extra step into what should be a quick and simple test. An alternative method for following the reaction is the use of quantitative colourimetric tests, which is commonly used in solid-phase peptide sythesis to detect primary amines.[107] Tests arising from protecting-group deprotection have also allowed facile reaction monitoring in peptide [108] and DNA synthesis.[109]

During the 1970s Schaefer used ^{13}C-NMR to analyse a variety of polymers. This was initially attempted on samples in the 'gel-phase',[110] but better results were obtained later using 'magic' angle spinning (MAS) NMR.[111] 'Gel-phase' ^{13}C-NMR spectra are obtained from swollen resin in deuterated solvent using a conventional NMR tube. This NMR technique is complicated by peak broadening effects, caused by two factors; the restricted motion of the resin, leading to dipolar coupling, and physical heterogeneity of the resin matrix, which results in equivalent atoms experiencing a different magnetic field. Dipolar coupling, Δ, has a strong angular dependence, as:

$$\Delta \propto r^{-3} (3 \cos^2 \theta - 1) \qquad \text{Eq. 1.3}$$

where r is the internuclear distance and θ is the angle between the dipolar coupled spins and the static magnetic field, B_o. 'Magic' angle spinning (MAS) NMR involves the sample being rapidly spun at the 'magic' angle (54.7°) to the static magnetic field. This reduces

dipolar couplings to zero and averages bulk magnetic susceptibility, reducing line-broadening significantly (Figure 1.23).[112]

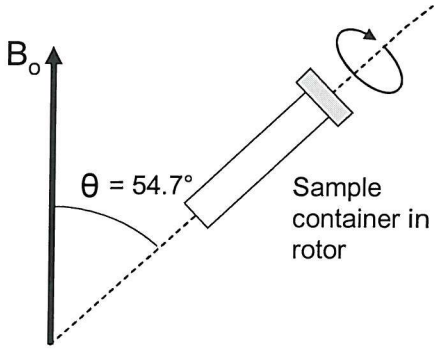

Figure 1.23: MAS NMR probe; the resin sample is rotated a 57.4° to the static field.

It was not until 1980 that Manatt and co-workers successfully used gel-phase NMR to follow peptide synthesis, using ^{19}F labelled protecting groups.[113] Gel-phase ^{13}C-NMR was also reported, but required long acquisition times due to the low natural abundance of the isotope.[114] This problem was overcome by Look and co-workers, who performed gel-phase ^{13}C-NMR of ^{13}C enriched materials.[115]

Due to the low chemical shift dispersion observed with ^{1}H-NMR spectra, the signals acquired using gel-phase ^{1}H-NMR are generally too broad to give useful information. The breakthrough for ^{1}H-NMR of resin bound substrates came with the application of MAS NMR techniques, in 1994.[116] This allowed high resolution 2D ^{1}H-NMR spectra of resin-bound substrates to be obtained, although this experiment required more sample.[117] More recently ^{19}F and ^{13}C-MAS NMR analysis has been used to accurately quantify resin loadings.[118]

Mass spectrometry (MS) monitoring of solid-phase reactions requires efficient linker-cleavage chemistry and a reliable ionisation technique, as demonstrated in 1995 by Bradley.[119] A polymer-bound substrate was cleaved from a Rink amide linker with TFA vapour. The ionisation matrix was added and allowed to crystallise around the bead, before conventional analysis by MALDI-TOF-MS. This technique has since been adapted for use with photo-labile linkers, which undergoes simultaneous cleavage and desorption during laser-assisted ionisation.[120]

Transmission-type infrared (IR) analysis of ground beads in KBr disks was first reported in 1971 by Frechet.[69] However, analysis in this manner was hindered by a peak flattening effect,[121] a problem not solved until the arrival of attenuated total reflection (ATR) infra-red spectroscopy, first described in 1996.[122] During this method the bead is flattened slightly between two surfaces (Figure 1.24).

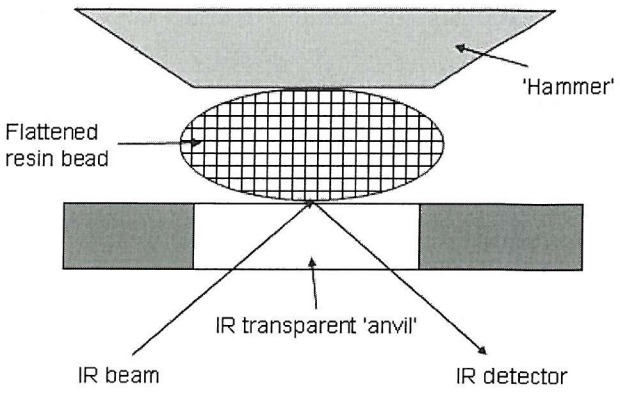

Figure 1.24: IR analysis using a ATR sample holder.

The IR beam is reflected off the bead surface, allowing the spectrum of the first few micrometers of the material to be recorded. This method is highly sensitive, and can be performed on a single bead. An alternative method for single bead analysis was developed at the same time, which used a microscope to focus the IR beam through the bead.[123]

1.4.5 Polymer Supported Reagents and Scavenging Resins

The problems associated with solid-phase synthesis, outlined in Table 1.2, have been the subject of intensive research and the fruits of this research are plain to see. The power of solid-phase synthesis originates from the facile separation of the immobilised substrate from the reagents. The alternative is to immobilise the reagents while the substrate remains in solution.[124] This solves the problems of bound-substrate analysis, whist still allowing rapid purification of excess reagents (Scheme 1.21).

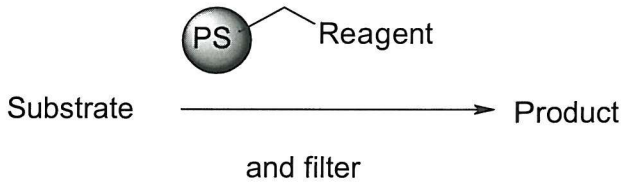

Scheme 1.21: Polymer supported reagents (PSR).

It is worth remembering that since the reactions of polymer supported reagents (PSR) are between a compound in solution and a tethered species, the reaction occurs within the support matrix and hence the outcome of the reaction is governed partly by the compatibility of the solvent and resin.[73]

The simplest polymer supported reagents are organic polymers loaded with simple functional groups, such as quaternary amines or sulphonic acids.[125] These resins

are made on a large scale for ion-exchange purposes, and are therefore relatively inexpensive. An example of their use was found in the early work of Cainelli in the formation of unsaturated nitriles (Scheme 1.22).[126]

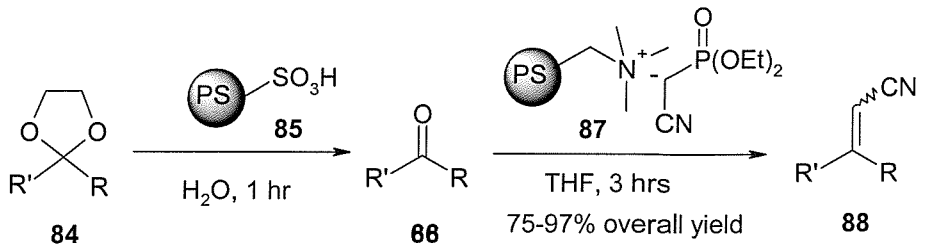

Scheme 1.22: Formation of unsaturated nitriles, using a supported Horner-Wittig reagent.

In the first step of this two step process, acetal **84** was treated with an excess of polymer supported sulphonic acid (**85**) to form ketone **86**. The reaction was filtered after the conversion was complete, and the second reagent was introduced directly to the filtrate.

In the second step, the Horner-Wittig reagent was supported on a quaternary amine resin **87**. This reagent was generated by deprotonation of the cyano-compound, followed by filtration of the anion through the quaternary amine functionalised resin. The supported reagent was added to ketone **86** in excess and was removed by filtration to give pure nitrile **88** in 75 to 97% yield as a mixture of E and Z isomers. As reagents **85** and **87** were immobilised they could also be applied to the acetal at the same time, without inter-bead reagent interaction. Mutual segregation of supported reagents is an extremely powerful feature of PSR and cannot be observed in solution or SPOS analogues.[113c]

The immobilisation of reagents onto resin *via* ionic interactions is a common feature of PSR.[127] Polymer supported reagents can be compatible with a greater variety of solvents than the corresponding unsupported reagent, opening up its use to previously incompatible reaction conditions.

In the example from Cainelli neither the ketone nor the resulting nitrile carried any permanent charge. If they had, the yield of the process would have been considerably lower, as the charged species could have remained within the resin after the reaction, due to ionic interactions. This process is called scavenging, and can be used to rapidly sequester a component of a mixture. Scheme 1.23 shows an example by Kaldor *et al.*,[128] where aromatic aldehyde **89** was reacted with primary amine **90** by reductive amination to give a secondary amine **92**.

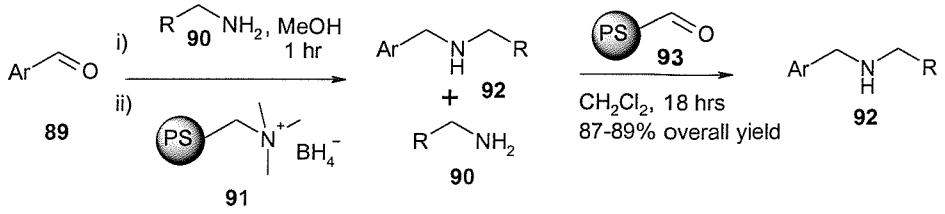

Scheme 1.23: Reductive amination of an aromatic aldehyde.

The first step involved the treatment of the aldehyde with an excess of the primary amine **90** to form the imine. The imine was then reduced *in situ* by polymer supported borohydride **91**. If the reaction was worked up at this stage chromatography would have been required as the excess amine was still present. In this case a rapid alternative to chromatography was used; the solution was shaken with an aldehyde resin (**93**) which sequestered the primary amine, in the presence of the secondary amine. The solution was then filtered to yield pure secondary amine **92** in 87-89% overall yield.

Other common scavenging resins used are isocyanates for the removal of nucleophiles,[129] and primary amines for the removal of electrophiles.[130] Like polymer supported reagents, these two scavenger resins can be used together, as inter-bead reaction will not occur. This strategy was applied by Hodges in the example shown in Scheme 1.24. [131]

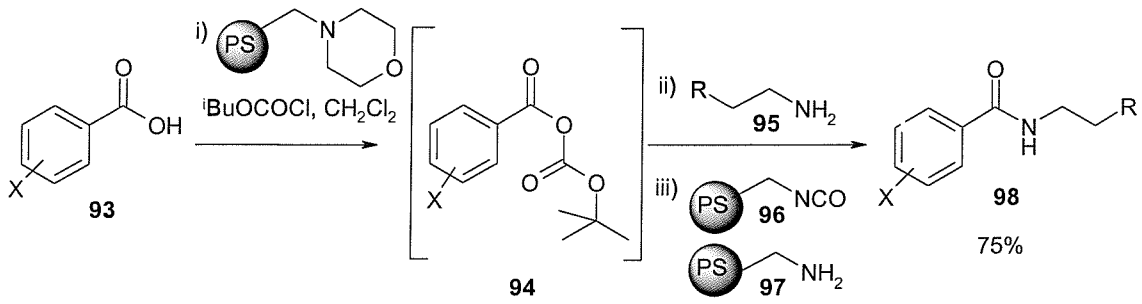

Scheme 1.24: Amide bond formation, using scavenger resins.

In the third step both amine (**97**) and isocyanate (**96**) resins were added to scavenge any active ester **94** or amine **95** from the reaction mixture. All the resins were removed by filtration to yield amide **98** in 75% yield and 97% purity.

Chapter 2: Polymer-Supported Diazonium Salts.

2.1 Introduction

Only in the last few years has the diazotisation reaction been applied to the solid-phase. Bräse and co-workers reacted resin-supported aniline **101** with ^{t}butylnitrite (^{t}BuNO$_2$) to give supported diazonium salt **102** (Scheme 2.1).[132-133]

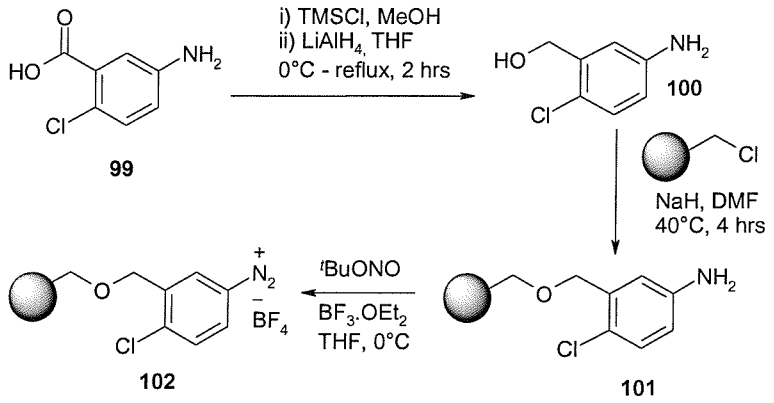

99 100 101 102

Scheme 2.1: Synthesis of a supported diazonium salt.

Polymer supported diazonium salt **103** was reacted with a range of primary amines to form a triazine, which acted as a linker for the synthesis of unsymmetrical ureas **106** (Scheme 2.2).[134]

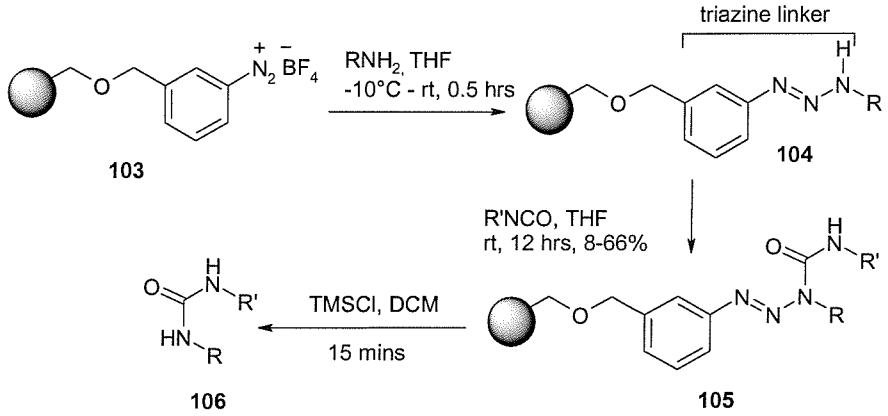

103 104 105 106

Scheme 2.2: Synthesis of ureas, using a triazine linker.

This approach was also used for the synthesis of amides,[134] arenes,[135] thioureas,[136] guanidines,[136] and amines.[137] A polymer supported reagent for the generation of diazonium salts has also recently been reported. Ley and co-workers used the cationic ion-exchange resin Amberlyst A-26 loaded with nitrite ions (**108**) to prepare diazonium salts (**109**), by mixing the resin with anilines (**107**) in concentrated HCl.[138] These salts were treated with a range of phenols (**110**) to give azo-dyes (**111**) (Scheme

2.3) in moderate to high yield, which were purified by catch-and-release using Amberlyst A-26 (OH^- form).

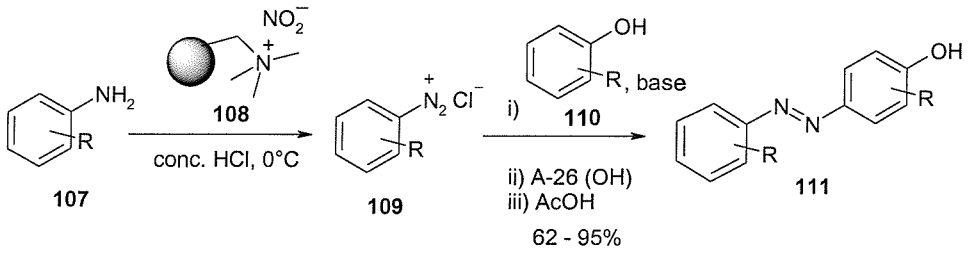

Scheme 2.3: Synthesis of azo-dyes, using polymer supported nitrite.

2.2 Objectives of Research

During this chapter the preparation of ion-exchange resin supported diazonium salts was attempted. It was proposed that the immobilisation of the diazonium salts would allow easy handling of these unstable materials. Supported salts could then be reacted with phenolic nucleophiles to give a library of azo-dyes (Scheme 2.4).

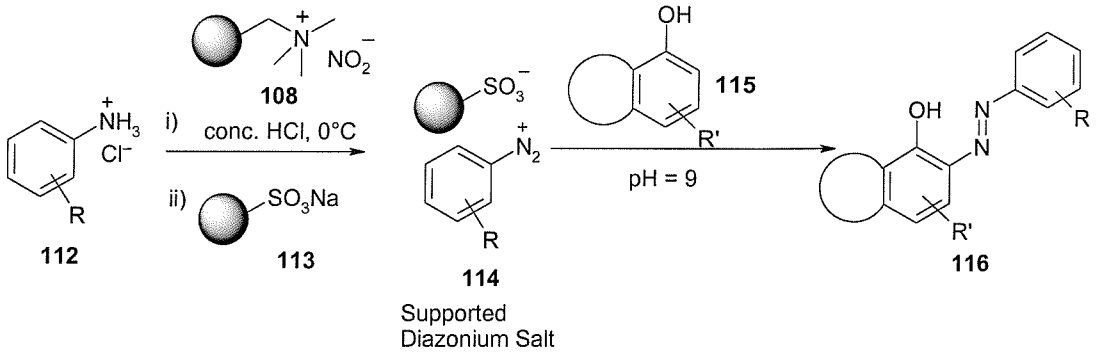

Scheme 2.4: The proposed synthesis of azo-dyes from supported diazonium salts: aniline and phenolic derivatives are defined in Table 2.1.

This library should give an indication as to the ability of this technique to support the wide range of diazonium salts used in modern azo-dye synthesis.

2.3 Supported Diazonium Salts

During the preparation of the supported diazonium salts, two ion-exchange resins were used, Amberlyst A-26 (SCX, 4.2 mmol/g) and Amberlyst A-15 (SAX, 4.7 mmol/g). These are relatively large (0.3-0.8 mm) macroporous polystyrene resins, with large cavities in the matrix interior (~250 Á). A-26 is commercially available with many counter ions loaded, and required no treatment prior to use, but A-15 required acid/base washing to remove synthesis by-products and ensure consistent H^+ loading.[140]

Following the work of Ley,[138] diazotisation of aniline (**112/5**) using A-26 supported nitrite **108** was performed in 12 M HCl (Scheme 2.5). At this acid concentration the nitrosating agent was nitrosyl chloride ($Cl^-{}^+N{=}O$).

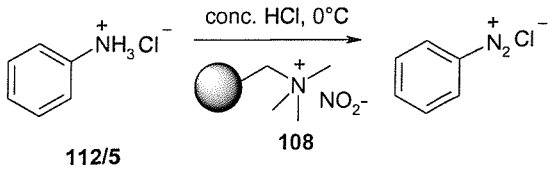

112/5 **108**

Scheme 2.5: Diazotisation of aniline hydrochloride using supported nitrite.

The stirring of resin-containing reactions can result in damage to the beads, which in turn can lead to problems during filtration. Macroporous beads are especially brittle due to high cross-linking, which makes them especially prone to damage by this procedure. During this work an orbital shaker was used, which resulted in good agitation of the reaction mixture without destructive shearing forces. Although the loading of the A-26 resin was supposedly 4.2 mmol/g previous reports of polymer supported reagents using this resin suggest loadings of around 1 mmoi/g.[124e] Due to the low cost of this resin it was used in excess, as further reaction of the diazonium salt with the supported nitrite was not possible.

The filtrate was passed through a solid-phase extraction (SPE) tube with a filter (Figure 2.1), containing A-15 (Na^+ form) (**113**) resin. The exchange of the sodium ions with the diazonium species allowed immobilisation of the reactive species and formation of the polymer supported diazonium salt, **114/5** (Scheme 2.6).[139]

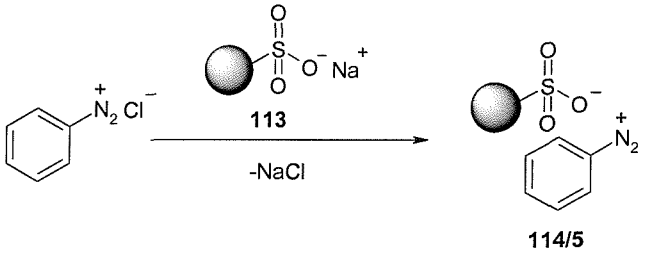

114/5

Scheme 2.6: Immobilisation of the diazonium salt on the A-15 resin.

As over 2 equivalents of diazonium salt were applied to the resin, a high level of exchange should have been achieved. Macroporous beads have relatively rapid exchange properties, due to the large cavities and channels within the bead ensuring efficient solvent flow.[141] The flow rate through the syringe was maintained at approximately 10 mL/min, in order to ensure efficient penetration and exchange of the diazonium salt with the resin beads. This flow rate also ensured that the resin bed was

not disturbed during the exchange process. Significant disturbance to the bed could result in a large proportion of the diazonium salt solution passing through the chamber without achieving optimal exchange (Figure 2.1).

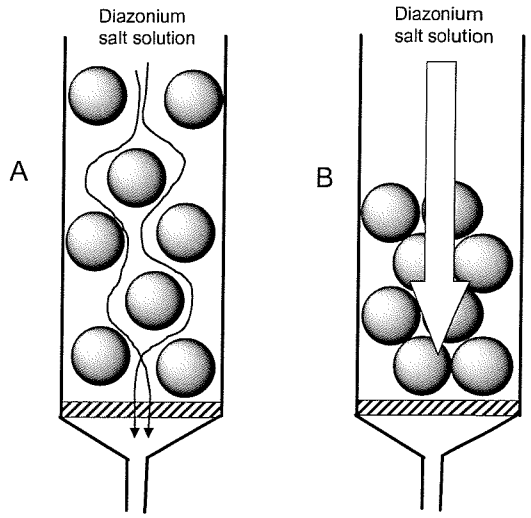

*Figure 2.1: Diazonium salt-flow though resin **113**; a) disturbance of the resin bed results in poor exchange kinetics; b) good exchange kinetics due to stable resin bed.*

The diazonium resin **114/5** was then washed with water and methanol to ensure complete removal of un-supported diazonium salt. The resin was dried in a flow of nitrogen and stored at 4°C. This process was repeated in a serial manner, whereby a syringe of resin **108** was held above a second syringe of resin **113** (Figure 2.2). A solution of aniline hydrochloride was then cooled to 0°C and passed slowly through the two syringes in a sequential manner (the whole reaction was kept cool by surrounding the A-26 resin with a jacket of ice/water).

This allowed production of the supported diazonium salt **114/5** in one step, although more equivalents of the supported nitrite **108** were required to ensure complete conversion of the aniline to the diazonium salt. This concerted methodology would probably be unsuitable for unreactive anilines, as any remaining starting material would also be sequestered by the A-15 resin, reducing its reactive load. Any lack of reactivity could be partially offset by a slower flow rate which would keep the aniline in contact with the supported nitrite for a longer time.

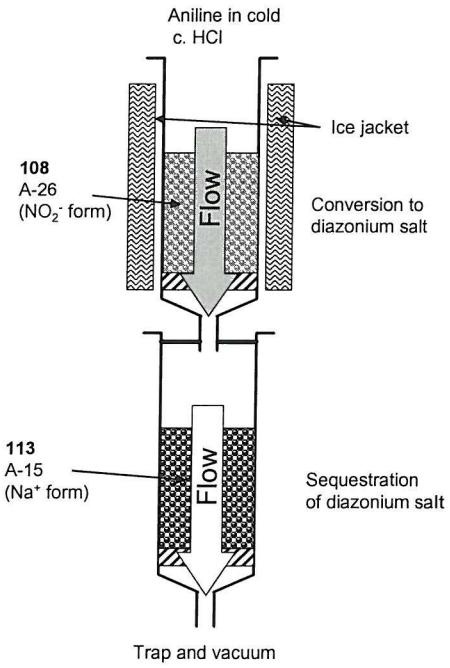

Figure 2.2: Concerted diazonium salt generation and immobilisation.

2.4 Reaction of Supported Diazonium Salt with H-acid

The supported diazonium salt **114/5** was reacted with a solution of phenolic nucleophile **115/a** (H-acid) at pH 9 to give azo-dye **116/a5** (Scheme 2.7).

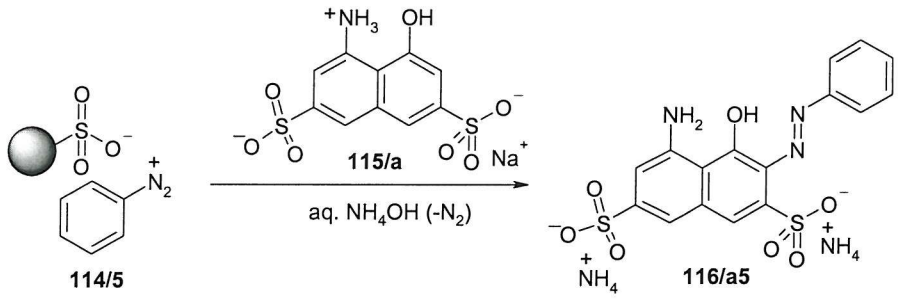

*Scheme 2.7: Reaction of a supported benzene diazonium salt (**114/5**), with H-acid (**50**).*

A SPE tube was loaded with the supported diazonium resin (**114/5**), to which a solution of H-acid in aqueous ammonium hydroxide was added. This maintained the pH of the media at around pH 9 during the course of the reaction. The syringe was attached to an orbital mixer, to ensure sufficient agitation of the reaction mixture. Upon addition of the ammonium hydroxide solution the supported reagent decomposed rapidly, so an excess was required. After approximately 40 minutes the evolution of gas had stopped, indicating the reaction was complete. The reaction mixture was filtered and the filtrate

collected. Rapid elution of the product from the bead was achieved, due to increased electrostatic repulsion between the anionic resin and dye (Scheme 2.8).

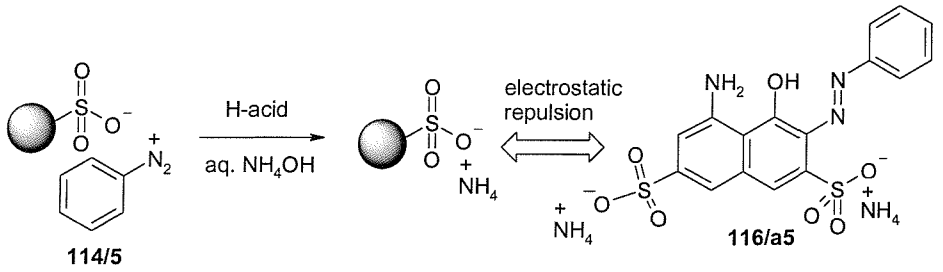

Scheme 2.8: Electrostatic repulsion allowed facile dye elution.

The filtrate was then reduced *in vacuo* to remove the excess ammonium hydroxide, and freeze-dried to give the dye **116/a5** in 82% yield and 83% purity (ELSD-HPLC analysis).

A potential problem associated with this technique was the possible low affinity between nitrosyl chloride and the A-26 resin. On treatment with acid at >6 M (pH -0.7) the supported-nitrite ions reacted to form the nitrosyl ion. This cationic species should experience an electrostatic repulsion from the cationic resin and be forced into solution, where it would react with aniline. Upon filtration the excess nitrosyl ions, along with the diazonium salt, should have passed through the filter and have been sequestered by the anionic A-15 resin. When the nitrosyl-loaded resin was added to the basic solution, the nitrosyl ions should be rapidly converted back to the anionic nitrite, and once again be released from the resin (Scheme 2.9).

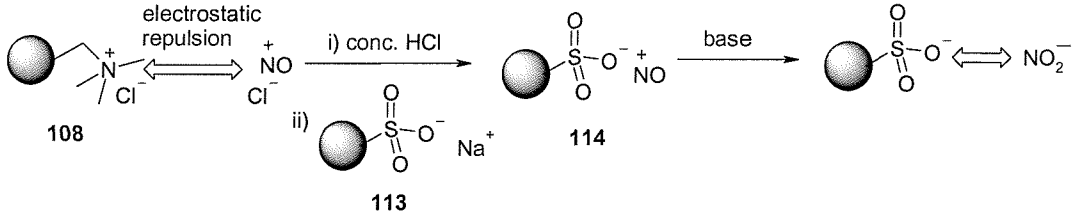

Scheme 2.9: The possible disassociation and sequestration of nitrosyl ions.

However, no evidence of involatile ammonium nitrite was found in the reaction eluent, when analysed by ELSD-HPLC. A possible explanation for this result was that the nitrosyl ions were converted back to nitrite ions when resin **114** was washed with water, and eluted from the matrix.

Not only did this approach to diazonium salt generation allow rapid production and facile handling of these species, but the supported salt had relatively good stability. An experiment was undertaken to estimate the initial loading and storage lifetime of these

supported species. A batch of supported benzene diazonium salt **114/5** was generated by the standard procedure, and stored at 4°C. Derivative **114/5** was chosen as it should provide representative behaviour of the diazonium salts used in this chapter. An aliquot of approximately 10 mg of resin was reacted (in duplicate) with an excess of H-acid to ensure the maximum possible amount of diazonium salts reacted to form the dye. The solutions were analysed (HPLC) to determine the amount of dye produced. HPLC analysis suggested that the half-life of supported benzene diazonium salt was about 6 weeks at 4°C (Graph 2.1).

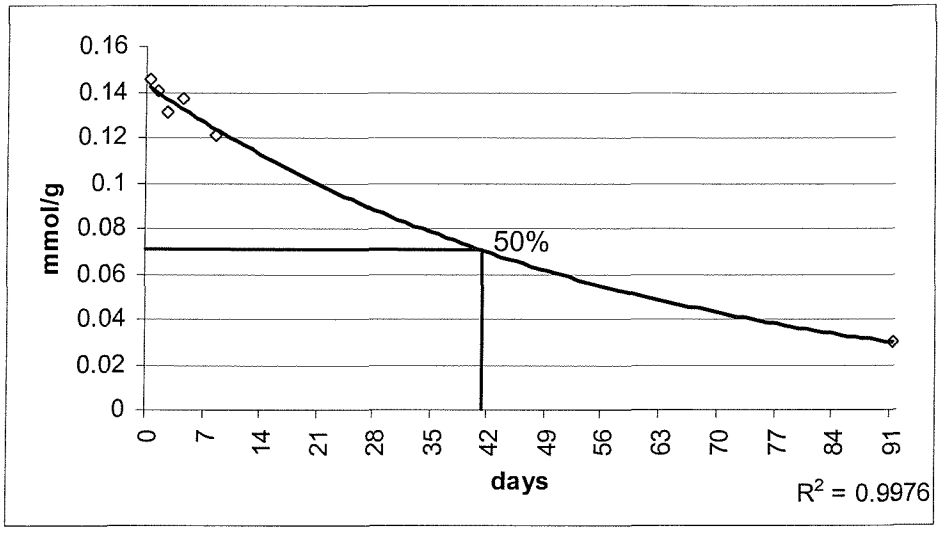

Graph 2.1: Decomposition plot of supported benzene diazonium salt; line shown is the calculated exponential line of best fit.

The amount of dye formed by the resin was initially 0.14 mmol/g of resin **114/5**, which was approximately 7 times lower than predicted for a loading of 1 mmol/g. This suggested that the remaining diazonium ions decomposed under the basic reaction conditions before reaction with H-acid was possible.

2.5 Library Synthesis

The technique of supporting diazonium salts on ion exchange resin was used to create a small library of azo-dyes in a parallel fashion, to give an insight into their value as supported reagents. The above technique was used to generate six supported diazonium salts, **114/1-6**, and these were each reacted with six phenolic nucleophiles, **115/a-f**, to give thirty-six dye products **116/a1-f6**. The anilines and nucleophiles, along with their codes, are listed below (Table 2.1).

*Table 2.1: Reagents used for the synthesis of dyes **116/a1-f6**, and their codes.*

	Anilines:		**Phenolic Nucleophiles:**
112/1	4-Chloroaniline	**115/a**	5-Amino-6-hydroxynaphthanlene-2,7-disulphonic acid (H-acid)
112/2	4-Bromoaniline	**115/b**	Phenol
112/3	4-Iodoaniline	**115/c**	4-Hydroxybenzene sulphonic acid
112/4	4-Nitroaniline	**115/d**	4-Nitrophenol
112/5	Aniline	**115/e**	3-hydroxy-naphthalene-2,7-disulphonic acid
112/6	4-Sulphanilic acid	**115/f**	4-hydroxy-naphthalene-1-sulphonic acid

Anilines **112/1-6** were transformed into a range of diazonium salts **114/1-6** with differing stabilities and reactivities. The phenolic nucleophiles used were half benzene-based and half naphthalene-based species, all of which are commonly used in dye synthesis. As reflected in the yields (Graph 2.2) and purities (Graph 2.3) of dye library **116/a1-f6**, some starting materials were more suited than others to this synthetic approach.

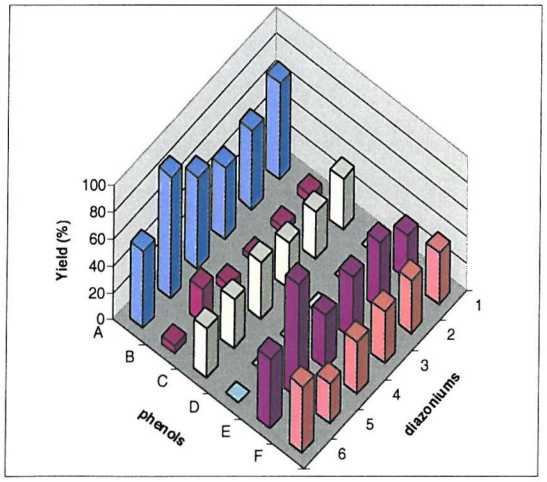

*Graph 2.2: Yield of Dyes **116/a1-f6**.*

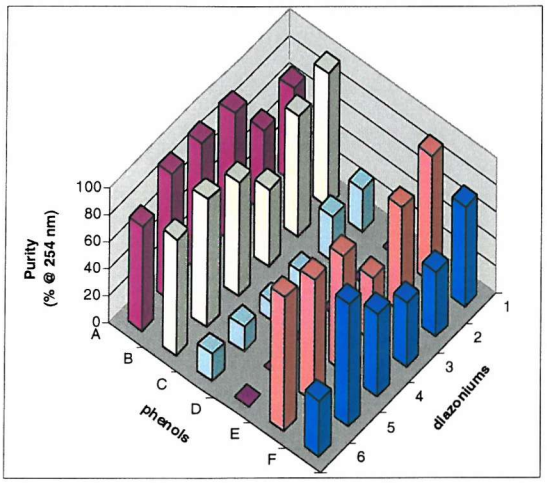

*Graph 2.3: Purity of dyes **116/a1-f6**.*

From Graph 2.2, it was observed that dyes containing the same phenolic component had similar yields, suggesting that the diazonium coupling reaction had a greater effect on the overall yield than the generation and stability of the supported diazonium salts. The yields originating from each supported diazonium salt varied from relatively high, when coupled to phenol **115/a** or **115/e**, to very low when coupled with phenol **115/b** or **115/d**. In the case of phenol **115/d**, no product was formed, because 4-nitrophenoate was unreactive towards diazonium electrophiles due to the delocalisation of the phenolate.

However, the distribution in yields for the remaining dyes could not be explained simply by the reactivity of the phenolic or diazonium salt components. Graph 2.3 shows that the reactions involving **115/b** resulted in products of high purity, suggesting a high level of conversion. However, Graph 2.2 shows that yields of the same reactions resulted in very low isolated yield. This suggested that the low yields observed were due in part to retention of the dye product inside the matrix. If the dye product was insoluble in the reaction solvent, it could precipitate and remain in the resin. Removal of precipated dye would have been possible by washing the resin with organic solvents, such as MeOH, but this would have also co-eluted the diazonium decomposition product, reducing the purity of the dye.

2.6 Conclusions

The immobilisation of the diazonium salts onto Amberlyst A-15 resin provided a powerful tool for the storage and handling of these reactive species. Treatment of the supported reagent with nucleophilic coupling agents allowed the rapid synthesis of azo-dye products in variable yield and purity. The rate of decomposition of the supported species at pH 9 required an excess of reagent to be used. This technique would probably be better suited to a synthetic approach where the nucleophilic coupling step was performed at lower pH, so that more of the supported reagent would be available for reaction with the nucleophile.

Chapter 3: Microwave-Assisted Convergent Azo-Dye Synthesis

3.1 Introduction

3.1.1 Microwave-Assisted Synthesis

When samples of water and chloroform are exposed to the same levels of microwave radiation, water increases in temperature at a much faster rate. To understand why this happens, it is necessary to examine the various methods of microwave heating.[142-144] When molecules in solution possessing a permanent dipole are placed in an electro-magnetic field they try to align themselves with the rapidly changing electric field component (Figure 3.1). If the frequency of the EM field is low (e.g. radio waves) the molecules will rotate in phase with the field. Although this results in a small energy gain by the molecules, the overall heating effect is small. If the frequency of the field is high (e.g. infra-red), the molecules do not have sufficient time to respond to the changing field, and do not rotate. As no energy is induced to the molecule heating does not occur.

If the field frequency is between these two extremes, such as is the case with microwave radiation, a third effect can be observed. The molecules interact with the electric field and try to align themselves but will always lag slightly out of phase due to friction with the adjacent molecules. This results in a lost of energy, which manifests itself as a heating effect called the *dipolar microwave* heating.

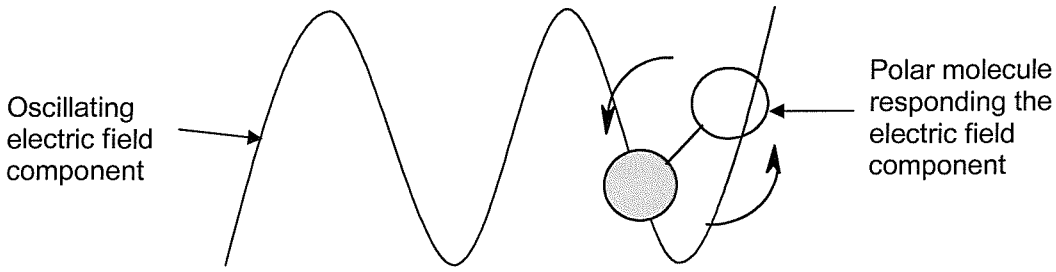

Figure 3.1: Molecules responding to microwave irradiation.

Materials possessing no permanent dipole, such as toluene or diethyl ether, do not oscillate, and are therefore described as microwave-inactive. Materials such as water, ethanol and DMF which have a relatively high permanent dipole all heat rapidly.[142-144]

A second method whereby materials in a microwave field can increase in temperature is known as *conduction microwave* heating. This occurs when solvated ions are placed in an electric field and move under its influence increasing the kinetic energy of the particles. This in turn results in an increased collision rate between ions and solvent converting kinetic energy into heat, which increases the temperature of the solution (Figure 3.2).

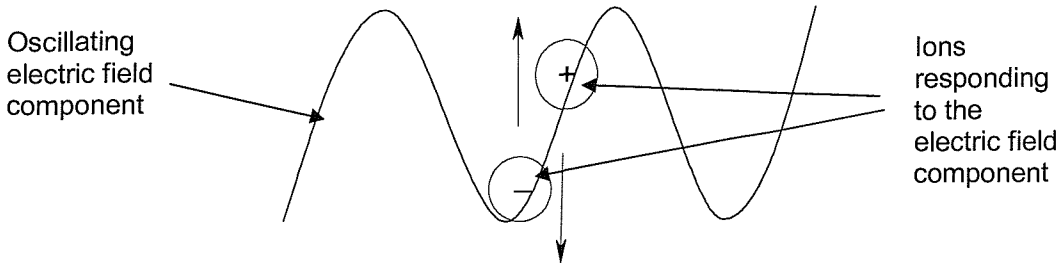

Figure 3.2: Ions responding to microwave irradiation.

This method of energy absorption is far more efficient than the dipolar mechanism, due to the interaction between a full charge and the field rather than a partial dipole charge.[142-144] So, is the behaviour of an organic solvent in a microwave field simply the result of its polarity? Unfortunately, this is not the case, as is demonstrated with acetone and ethanol. These two solvents have similar dielectric constants (i.e. dipoles), but when placed in the same microwave electromagnetic field ethanol will heat up at a much faster rate. This is due to another physical parameter, the 'loss tangent', tan δ, which is a measure of the ability of a solvent to be heated under microwave irradiation:

$$\tan \delta = \varepsilon'' / \varepsilon' \qquad \text{Eq. 4.1}$$

where ε'' is the loss factor, which is proportional to the efficiency by which the absorbed microwave energy can be converted in to heat, and ε' is the relative permittivity, proportional to the dielectric constant, which represents the ability of the material to absorb and store electrical potential energy while in an electric field.

Table 3.1: Loss tangents and dielectric constants for common solvents.

Solvent	**Dielectric constant (ϵ_s)** [a]	**Tan δ (@ 2.45 GHz)**
Acetone	21	0.054
Acetonitrile	38	0.062
Chloroform	4.8	0.091
Water	80	0.12
Dimethyl formamide	37	0.16
Dimethyl sulphoxide	47	0.82
Ethanol	24	0.94

a) The dielectric constant, ϵ_s, is the ratio of the permittivity of the material to the permittivity of free space, 8.85 x 10^{-12} farads / m.

As can be seen in Table 3.1, the tan δ of acetone and ethanol are very different, explaining the differing heating rates.[145]

Microwave radiation has been used in food preparation for over 50 years, but it was not until the 1970's that microwave heating was used for synthetic chemistry. Initial work undertaken in the late 1970s to mid-1980s was performed in domestic microwave ovens.[147-148] Domestic microwaves are known as multimode reactors, because there is an uneven distribution of microwave field inside the reactor creating hot-spots in certain regions (Figure 3.3a). During the preparation of food this heterogeneous character is not really a problem, especially since the food can be rotated inside the cavity to average out any difference in field strength. However, when this equipment is put to scientific use the unpredictable fields results in poor reproducibility. Heating in domestic microwaves also does not allow the reactor temperature or pressure to be monitored, making the use of flammable solvents and sealed vessels a hazardous endeavour.

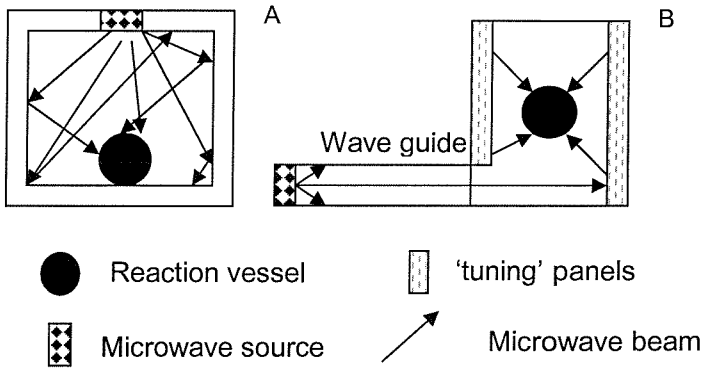

Figure 3.3: Schematics of microwave reactors; a) multi-mode; b) mono-mode.

Recent advances in microwave reactor design have allowed the construction of microwave cavities which allow homogenous and reproducible field strength within the reactor (Figure 3.3b).[148] This can be achieved by 'tuning' the reactor with movable microwave reflectors until a uniform field is obtained. This tuning is performed while the reaction vessel, solvent and reagents are in the field, so that their interaction with the field is taken into account. The latest 'mono-mode' reactors also allow accurate measurement of the temperature and pressure of the reaction vessel, resulting in a more reproducible and safe experimental system.

Reactions can also be performed in sealed vessels, which allow temperatures well above a solvent's boiling point to be reached. Microwave-assisted chemistry has been used to accelerate a wide variety of reactions.[144]

3.1.2 Solid-Phase Extraction.

One of the main attractions of solid-phase chemistry is the rapid separation of supported product from excess reagents by filtration and washing.

Combinatorial solution-phase synthesis has gained popularity partly due to its simplicity and ease of reaction monitoring. However, a serious drawback is that purification of large solution libraries is very time consuming. Consequently, many techniques have been developed to minimise time spent on this process, including the use of scavenger resins,[129-130] polymer supported reagents,[124] liquid-liquid extraction,[149] and solid-phase extraction (SPE).

SPE is similar to traditional flash chromatography, but the mobile and stationary phase are optimised so that the retention factors of the components to be separated are at opposite ends of the spectrum.[150] The component with the higher retention factor will be eluted rapidly, while the other component will be held on the stationary phase. SPE can be used in two ways; either the desired product can be extracted onto the resin, and eluted using a second solvent, or the excess reagents can be extracted onto the resin and the desired product eluted directly (Scheme 3.1).

Stationary phases can be categorised into 4 main groups; ion-exchange, normal-phase, reverse-phase and fluorous phase.Ion-exchange SPE is the most widely used, as many combinatorial transformations involve the modification of apolar scaffolds with highly polar reagents, such as acids or bases. The separation of the desired product can therefore be achieved by passing it through cationic, anionic or mixed bed (a mixture of cationic and anionic) ion-exchange media.

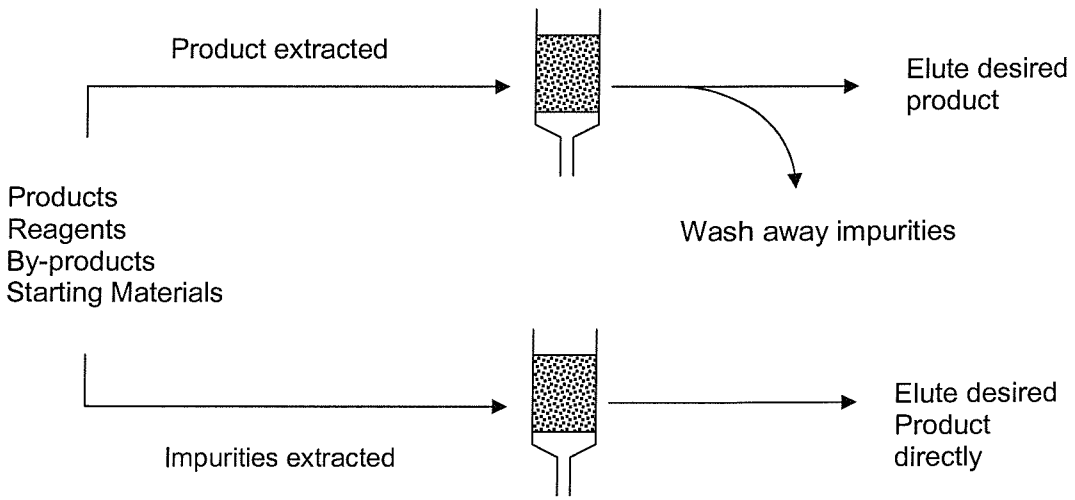

Scheme 3.1: SPE methodologies.

Boger and co-workers demonstrated this with the purification of biaryl **118** after a Pd-C catalysed coupling.[151] TEA and HI were removed by successive treatment of the

reaction mixture through strongly acidic Dowex 50W-X8-200, and strongly basic Amberlite IRA-400, to yield biaryls in 70 to 95% yields (Scheme 3.2).

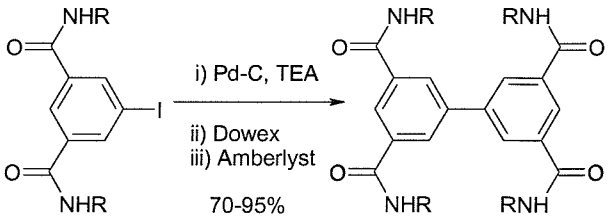

117 118

Scheme 3.2: Bogers biaryl synthesis using SPE.

Normal-phase SPE, typically using SiO_2, is similar to conventional silica flash chromatography. However, the solvent is chosen to immobilise either the desired product or reagents on the polar stationary phase. Since a short column length is used, the retention factor of the retained product must be very low to minimise premature elution. This technique was applied by Nilsson for the separation of *N*-alkylated amino-acid **119** from carbohydrate derived alcohol **120**.[152] The alcohol was eluted with DCM/MeOH (9:1) and desired product **119** removed with DCM/MeOH/water (65:35:5) in 31 to 99% yield and >90% purity (Scheme 3.3).

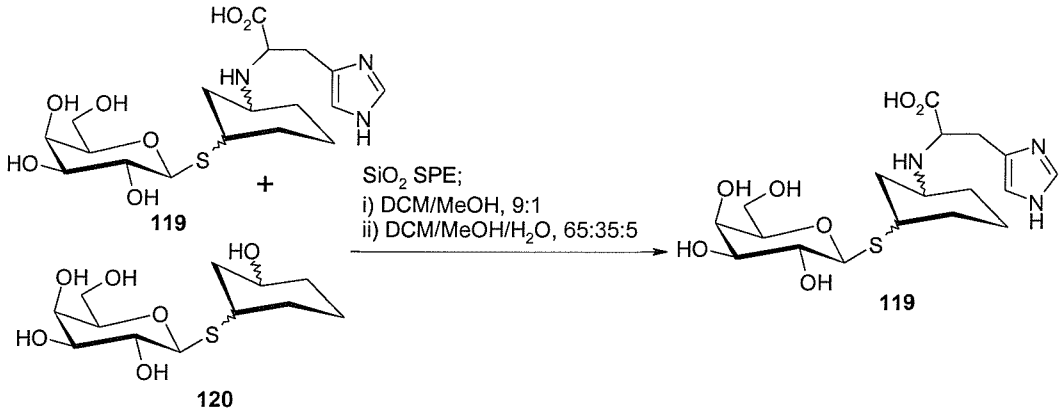

Scheme 3.3: Nilsson's purification of N-alkylated amino acids using SPE.

Reverse-phase SPE is used less, as strong affinity for hydrophobic media is rarely a property of common reagents and scaffolds.[153] However, the hydrophobicity can be introduced to the scaffold by the use of hydrophobic tags.

An example of this is the work of Hindsgaul and co-workers, who attached an *p*-methoxyphenyloctyl tag to a disaccharide acceptor.[154] The tagged acceptor was reacted with an excess of a disaccharide donor, and subsequent purification by RP-SPE yielded

the tagged trisaccharide in high yield. The aromatic ring incorporated into the tag also allowed the polysaccharides to be observed by RP-HPLC using UV/vis detection.

The final category of SPE media is the fluorous phase. In a similar manner to fluorous-liquid/liquid extraction,[155] this technique allows the retention of fluorinated species on to a fluorous SPE media. This technique was used by Curran and co-workers during the synthesis of allyl alcohol **122** with fluorinated allylstannane **121**.[156] This reagent was prepared by the reaction of allyl magnesium bromide with tris[2-(perfluorohexyl)ethyl] tin bromide and was used to allylate a series of aldehydes (Scheme 3.4).

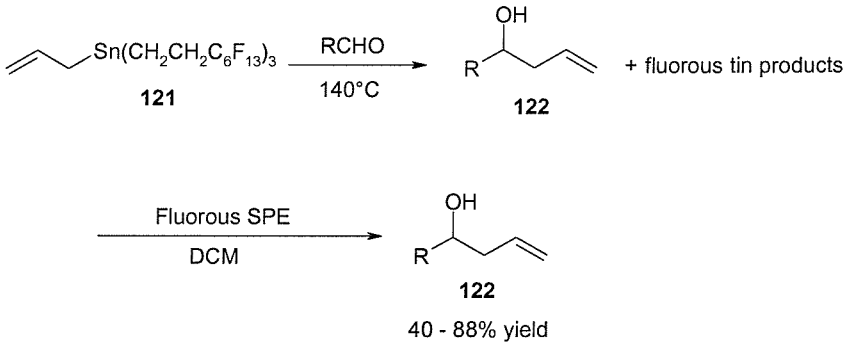

Scheme 3.4: Curran's synthesis of allylic alcohols using fluorous-tagged reagents.

The reaction mixture was then passed through a fluorous SPE column, to yield allylic alcohol **122** in 40 to 88% yield and 76 to 99% purity, without contamination with fluorous by-products.

3.2 Objectives of Research

During this chapter the convergent synthesis of azo-dye **125** was attempted by the substitution of disubstituted monochloro-triazine **124** with azo-dye **125** (Scheme 3.5).

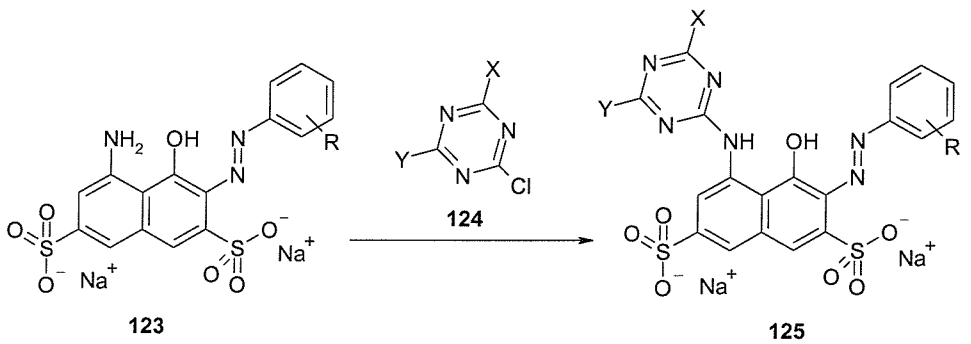

*Scheme 3.5: Synthesis of azo-dye **125** via a convergent synthesis.*

A convergent synthesis of these species would reduce the number of steps involving sulphonated species, hence minimising time spent on their time-consuming purification. The substitution of monochloro-triazines with primary amines is normally

performed at high temperature and high pH.[157] In order to achieve substitution with poor nucleophiles, extreme temperatures would be required. It was hoped that the high temperatures would be achieved through microwave heating to enable this reaction to proceed.[158-159] During this synthesis, the purification of azo-dyes was achieved using reverse-phase solid-phase extraction (RP-SPE).

3.3 Synthesis of H-acid Derived Dyes

During sections 2.3 and 2.4 the generation and use of polymer supported diazonium salts was investigated. During this chapter the technique was applied to the synthesis dyes **123/1-8** (Scheme 3.6).

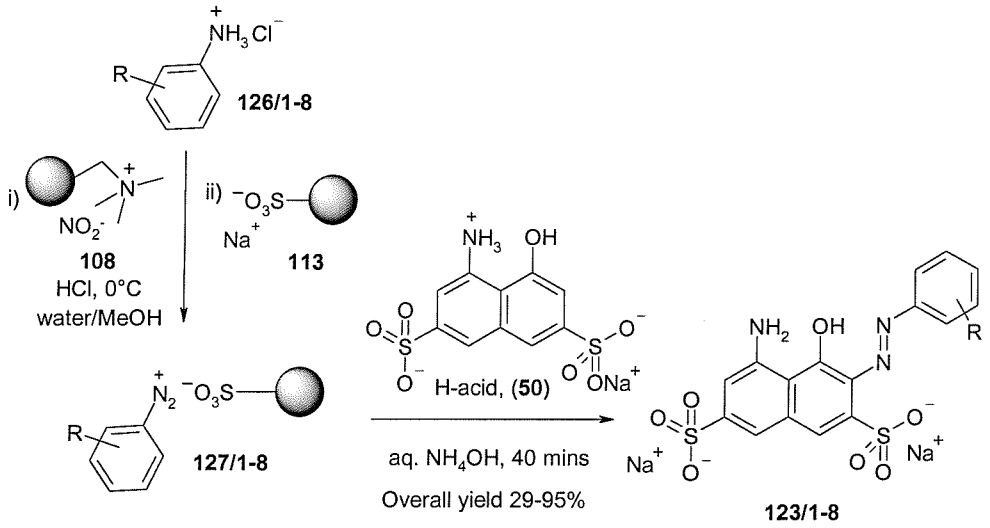

*Scheme 3.6: Synthesis of dyes **123/1-8** using support diazonium salts: For definition of R-groups, see Table 3.2.*

The diazotisation reaction was optimised using aniline (**126/8**) as it should display a representative reactivity towards nitrosation and diazonium salt stability. 95 mmol of aniline required for the reaction dissolved into concentrated aqueous HCl. At this concentration (12 M, pH -1) the nitrosating agent was nitrosyl chloride (**28**), the most reactive form, and the diazotisation reaction should be complete within minutes. However, this approach was later modified, as the substituted anilines (**126/1-7**) proved to be less soluble in this solvent, resulting in slow reaction and precipitation of the diazotisation salts. A mixture of concentrated aqueous HCl in methanol allowed complete dissolution of the reagents and intermediates. However, the drop in acid concentration from 12 M to 1 M (pH -1 to 0) altered the equilibrium towards the less reactive nitrous acidium ion (**26**) as the major nitrosating agent, and longer reaction times were required to fully convert the anilines.

After the reaction was complete, the mixture was filtered and the filtrate was passed through approximately 0.5 equivalents of Amberlyst A-15 resin. It was observed that if A-15 (sodium form) (**113**) was used, higher yields of dyes **123/1-8** were obtained compared to when using the H^+ form.

The yields of dyes **123/1-8** (Table 3.2) were dependant on several factors. As the reaction was performed in a highly basic solution, the reaction timescale was limited by the time it took for the diazonium salt to completely decompose. During the reaction the diazonium salt also reacted with H-acid (**50**) to form dye **123/1-8**. The final yield therefore was largely proportional to the ratio of the rates of the decomposition and coupling reactions. This can be seen from the reactions between halo-benzene diazonium salts and H-acid. The more reactive fluoro- and chloro-derivatives gave a moderate yield (68%) but the less reactive iodo-derivative gave a poor yield of 32%. Although it was possible that the yield of the iodo-derivative could be increased with a longer reaction time, after 40 minutes the amount of diazonium salt remaining would be negligible.

*Table 3.2: Yields and purities of dyes **123/1-8**.*

Dye	Aniline 126 used	Yield	Purity [a]
123/1	6-Ethyl-2-methylaniline	29%	95%
123/2	4-Iodoaniline	32%	95%
123/3	4-Bromoaniline	64%	87%
123/4	4-Chloroaniline	68%	75%
123/5	4-^{t}Butylaniline	64%	95%
123/6	2-Fluoroaniline	68%	40%
123/7	2,4,6-Trimethylaniline	95%	90%
123/8	Aniline	95%	88%

a) HPLC @ 254 nm, after C-18 purification.

The yields from the alkylbenzene diazonium salts were more varied than expected. The electron donation into the aromatic ring should result in reduced reactivity towards nucleophiles. However, the yields of **123/7** and **123/8** were the same (95%), suggesting that the inductive effect from the methyl groups did not affect the diazonium salt reactivity. However, not all the alkylbenzene diazonium salts achieved such good yields. The 6-ethyl-2-methyl- derivative (**123/1**) was only isolated in poor yield (29%), and the 4-^{t}butyl-derivative (**123/5)** was isolated in moderate yield (64%). This variety of yields suggests that the isolated yield was less dependent on the reaction kinetics, and more on other factors. It was possible that the lower yields were due to the low solubility of the diazonium salt during its formation in the MeOH/HCl mixture, resulting in its filtration and

hence a low diazonium salt loading on the A-15 resin. Also possible would be the poor solubility of the dye in the reaction solvent resulting in precipitation of the dye within the polymer support.

The crude purity of the dyes ranged between 22% and 95%. In order to obtain these dyes in pure form, chromatography was required. However, neither silica nor alumina stationary phase was suitable for their purification, as they were too polar. Alternative methods of purification tried were dialysis[160] and reverse osmosis,[161] but investigation into their use showed them to be inefficient at purifying species of such low molecular weight and generally unsuitable for parallel purification.

An alternative solution to the purification of the dyes was the use of reverse-phase solid-phase extraction, which allowed such separations in a rapid time and solvent efficient manner. The columns used in this chapter were Supelco's Supelclean C-18 cartridges, which contained silica functionalised with octadecyl (C-18) alkyl chains, so that 10% of the stationary phase was carbon. The remaining unfunctionalised sites were then acetylated to ensure the polar nature of the silica support particle was totally suppressed and to stop dissolution of the silica into aqueous phase. The columns were attached to a 6-channel solvent pump, which allowed rapid parallel purification (Scheme 3.7).

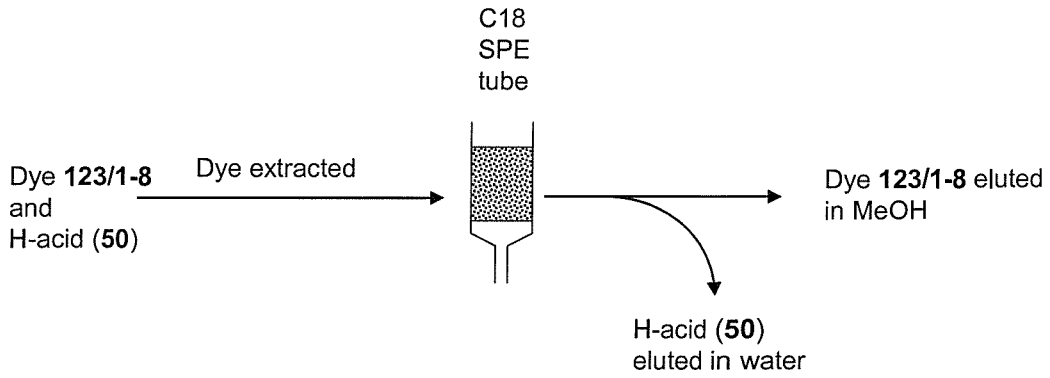

*Scheme 3.7: Purification of dye **123/1-8** with RP-SPE.*

When a mixture of dye **123/1-8** and residual H-acid (**50**) was passed through the column eluting water, the H-acid displayed no affinity for the stationary phase. Dye **123/1-8** remained bound on the column until eluted with MeOH. This method was used to purify dyes **123/1-8** and resulted in high purity in all cases except **123/6** where a second component was observed to co-elute.

NMR assignments of these dyes was achieved by H-H, C-H and long range C-H coupling experiments. Due to the almost uninterrupted conjugation of the molecule, small structural alteration resulted in variation in chemical shifts in the dye series. The ^{13}C-NMR

spectra were difficult to assign with certainty, due to the close proximity of the quaternary carbon signals. Meta-related coupling of ~2 Hz between protons 6 and 8 were observed in many cases (Figure 3.4). This allowed unambiguous assignment of the remaining proton at the 1 position.

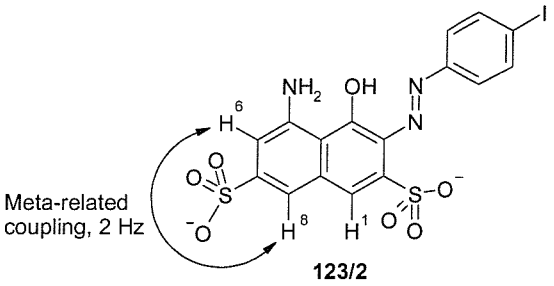

Figure 3.4: Meta-related coupling between protons 6 and 8.

3.4 Parallel Monochloro-Triazine Synthesis

Monochloro-triazines (**124/aa-ee**) were synthesised by the sequential substitution of cyanuric chloride by amines (Scheme 3.8).

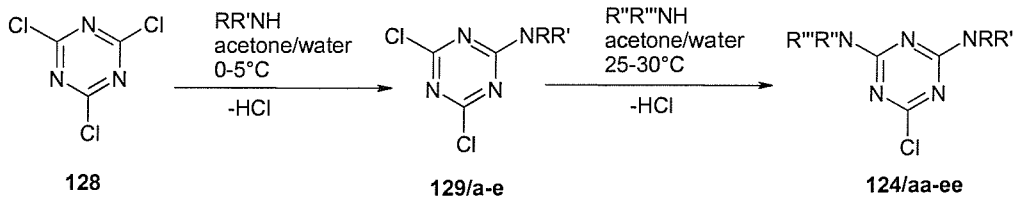

128 **129/a-e** **124/aa-ee**

Scheme 4.8: Nucleophilic substitution of cyanuric chloride: For definition of alkylamino substituents see Table 3.3.

*Table 3.3: Aminoalkyl groups incorporated into monochloro triazines **124/aa-ee**.*

Code	Aminoalkyl group	Structure
a	benylamino	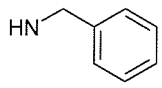
b	cyclohexylamino	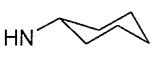
c	*N,N*-dibutylamino	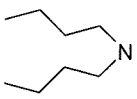
d	ethanolamino	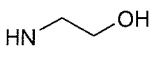
e	furfurylamino	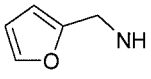

In order to ensure that significant over-substitution did not occur, the reaction temperature did not exceed 5°C for the first substitution or 30°C for the second. In order to allow rapid multiple parallel synthesis of the monochloro-triazines, it was desirable that no column chromatography or liquid-liquid extraction should be required.

In order to achieve this, during the reaction cyanuric chloride (**128**) and dichloro-triazine intermediates (**129/a-e**) were precipitated before respective amine addition, followed by reaction mixture filtration and washing with water to remove excess amine. Cyanuric chloride is often used as a suspended reagent whist still demonstrating excellent reactivity.[162-163]

To generate a finely-divided and therefore highly reactive suspension, cyanuric chloride (**128**) was first dissolved in acetone and added dropwise to water, cooled in ice. The addition of two equivalents of amine yielded the dichloro-triazine, **129/a-e**. The second equivalent was required to neutralise the acid generated during substitution, allowing the reaction to proceed to completion. The reaction mixture was then filtered and the **129/a-e** was washed with ice-cold water to remove remaining amine. The intermediate was then redissolved in acetone, re-precipitated with the addition of water and converted to the monochloro-triazine products **124/aa-ee** by the addition of a further two equivalents of amine. The product was then recovered by filtration. Although this method was suitable for the synthesis of one triazine, parallel small-scale filtrations resulted in significant loss of material, especially when dealing with intermediates which were oils.

A second approach was investigated, which involved reactions in centrifuge tubes attached to an orbital shaker. Once the reaction was complete, the sample was centrifuged to compact the product in the base of the tube. The excess amine could be removed by decantation, addition of further water, shaking, centrifugation and decantation. This approach allowed the process to be undertaken in a parallel manner (Scheme 3.9).

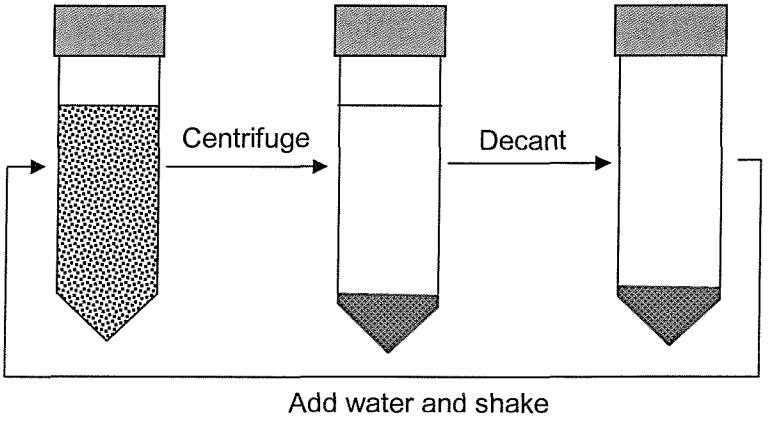

Scheme 3.9: Purification of triazine suspension by centrifugation/decantation.

Qualitative ninhydrin tests demonstrated the efficient removal of excess primary amines from the triazine.

The yields of monochloro-triazines **124/aa-ee** varied, as the low density of certain materials resulted in inefficient separation by centrifugation. The purity of the monochloro-triazine product also varied, as symmetrical disubstituted products were also formed. These impurities were generally low in quantity, except where highly nucleophilic amines were used in the first step. Because of this, monochloro-triazines **124/aa-ee** were synthesised in such a way as to substitute with the least nucleophilic element first, and the more nucleophilic element second.

The symmetrical monochloro-triazines **124/aa**, **124/bb**, **124/cc** etc. were made by the addition of 4 equivalents of amine to a cyanuric chloride suspension at room temperature. The product was then purified by centrifugation/decantation to give the monochloro-triazines in high purity and moderate yield, as no trisubstituted-triazine was synthesised.

Benzylamino- and furfurylamine- dichloro-triazine intermediates were used when possible, due to their efficient purification by the centrifugation/decantation method. It proved convenient to synthesise two groups of monochloro-triazines according to these common substituents;

- **124/ab** to **124/ae**, where the benzylamino-dichloro-triazine intermediate was used,
- **124/be** to **124/de**, where the furfurylamino-dichloro-triazine intermediate was used.

The remaining monochloro-triazines proved to be inaccessible using this technique, because either the intermediate or disubstituted products were not dense enough to be separated by centrifugation. These were synthesised in a conventional manner and was purified using liquid-liquid extraction. The yields and purities of all monochloro-triazines are shown in Table 3.4.

*Table 3.4: Yields (purities) of monochloro-triazines **124/aa-ee**.*

	a [a]	**b**	**c**	**d**	**e**
a	68% (95% [b])	73% (69%)	67% (94%)	58% (84%)	56% (64%)
b		50% (93%)	77% (93%)	41% (95%)	73% (57%)
c			38% (95%)	51% (93%)	67% (94%)
d				95% (95%)	58% (78%)
e					63% (87%)

a) For alkylamino groups see Table 3.3: b) HPLC @ 254 nm.

3.4.1 Temperature NMR Study of Monochloro-Triazine

The NMR spectra of these compounds were complicated by multiple signals originating from rotomeric activity. This behaviour was investigated using ^{13}C-NMR temperature studies on **124/cc**.

When nitrogen atoms are located next to aromatic rings, the hybridisation of the bonding nitrogen orbitals is not pure sp^3. Instead, the substituents have more sp^2 character and the lone pair resides in an orbital with more *p*-character, as it can then delocalise with the aromatic π-system. This results in a more electron rich ring, slightly more in-plane nitrogen substituents and the low lone-pair nucleophilicity. Previous NMR [164-166] and X-ray [167] studies of monochloro[1,3,5]triazines showed that these molecules exhibit restricted rotation around the exocyclic C-N bonds (Scheme 3.10).

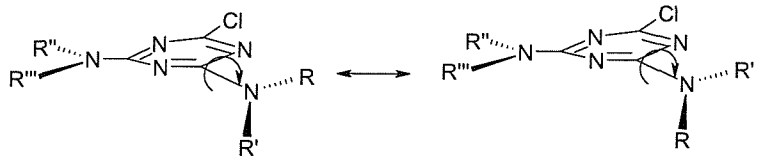

Scheme 3.10: monochloro-triazines display rotomeric behaviour.

Due to the stabilisation acquired while the nitrogen *p*-orbital is conjugated into the aromatic ring, these studies only reported the presence of planer species, where all nitrogen *p*-orbitals were aligned with the π-system.

The ^{13}C NMR spectrum of monochloro-triazine **124/cc** at 25°C, however, showed 3 signals of approximately equal integration for each carbon in the dialkylamino substituents, suggesting that in the case of **124/cc** the molecule can exist in either the in-plane/in-plane rotomer, or the out-of-plane/out-of-plane form (Figure 3.5).

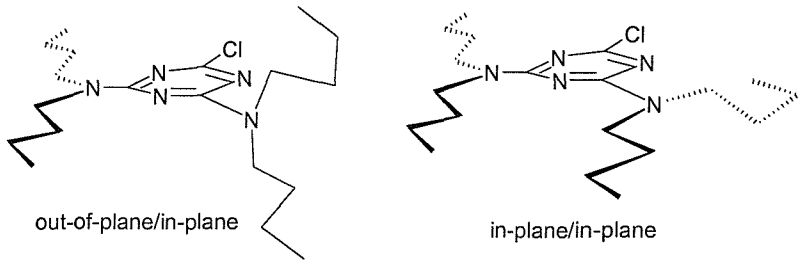

*Figure 3.5: The suggested conformation of **124/cc**, in two rotomeric conformations.*

However, a variable-temperature NMR study of monochloro-triazine **124/cc** showed that only two of the three signals converged when the temperature was raised, in

agreement with a previous study of this molecule (Figure 3.6).[168] This suggested that remaining signal could have originated from the dichloro-impurity **129/c**, detected in small quantities (5%) by LC/MS.

Reanalysis of compound **124/cc** by flame-detector gas-chromatography, a more reliable quantitative detection method, suggested the monochloro-triazine impurity was present at 16%, but this would not explain the approximate 1:1 molar ratio suggested by ^{13}C-NMR.

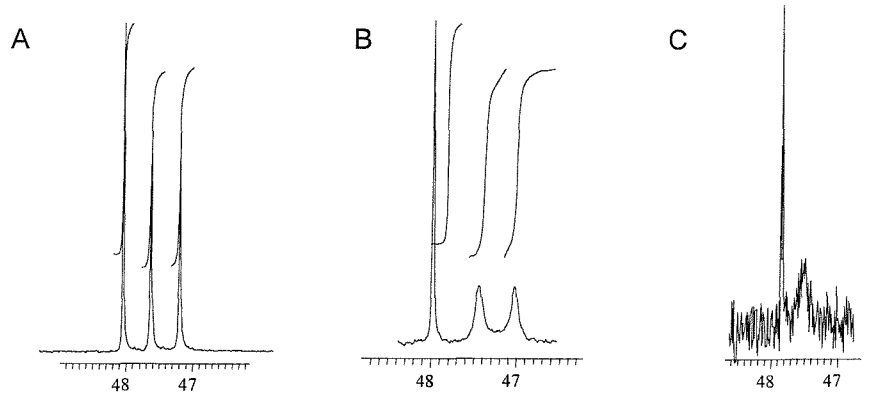

*Figure 3.6: ^{13}C NMR the α-carbon of **124/cc**, at 25.4°C (A), 50°C (B) and 80°C (C).*

Multiple signals were observed from most of the ^{1}H- and ^{13}C-NMR monochloro-triazines **124**, and subsequently the NMR spectra of dyes **125** also displayed complex multiplet signals for the triazine alkylamino-substitutents.

3.5 Microwave-Assisted Substitution of Monochloro-Triazines

Before synthesis of the dye **125** was attempted, the reaction of H-acid (**50**) and monochloro-triazine **124/bc** was undertaken (Scheme 3.11).

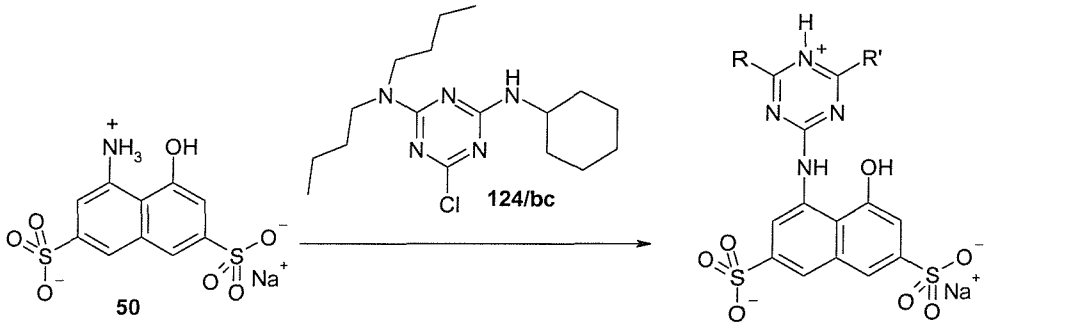

R = N(^{t}Bu)$_2$ · R = NH(cyclohexyl) **130/bc**
R = R' = NH **130/bb**

*Scheme 3.11: Proposed reaction of **50** and **124/bc**.*

This reaction was attempted in a variety of organic polar solvents, which could conceivably dissolve both reagents at high temperature without reacting with the monochloro-triazine (Table 3.5). After 600 seconds of irradiation, the reaction mixtures were analysed by HPLC to confirm reaction progress.

*Table 3.5: Crude purities of **130/bc** after reaction in a variety of solvents.*

Solvent	Temperature	Pressure (bar)	Time (s)	130/bc purity [a]
Dioxane	130°C	2.5	600	0
Acetonitrile	130°C	3.0	600	0
DMF	130°C	1.2	600	39
DMF	150°C	2	600	19
DMSO	130°C	1.0	600	59

a) HPLC @ 254 nm.

Of these solvents, reaction in acetonitrile and dioxane resulted in no product, where as reaction in DMSO and DMF yielded **130/bc**. When the reaction was performed in DMF, reactions at both 130°C and 150°C were performed. The results suggest that the increase in temperature resulted in degradation of the product, as a lower purity was observed. Reaction progress in dioxane and acetonitrile was hindered by the insolubility of H-acid. In an attempt to find more suitable solvents for this reaction, a mixture of water and acetonitrile was tried. The reaction of **50** and monochloro-triazine **124/bc** in a 3:1 mixture of water/acetonitrile resulted in consumption of the triazine in 10 minutes (Figure 3.7). An excess of **50** was used in this reaction in order to achieve complete consumption of the monochloro-triazine. If excess monochloro-triazine was used, the reaction did not progress to completion, resulting in a more complex purification process.

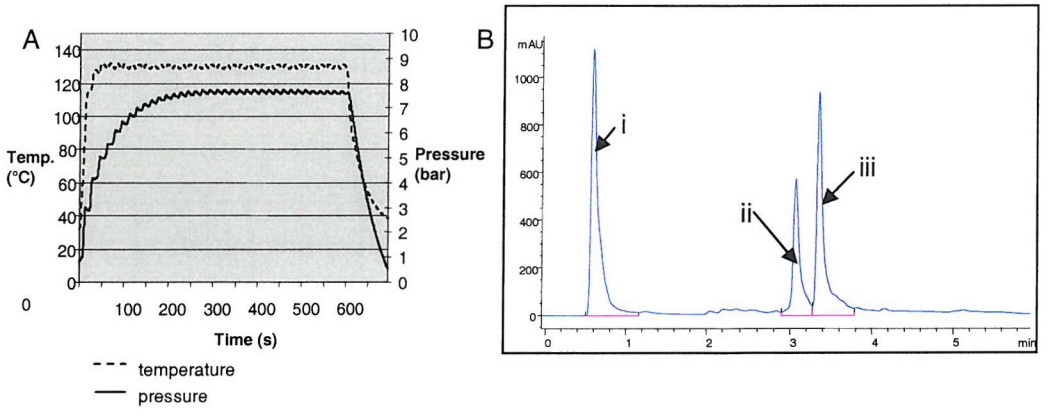

*Figure 3.7: a) temperature and pressure plotted vs. time for synthesis of **130/bc**; b) HPLC of reaction mixture {i = **50**, ii = **130/bb**, iii = **130/bc**}.*

The temperature vs. time graph (Figure 3.7a) showed that the reaction mixture was a strong absorber of microwave radiation. In approximately 40 seconds the reaction had reached the desired temperature, and was retained there using only limited power. This rate of temperature increase was faster than with pure water, suggesting that the ionic nature of the reagent increased the adsorption of the radiation by the conduction mechanism.

The HPLC of the crude reaction mixture (Figure 3.7b) showed excess **50** (0.59 minutes) and two new products peaks (3.06 and 3.35 minutes). LC-MS of the mixture suggested that they corresponded to two different derivatives of **130**; **130/bb** and **130/bc**. The synthesis of **130/bb** as a by-product was possible, as the precursor monochloro-triazine **124/bb** was present in small quantities (7%, HPLC @ 245 nm) as a by-product of the synthesis of **124/bc**. However, this does not explain the 37% impurity of **130/bb**.

Separation of **130/bc** from residual **50** was efficient using RP-SPE. However, purification of **130/bc** from its symmetrical impurity, **130/bb**, proved to be impractical *via* RP-SPE. This was not surprising, since SPE relies on large differences in component-affinity to the stationary phase. These two species should have also most identical affinities, and were therefore inseparable by this technique.

In an attempt to synthesise a single derivative of **130**, the reaction between **50** and **124/cc** was attempted, using identical conditions to the previous reaction. As this monochloro-triazine was symmetrical, no minor unsymmetrical monochloro-triazine impurities were present and hence no side-reactions could occur. However, despite increasing the reaction time and temperature, this reaction did not yield **130/cc**. This result came as a surprise, as this triazine should have had very similar activity towards the nucleophile as **124/bc**.

3.6 Microwave-Assisted Synthesis of Azo-Dyes

After the variable results in section 3.5, similar reactions were performed using dyes **123/1-8** (Scheme 3.12).

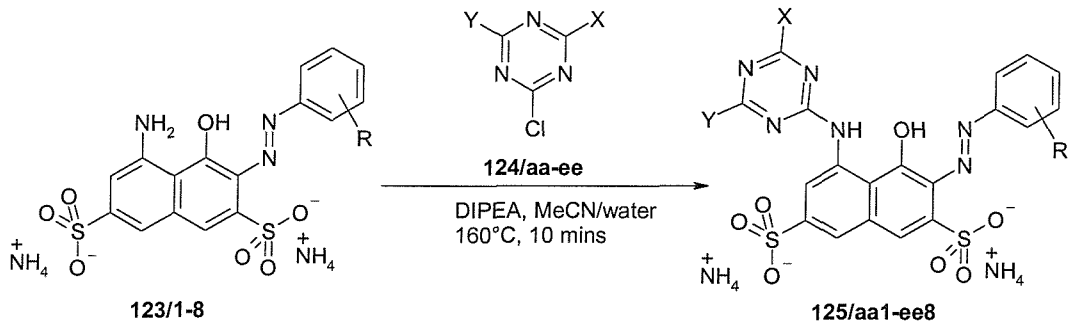

*Scheme 3.12: Reaction between **123/1-8** and monochloro-triazines **124/aa-ee**.*

As the primary amine *p*-orbital was spread over a larger delocalised system, dyes **123/1-8** should be less nucleophilic than H-acid and hence higher temperatures were used to ensure successful substitution.

Initially, this reaction was attempted using monochloro-triazine **124/bc** and dye **123/8** in MeCN/water. From the outset this reaction was performed at 160°C, twice the boiling point of acetonitrile, which gave a reactor-pressure of 11 bar. Although this pressure did not approach the pressure-limit for the equipment, during these experiments reactor venting did occur and hence no higher temperatures were applied.

Reactions involving these two species were at first unsuccessful despite increasing the reaction times. After speculation at this difference in reactivity between H-acid and its derived dyes, it was hypothesised that the ammonium counter ion could have caused a side reaction with the monochloro-triazine, causing its conversion to the unreactive tri-substituted product, **131** (Scheme 3.13).

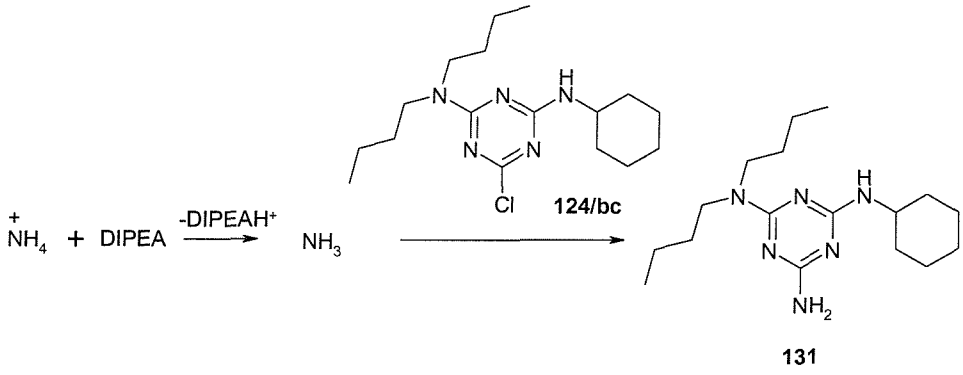

*Scheme 3.13: Proposed side-reaction between ammonia and **124/bc**.*

In an attempt to halt this side-reaction, dye **123/8** was passed through A-15 (Na^+ form) resin (**113**) to exchange the ammonium ions with sodium. The dye solution was then reacted with **124/bc** in MeCN/water at 160°C for 10 minutes to give dye **125/bc8** in 51% yield and 70% purity.

The production of the symmetrical by-product **125/bb8** was also observed by LC-MS (Figure 3.8b). SPE was highly effective at removing excess dye **123/8**, but ineffective at separating the two newly formed dyes **125/bb8** and **125/bc8**.

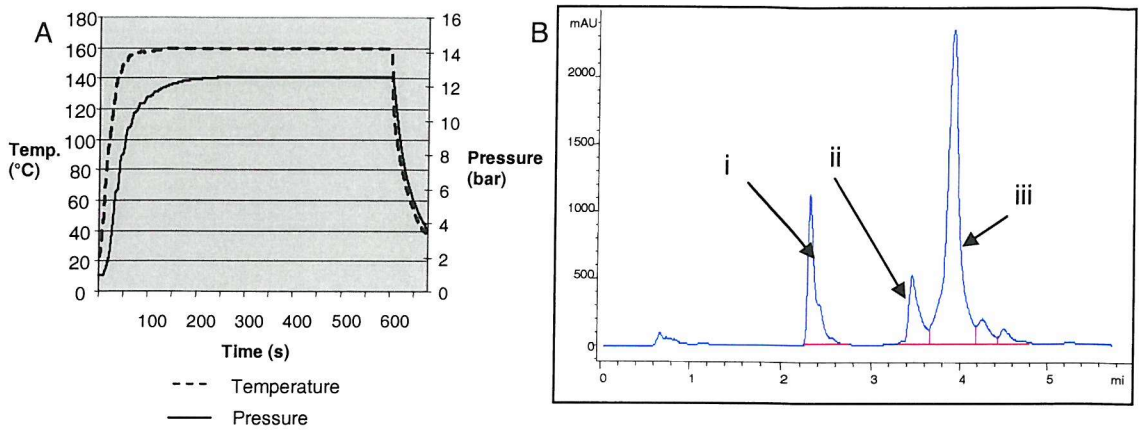

*Figure 3.8: a) Temperature and pressure plotted vs. time for synthesis of **125/bc8**: b) HPLC of reaction mixture (i = **123/8**, ii = **125/bb8**, iii = **125/bc8**).*

In view of this successful reaction, substitution of monochloro-triazine **124/bc** using dyes **123/1-3** was attempted, which gave the corresponding dyes **125/bc1-3** in variable yields (Table 3.6). RP-SPE purification of the reaction mixtures successfully removed excess dye **123/1-3** but proved ineffective at separating the desired product from the symmetrical by-products.

*Table 3.6: Yields and purities of dyes **125/bc1, bc2, bc3, bc8.***

Product	Yield (%)	Purity [a]
125/bc1	67	82
125/bc2	20	48
125/bc3	12	47
125/bc8	51	70

a) HPLC @ 254 nm.

After successful synthesis of these four dyes, it was necessary to expand this small array into a 96-member library, containing 8 azo-functionalities and 12 triazinyl-functionalities. The results of library synthesis should allow a greater understanding of the reaction. These reactions were performed in groups of 6, so that RP-SPE of the reaction mixtures could be carried out in parallel using a 6-channel solvent pump.

However, none of the 12 remaining attempted reactions performed yielded the desired product. It was possible that these reactions did not progress due to the low solubility of the monochloro-triazines in water/MeCN at 160°C. The reaction between **123/8** and triazines **124/be**, **ce**, **de** and **ee** was repeated in DMF, ensuring that all reagents were fully dissolved during the reaction. However, still no reaction progress was

observed. This suggested that the difference in reactivity between triazines was solely down to intermediate stability.

During the $S_n(AR)$ reaction between the monochloro-triazine **124** and an amine, an anionic intermediated **132** is formed (Scheme 3.14)

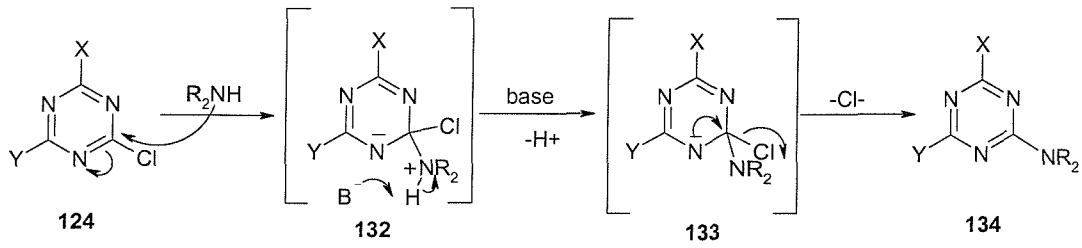

*Scheme 3.14: $S_n(AR)$ reaction involving amine and monochloro-triazine **124**; X = Y = aminoalkyl groups.*

Electron donation into the triazine ring from the aminoalkyl groups de-stabilises the anionic intermediate **132** resulting in a high activation barrier. This reaction therefore requires high temperatures to proceed. However, during the attempts to form dyes **125/aa1-ee8** it was observed that only monochloro-triazine **124/bc** successfully formed the final dye. The combination of electron donation from groups b and c should have resulted in **124/bc** being one of the most electron rich, and hence deactivated, monochloro-triazines used, and hence the results cannot be explained by this mechanism.

3.7 Conclusions

The application of polymer supported diazonium salts in the synthesis of dyes **123/1-8** only yielded pure dyes in a two cases. However, when used in conjunction with RP-SPE facile and rapid production of pure dyes was possible. Efficient synthesis of monochloro-triazines **124/aa-ee** was generally successful using parallel solution-phase chemistry, although non-crystalline derivatives were not accessible by this route.

The convergent synthesis of dyes **125/aa1-ee8** proved to be successful in only a few examples. In all successful examples, symmetrical triazine by-products were observed in significant proportions, which could not be separated by RP-SPE. To further understand the mechanism of this process it would be essential to achieve reaction with a wider range of monochloro-triazines to ascertain the important factors contributing to monochloro-triazine reactivity.

Chapter 4: Solid-Phase Azo-Dye Synthesis using the Marshall linker

4.1 Introduction

4.1.1 Dyes and the Solid-phase

Early uses of dye in combination with supported materials included photometric tests to ascertain the loading of specific chemical groups within the support. These tests can function in a qualitative[107] or quantitative[171] manner, involving generation of dyes directly on the support,[172] or into solution.[173,107] An example of a qualitative test where the dye remains within the bead is found in work by Taddai and co-workers.[174] Treatment of resin **136** with Malachite Green (**137**) in the presence of a base resulted in a green colouration in the presence of carboxy groups (Scheme 4.1).

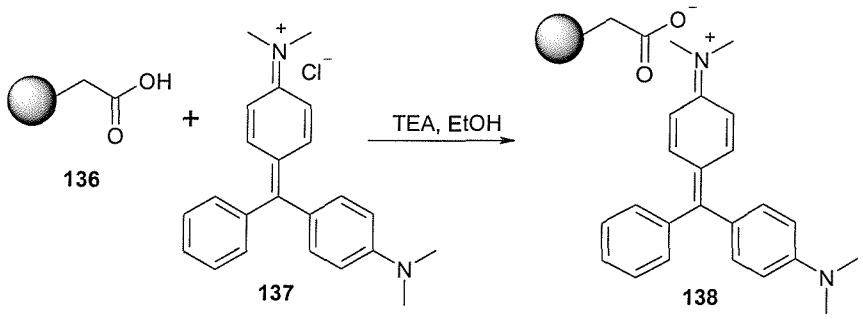

Scheme 4.1: Taddai's Malachite Green test.

The test was successfully used to detect the presence of as little as 1% carboxylic acid functionality on a range of aliphatic and aromatic carboxylic acids. More recently dyes have been used with resin beads to assay mixtures of large peptide libraries for activity. An example of this approach is the work of Kilburn and co-workers where a library of supported hosts with peptidic side-arms (**140**) was treated with a tri-peptide guest linked to Disperse Red Dye 1, **139** (Figure 4.1).[175]

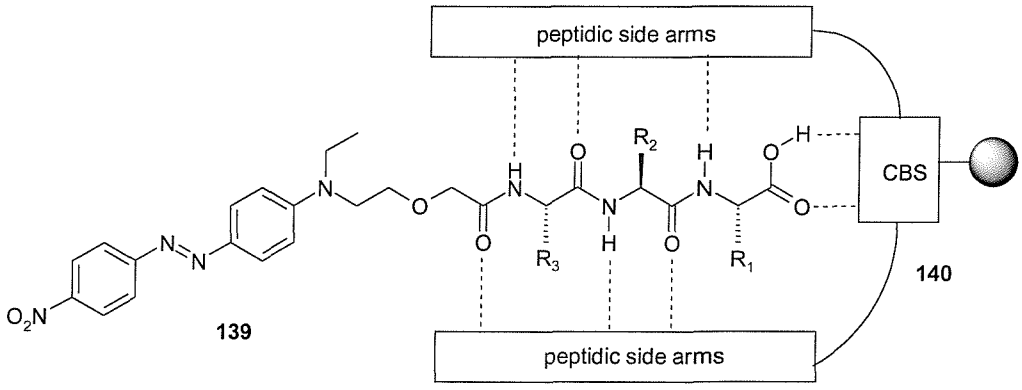

Figure 4.1: Peptidic host/guest dye based assay; CBS = carboxylic acid binding site.

Highly coloured beads were picked out, the guest dye/peptide removed and the unknown host peptide identified by Edman sequencing.[176]

Only recently have groups attempted to synthesise dyes in a combinatorial manner,[177] or on solid-phase,[128] but this approach has not yet been applied to the synthesis of azo-dyes. As an example, solid-phase methodology has been successfully applied by Balasubramanian and co-workers for the synthesis of cyanine dyes.[179] The group utilised supported sulphonyl chloride (**144**) as a tool for purifying and activating dye intermediate **143** (Scheme 4.2) which allowed the generation of a 3 x 3 array of varied cyanine dyes (**147**) in yields ranging from 0 to 79% with 0 to >95% purity.

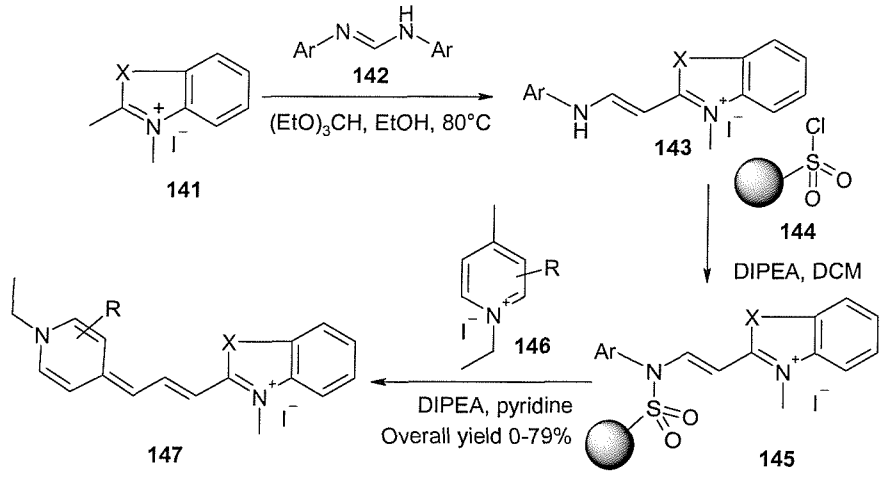

*Scheme 4.2: Cyanine dye synthesis, via supported intermediate **143**.*

4.1.2 Sulphur-based Safety-catch Linkers

The diversity of compounds synthesised on solid-phase is partly determined by the functional group through which they are bound to the resin (e.g. COOH, OH, NH_2). This point of attachment can become a part of the structure of the cleaved compound, and hence influence the properties of the material. This problem can be partly overcome by the use of 'traceless' linkers, so called because their point of attachment is not evident after cleavage.[180-181] An example of this are the sulphur based linkers,[182-184] an application of which was demonstrated by Suto and co-workers in 1997 (Scheme 4.3).[185]

During this example, this traceless-linker functioned in a safety-catch manner. A two-step procedure was required to release the tethered substrate; the first to activate the linker, and the second to release the compound into solution. The activation of resin **150** was achieved by oxidation of the thioether with *m*-CPBA to give the sulphone **151**. Treatment of the resin **151** with a variety of amines cleaved the compound into solution to give 6 pyrimidines (**152**) in 50 to 93% yield and 50 to 96% purity.

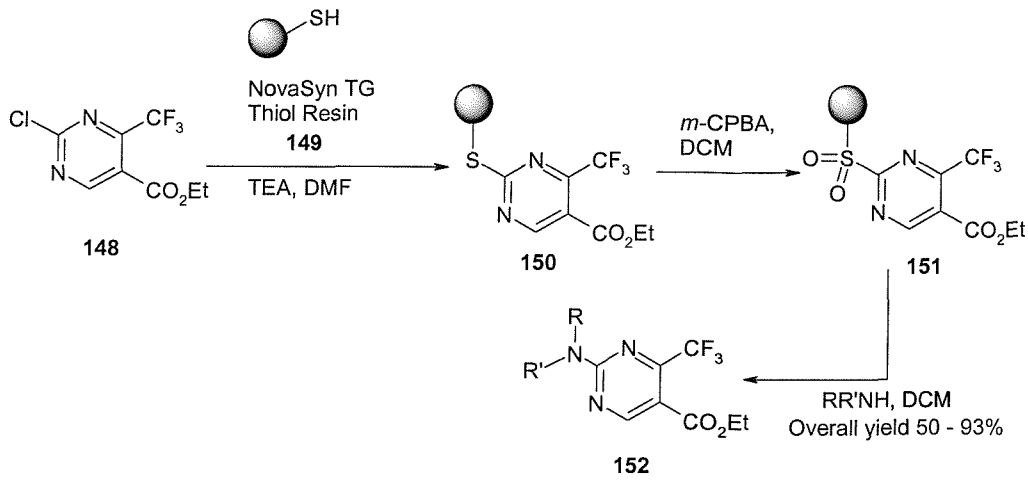

Scheme 4.3: Suto's pyrimidine synthesis using a safety-catch linker.

A similar sulphur-based linker was used previous to this by Marshall and Liener in 1970 for the synthesis of peptides.[186] An amino acid supported on resin by a 4-hydroxythiophenol linker (**153**) was treated with hydrogen peroxide in acetic acid, which oxidised the thioether to the sulphone (**154**). The resulting electron withdrawal activated the ester, and treatment with an amine released amino-acid **155** into solution in one step (Scheme 4.4).

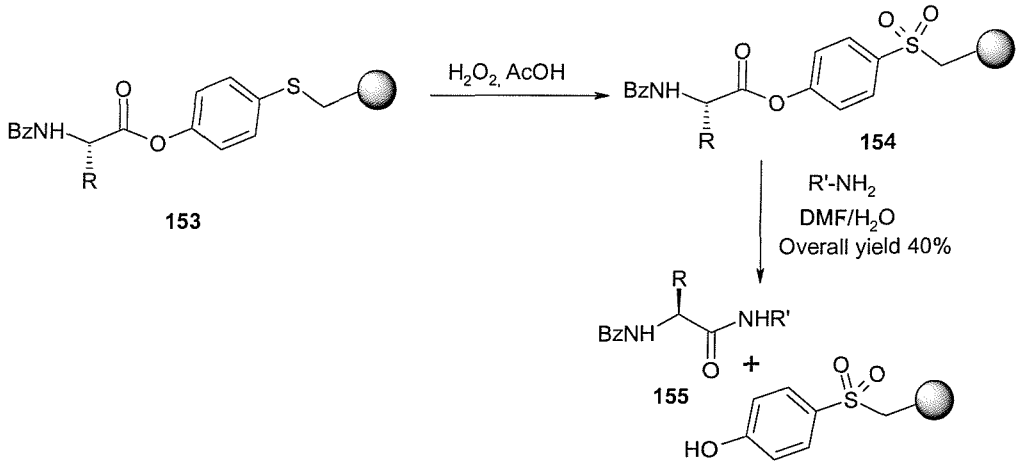

Scheme 4.4: Marshall's 4-hydroxythiophenol linker.

This linker has recently been applied to the synthesis of non-peptidic amides.[187] Dressman adapted the linker for the synthesis of unsymmetrical ureas,[188] while examples involving the cleavage of acids from the Marshall linker show that the oxidative 'activation' step is not always necessary to affect cleavage.[189-190]

4.2 Objectives of Research

The solid-phase synthesis of dye **125** could, theoretically, be achieved using a variety of points of attachments to immobilise the compound onto the resin (Figure 4.2).

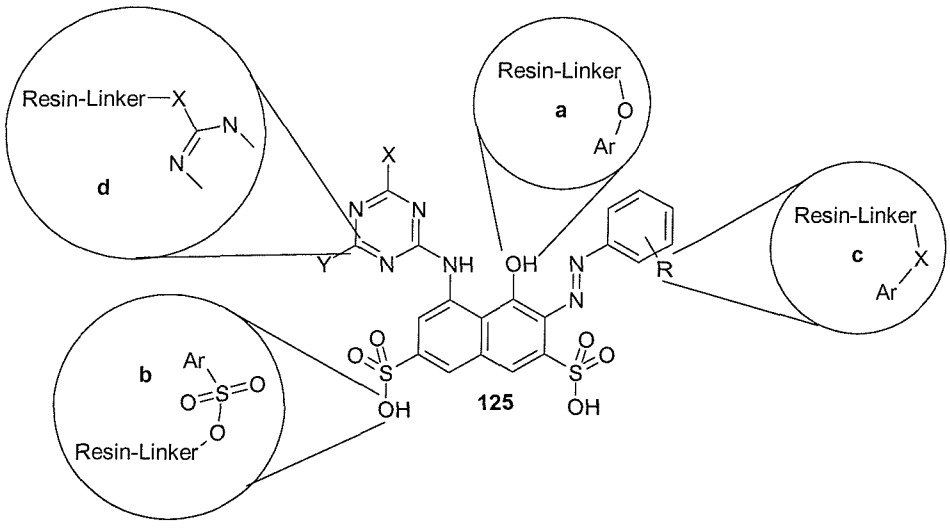

*Figure 4.2: Possible points of attachment for the solid-phase synthesis of dye **125**.*

The use of the phenol group as a handle (a) would slow diazonium coupling reactions at the naphthalene 3-position (no naphtholate ion). Attachment *via* esterification of an aryl sulphonic acid (b) would provide an unstable linkage at pH 9 – the conditions required for the diazonium coupling reaction. Attachment *via* the aryl-azo R-groups (c) is feasible, but would result in a reduction of possible diversity in the dye products as a defined point of attachment on the phenyl-azo ring would be required.

A forth option for the synthesis of dye **125** on the solid-phase was the use of the 4-hydroxythiophenol Marshall linker (d). This could be used to construct the dye through sequential substitution of immobilised triazine **156** (Scheme 4.5).[191]

Thioether oxidation of resin **158** to the sulphoxide would activate the linker to nucleophilic substitution. Potential problems lie in the presence of other functional groups, which could oxidise preferentially. Oxidation of nitrogen to the N-oxide could occur at the triazine- or azo-nitrogen atoms.[192] However, as the thioether is the most reactive site towards oxidation a less reactive oxidising agent, like H_2O_2, or only 1 equivalent of a faster oxidising agent could be used to selectively oxidise the thioether to the sulphoxide. Although the sulphoxide would not give as much electron withdrawal character as the sulphone, it should still allow ample activation to release the dye **124** on addition of a second amine.

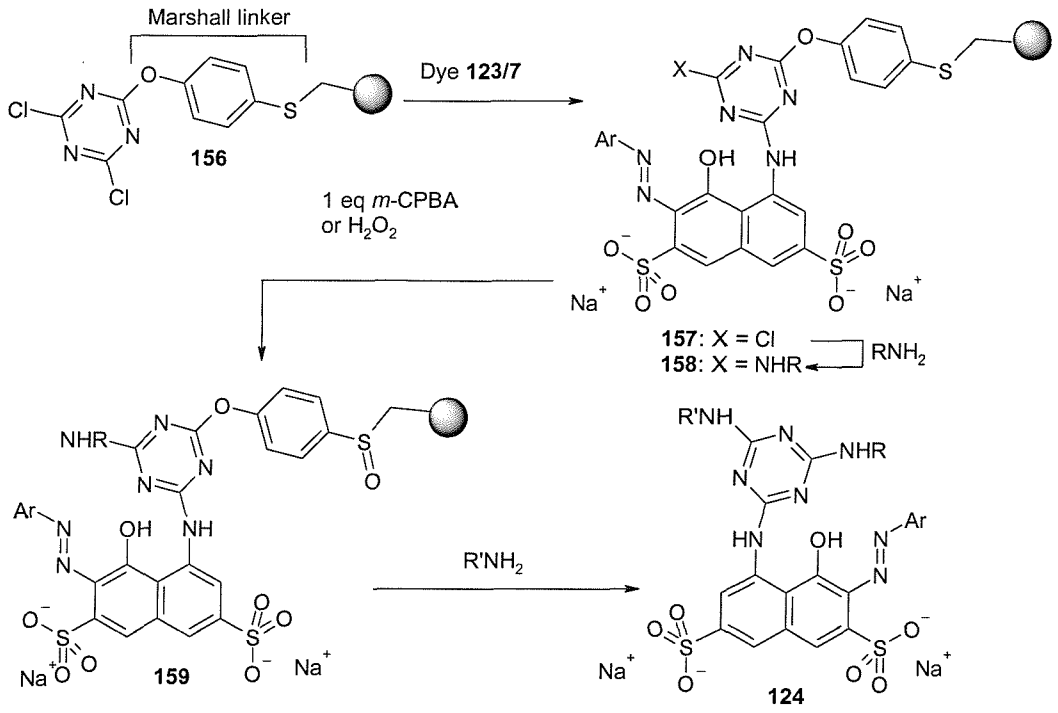

*Scheme 4.5: Proposed solid-phase synthesis of **124** using the Marshall linker.*

To best exploit the advantages provided by a solid-phase synthesis of azo-dyes, it would be advantageous to perform the maximum number of reaction steps on the resin. Although the synthesis of dye **123/7** was performed in solution the remaining steps were performed on the solid-phase. Since the introduction of diversity into the dyes was established while the dye was supported, the overall technique would allow rapid synthesis of dye-libraries.

4.3 Solution-Phase Synthesis of Azo-Dyes Using a Marshall Linker

A solution-phase synthesis was performed in order to assess the suitability of these reactions to the synthetic route before attempting them on the solid-phase. Acid **161** was preactivated with HOBt and DCC, before being coupled with benzylamine, to give amide **162**.[193] This species was reacted with cyanuric chloride at 0°C to give the triazine **163** in good yield (Scheme 4.6).

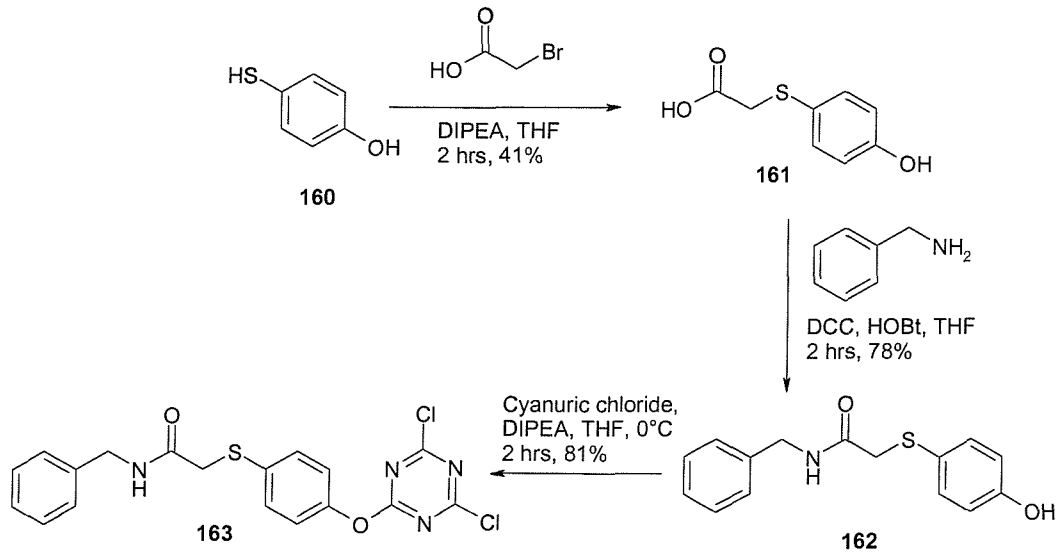

*Scheme 4.6: Synthesis of dichloro-triazine **163**.*

Triazinylation of H-acid derived dyes is usually performed using cyanuric chloride, due to its high electrophilicity, but reaction of the less reactive dichloro-triazine **163** with dye **123/7** still yielded monochloro-triazine **164** in moderate yield (Scheme 4.7). This reaction was performed using water/THF as solvent, as without the aqueous component dye **123/7** was insoluble. No hydrolysis of the triazine was observed during this reaction.

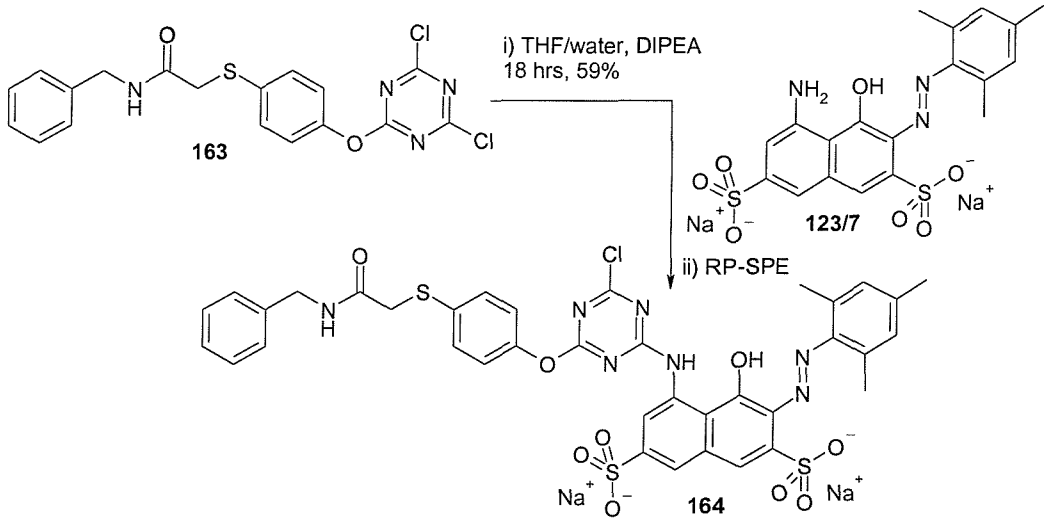

*Scheme 4.7: Synthesis of dye **164**.*

The purification of this species was achieved first by conventional liquid-liquid extraction to remove excess **163**, followed by RP-SPE to remove remaining **123/7**. Separation of dyes **123/7** and **164** in this manner was efficient, due to a high affinity between the column and the desired dye product.

Monochloro-triazine **164** was treated with excess cyclohexylamine, to give rapid conversion to the trisubstituted triazine **165** (Scheme 4.8). RP-SPE ensured complete removal of excess amine, which if left would react with the activated triazine during the next step.

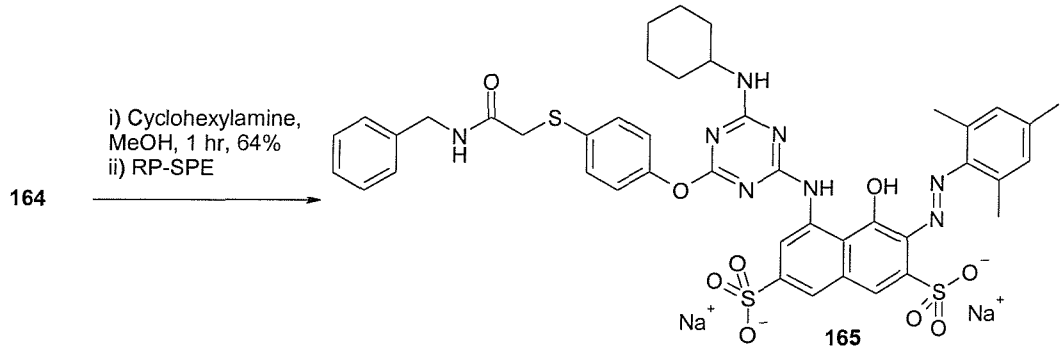

*Scheme 4.8: Synthesis of **165**.*

Oxidation was attempted using hydrogen peroxide, which should have selectively oxidised the thioether to the sulphoxide **166** in the presence of the azo- and triazinyl-functionality (Scheme 4.9). However, despite long reaction times no evidence of oxidation was observed by LC/MS. This was not totally unexpected, as the oxidation of thiophenols with hydrogen peroxide normally only occurs with electron rich thiophenols.[194] The addition of catalytic acetic acid is often used to increase the reactivity of hydrogen peroxide, but this could also result in the oxidation of the two other sensitive groups,[192] and was not used.

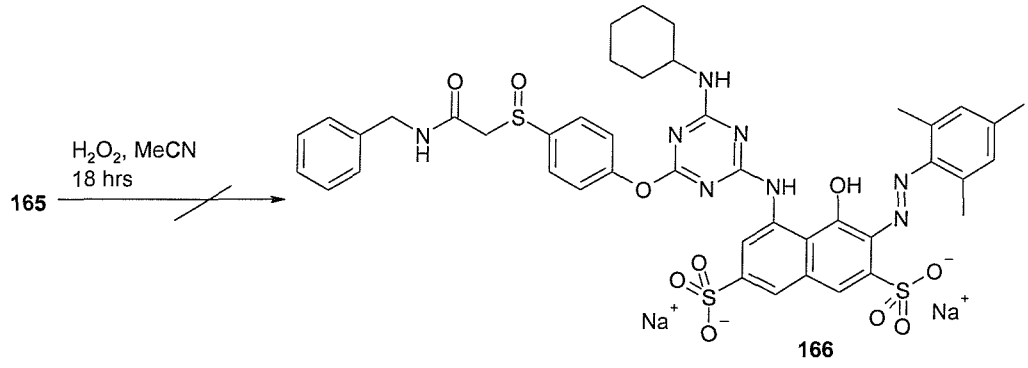

*Scheme 4.9: Attempted synthesis of sulphoxide **166**.*

The second attempt at this conversion involved 1.1 equivalents of *m*-CPBA. Although the oxidation of **165** was observed (HPLC), attempts to isolate **166** by RP-SPE in MeCN/water were unsuccessful, LC-MS of the resulting material suggesting it was the hydroxy-substituted dye, **167** (Figure 4.3).

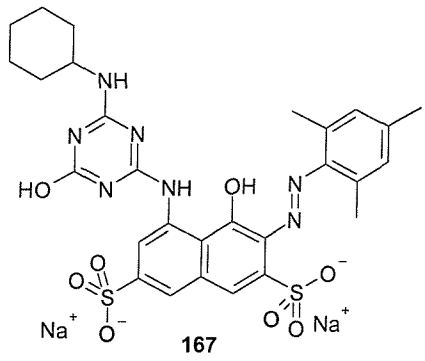

167

*Figure 4.3: Proposed dye **167**.*

It was proposed that addition of the second amine directly to the reaction mixture without isolation of the sulphoxide would yield the desired dye **124/bc7** (Scheme 4.10).

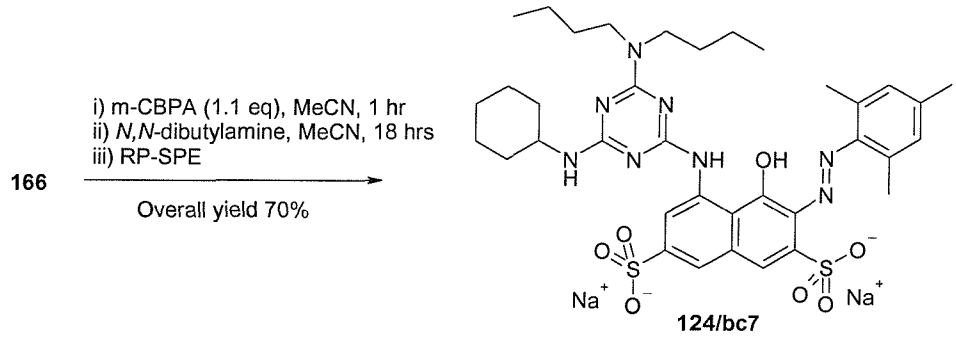

*Scheme 4.10: Synthesis of dye **124/bc7**.*

The oxidation of **166** using 1.1 equivalents of *m*-CPBA was followed by the addition of 10 equivalents of *N,N*-dibutylamine. This yielded dye **124/bc7** in 70% yield, without the symmetrical by-product (**124/bb7**) found in the convergent synthesis, discussed in Chapter 4. Crucially, there was no MS or HPLC evidence to suggest formation of *N*-oxides during the oxidation step, suggesting that *m*-CPBA was reacting selectively with the thioether in the desired manner. The successful solution-phase synthesis of dye **124/bc7** allowed the route to be applied to the solid-phase.

4.4 Solid-phase Azo-Dye Synthesis Using a Marshall Linker

Acid **161** was coupled to aminomethyl ArgoPore resin in accordance with previous work in the group (Scheme 4.11).[192] A qualitative ninhydrin test confirmed complete consumption of the free amine group, and elemental analysis suggested a loading of 0.65 mmol/g.

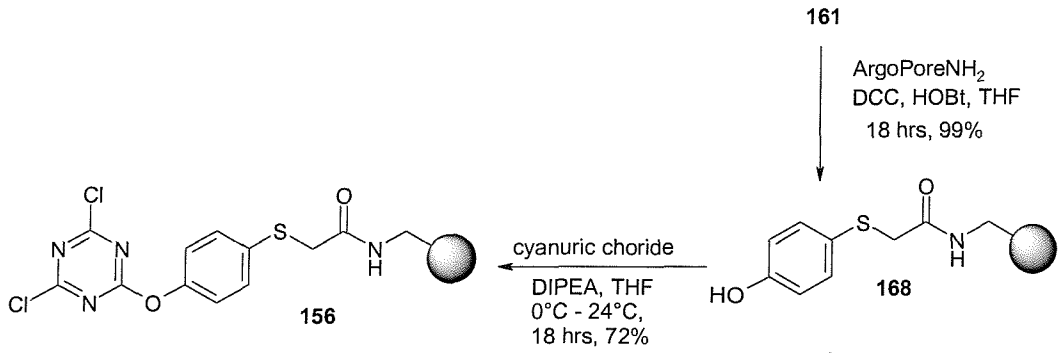

*Scheme 4.11: Synthesis of dichloro-triazine resin **156**.*

Three equivalents of cyanuric chloride were used in the conversion of **168** to **156**. The reaction was undertaken at 0°C for the first hour of reaction, and in an attempt to achieve quantitative conversion the reaction temperature was allowed to rise to 24°C. Despite the use of a relatively high temperature for this conversion, elemental analysis of the resin only suggested a 72% conversion to the dichloro-triazine. IR analysis showed complete disappearance of the broad peak corresponding to the hydroxyl stretching frequency.

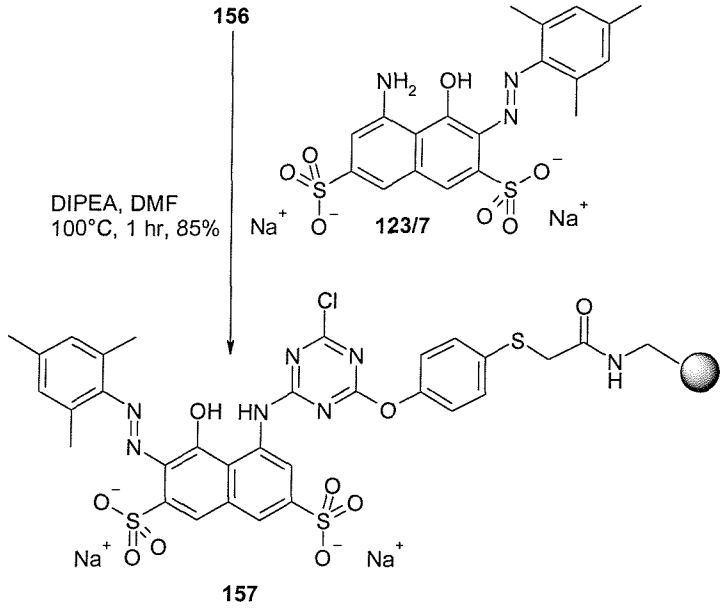

*Scheme 4.12: Synthesis of resin **175**.*

The substitution of resin **156** with dye **123/7** was initially performed using a 2-fold excess of dye with respect to the triazine in DMF. However, at room temperature this conversion was very slow, and after 24 hours sulphur elemental analysis suggested a substitution of less than 5%. Digital microscope images of these beads showed little colouration of the matrix (Figure 4.2a).

In order to increase the loading of the dye, the reaction was undertaken at 100°C in a microwave cavity (Scheme 4.12). It was hoped that the increase in temperature would force the substitution of the triazinyl resin by the dye, without significant levels of dichloro-triazine hydrolysis. The reaction was irradiated for 10 minute periods followed by the removal of an aliquot for microscope imaging (Figure 4.2b).

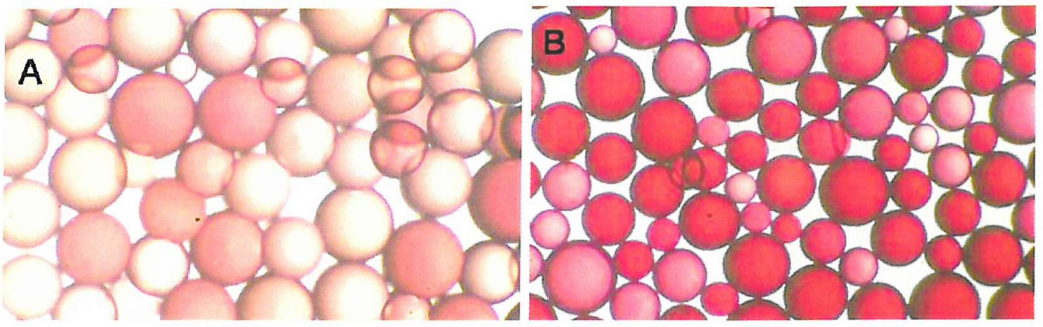

*Figure 4.2: Microscope images of resin **157**; a) after room temperature synthesis for 24 hours, b) after microwave synthesis for 60 minutes.*

In this manner it was ascertained that after 60 minutes of irradiation the reaction had reached its conclusion, and the resin was filtered and washed. Elemental analysis of the resin confirmed an increase in dye loading, as the sulphur content increased from 2.1% to 3.9%, corresponding to a loading of 0.41 mmol (85% yield).

Resin **157** was treated with cyclohexylamine to substitute the final chlorine group (Scheme 4.13).

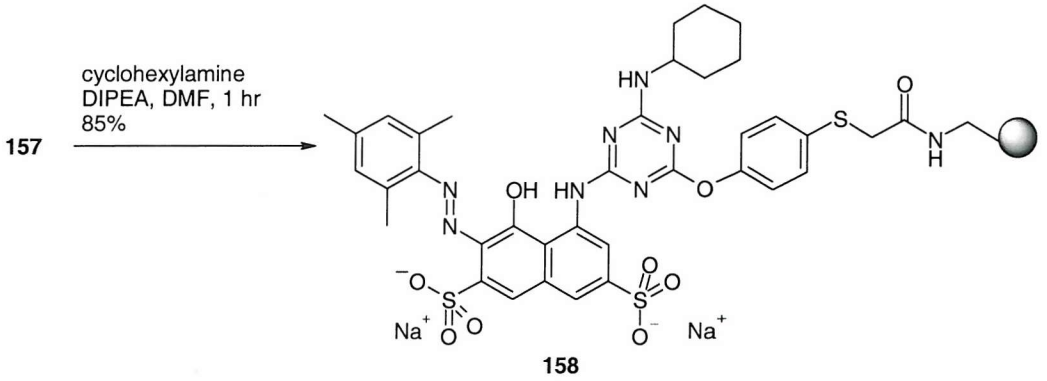

*Scheme 4.13: Synthesis of resin **158**.*

At first ten equivalents of amine were used to ensure rapid reaction. This technique resulted in low levels of dye cleavage from the beads, possibly due to premature substitution of the linker by the amine, in a manner similar as report by Dressman.[188] Hence the experiment was repeated using only 3 equivalents of

cyclohexylamine and 3 equivalents of DIPEA, which stopped further release of coloured material from the solid-phase.

Resin **158** was treated with 2 equivalents of *m*-CPBA (0.14 M) in acetonitrile at room temperature for 1 hour. More equivalents of oxidant were applied during the solid-phase approach than during the solution-phase analogue, in accordance with previous work.[182] It was perceived that this short reaction time would not result in significant oxidation of the triazine- or azo-groups by excess oxidant. However, treatment with 10 equivalents of *N,N*-dibutylamine (0.74 M) for 24 hours did not yield dye **124/bc7** into solution. This reaction was repeated using 10 equivalents of oxidant for 24 hours in an attempt to force the oxidation to completion. Microscope-images of these beads showed significant reduction in colour intensity, suggesting oxidation of the supported-dye. Treatment with 10 equivalents of *N,N*-dibutylamine for 24 hours did not result in the cleavage of any material from the resin.

The lack of cleaved material may have been due to several reasons.

- Dye **124/bc7** was formed, but did not leave the matrix due to a strong affinity for the support.
- The structure of the supported species was not as predicted, due to the microwave synthesis of resin **157**.

The successful solution-phase approach to this synthetic route demonstrated that the oxidation/substitution step proceeded in the presence of the azo-functionality, and hence this was unlikely to cause problems during the solid-phase approach. The lack of cleaved material from the resin could have been due to π-π dye-matrix interactions, but it would be unlikely that these forces would be strong enough to retain the dye so effectively.

During the supported synthesis the only significant modification to the reaction conditions was the use of high temperatures for the synthesis of dye **157**. During these elevated temperatures undesired processes could have modified the structure of the linker/dye so that subsequent oxidation/substitution would not release any material.
A possible side reaction which could cause a permanent immobilisation of the dye on the resin was a variation on the Vilsmeier reaction (Scheme 4.14).

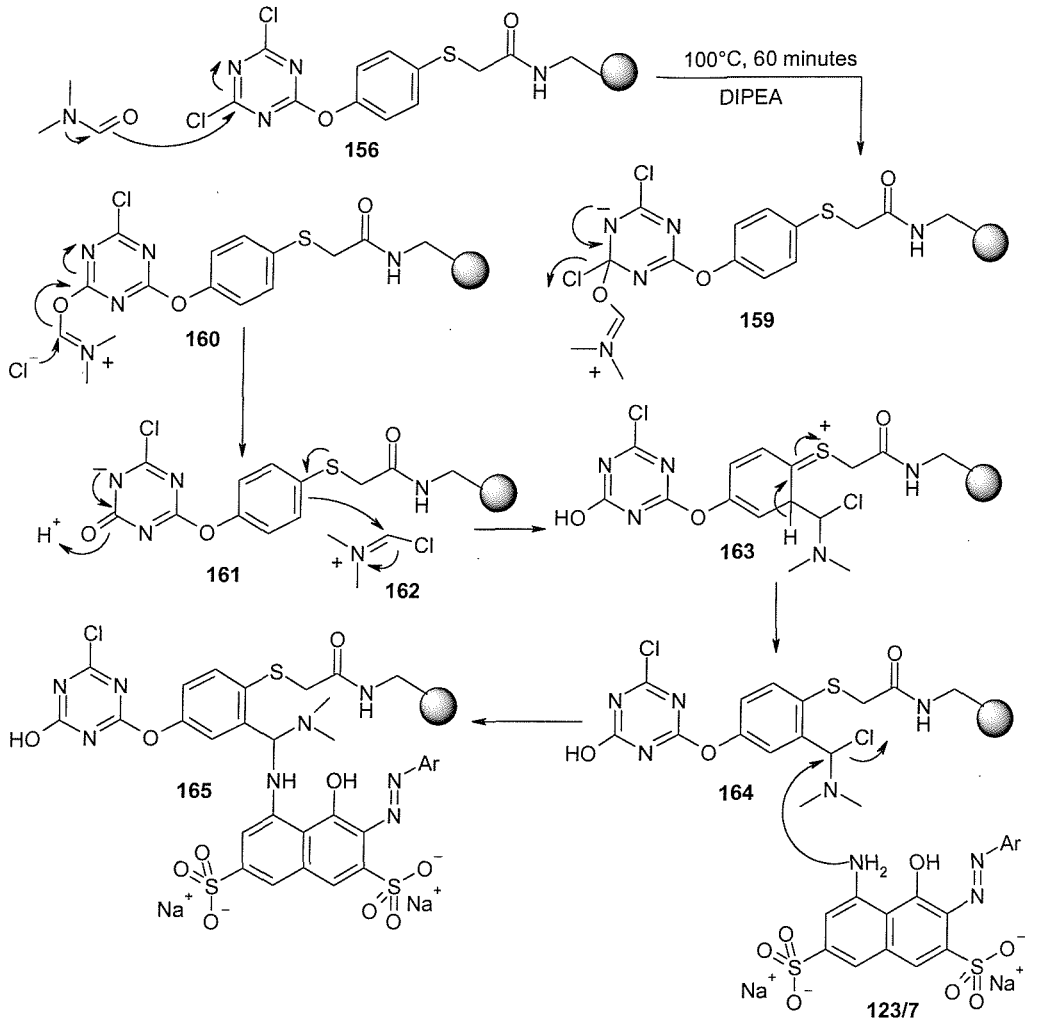

*Scheme 4.14: Possible reaction of resin **156** with DMF and dye **123/7**.*

The DMF could react with supported triazine **156** to form the chloromethylene-dimethyl-ammonium ion (**162**) analogous to the Vilsmeier reaction. Cyanuric chloride is reported to react in this manner at room temperature.[195] The Vilsmeier intermediate is known to react with electron rich aromatic systems,[196] to give aldehydes after an aqueous work-up. However, without the presence of water, substitution of the chlorine would be possible by dye **123/7** to give a highly coloured resin. The only other aprotic possible solvent which would dissolve dye **123/7** was DMSO, but this solvent has been demonstrated to be reactive towards electrophiles at high temperatures.[197]

4.5 Conclusions

The solution-phase synthesis of dye **124/bc7** was successful, demonstrating that the oxidation of the thioether was possible in the presence of other oxidation sensitive functional groups. The oxidation/substitution step was performed as a one-pot procedure, as isolation of unstable sulphoxide **166** was not possible by RP-SPE.

During the solid-phase approach, the substitution of dichloro-triazine resin **156** with dye **123/7** was slow, and high temperatures were used to achieve a significant degree of dye loading. The oxidation/substitution of resin **158** did not cleave dye **124/bc7** into solution, despite attempts to force the reaction with high reagent concentration. The successful results from the solution-phase synthesis suggest that the use of high temperatures during the solid-phase approach was the cause of the ineffectual dye cleavage.

Chapter 5: Towards Automated Digital Image Analysis of Resin Beads

5.1 Introduction

5.1.1 Resin Bead Characterisation.

Beads for solid-phase organic synthesis are usually prepared by suspension polymerisation, a technique capable of generating beads from 25-500 μm.[72] The size distribution of a batch of beads is an important parameter, and is usually measured using light scattering methods (Figure 5.1).[198] Beads size will affect kinetics of reactions performed on it [199] and is affected by many factors, including the synthesis conditions, the degree of cross-linking and solvent in which they reside.[73]

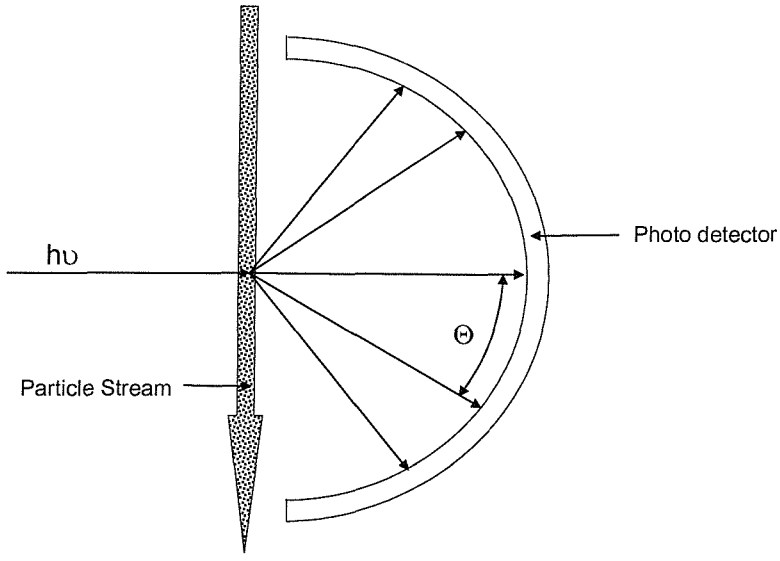

Figure 5.1: Light scatting methods can be used to determine the size distribution of a bead sample.

The incoming light, usually generated by a laser, interacts with the bead sample suspended in a stream of carrier fluid, diffracting the light beam. The diffraction pattern projected onto a photo detector allows the determination of the particle size present in the stream, since the smaller the particles the greater the interaction with the beam resulting in radiation scattering at large Θ-values.

5.1.2 Digital Image Analysis

Digital image analysis (DIA) is a broad concept covering sample preparation, image acquisition, image analysis and presentation of the recovered data.[199] The use of early imaging systems were very expensive and required a significant grounding in computing, and were therefore mostly used by computer scientists. However, since the advent of the charge-coupled device (CCD), the personal computer, and improvement in

graphical user interfaces, the availability and use of image-analysis systems has quickly expanded into numerous areas.

CCDs are essentially either 1 or 2-dimensional arrays of tiny photosensors etched onto silicon wafers.[200] Each sensor, or element, generates a flow of electrons proportional to the amount of light that falls on it during a certain period of time (Figure 5.2).

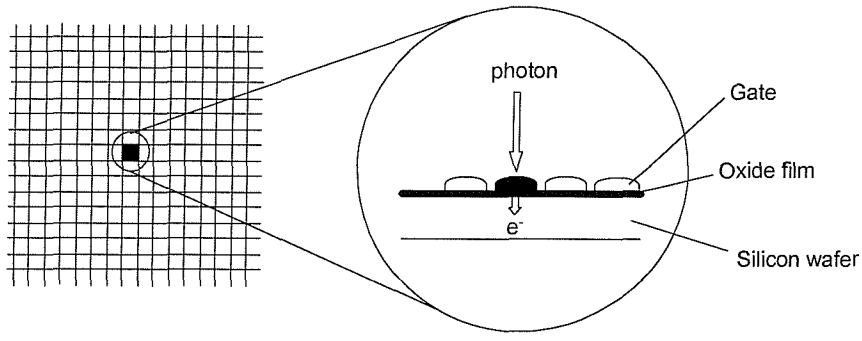

Figure 5.2: The basic structure of a 2-dimensional CCD array.

The signal from each element is collected and fed into a computer, which transforms the signals into an image. 1-Dimensional CCD arrays can be used to acquire images by scanning the object one 'line' at a time, but as this is inherently time consuming this approach is normally reserved for observing static systems, such as electrophoresis gels.[201] 2-Dimensional CCD arrays are becoming standard for most imaging applications, and will be the focus of this discussion.

The number of elements in a 2-dimensional CCD is proportional to the number of pixels, and hence the resolution, of the image generated using it. The physical size of each element can affect its signal response and the range under which it can function. The larger the surface area of the element the greater the amount of light which it can collect, and the greater the flow of electrons it can produce, which results in higher sensitivity and wider range under which it can give a linear response (dynamic range).

Digital images are composed of arrays of pixels (picture element) arranged in rows (X-direction) and columns (Y-direction). Each pixel has an associated intensity-value, which gives information about the amount of light falling on the respective element at the time of measurement. As it is a digital image, the intensity-values are integers and their size depends on the bit-depth of the image. For instance, in a greyscale (black and white) 8-bit image the binary pixel intensity-values can be from 00000000 to 11111111 representing 256 possible values, where the lowest value indicates the darkest pixel and the highest the lightest one (Figure 5.3).

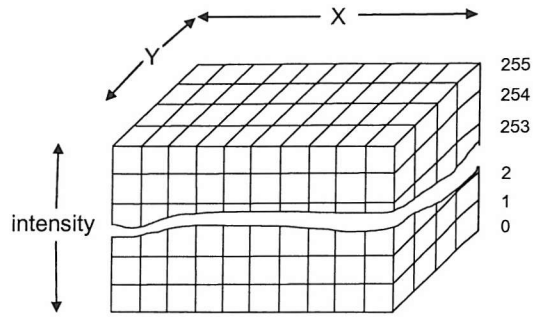

*Figure 5.3: Conceptual view of a greyscale 8-bit digital image composed of X * Y pixels, each of value 0 to 255.*

Hence, 10-bit images have 1024 possible levels of intensity, 12-bit images have 4096 possible levels, and so on. The number of pixels in the image (resolution) and the bit-depth of each pixel are important factors when performing image analysis. To demonstrate this, Figure 5.4 shows three representations of an object, with varying bit-depth and resolution.

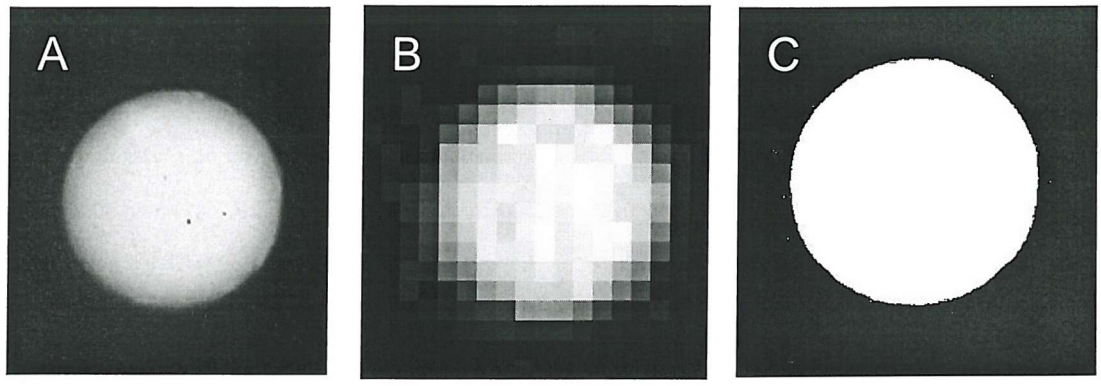

*Figure 5.4: Greyscale images of an object; a) 8-bit, 350*400 pixel resolution; b) 8-bit, 18*20 pixel resolution; c) 1-bit, 350*400 pixel resolution.*

Image 5.4a shows a gradual change from the background intensity to that of the object. Information regarding both the shape and brightness of the object is present. In the second image (5.4b) the information regarding the intensity of the object is present, but due to low resolution the perimeter of the object is not clear. In image 5.4c the perimeter is well defined, as this in a 1-bit image, but as the intensity value is either 0 or 1 it is no longer representative of the actual brightness of the object.

Colour images require three intensity values per pixel in the place of a greyscale images one. The three values correspond to the red, green and blue (RGB) components of the pixels colour. RGB values are also integers, and have a range depending on the

bit-depth of the image. Colour CCDs are more complex than greyscale models, as each element is constructed of three regions. The element-regions which correspond to each of the red, green or blue components are covered with filters which only let photons corresponding to desired light through.

If image acquisition is performed in the correct manner large quantities of information regarding the object can be extracted. Digital image analysis is widely used in many disciplines of science, including the analysis of satellite photography,[202] astronomy [200] and studies of highly-ordered polymers,[203] although most examples currently being reported are biologically orientated.[204-205] Special interest is currently associated with the analysis of microarrays,[206] used in the study of genomics, and 2D electrophoresis gels,[207-208] used in the study of proteomics (Figure 5.5).

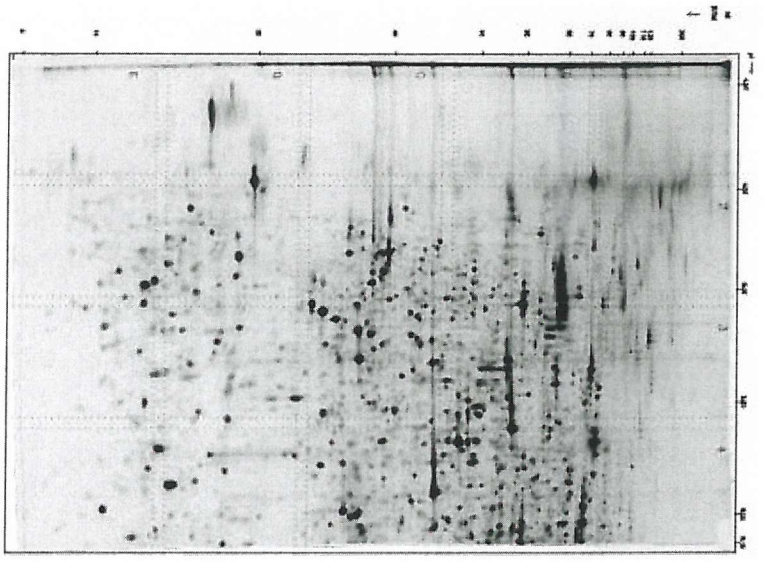

Figure 5.5: 2D-electrophoresis gel.[209]

The gel-images require rapid automated analysis to identify the presence of proteins distributed within the gel. The data can be used in a comparative sense between gels, or to control robotic equipment to remove samples for analysis.

5.2 Objectives of Research

This chapter describes attempts to develop an automated digital image analysis system which is capable of extracting pixel-intensity data from images of resin beads. If successful, this system could be used to accurately measure the colour of azo-dyes supported upon them allowing dyes synthesised by solid-phase techniques to be rapidly analysed without the need for dye cleavage or its application to paper (Scheme 6.1).

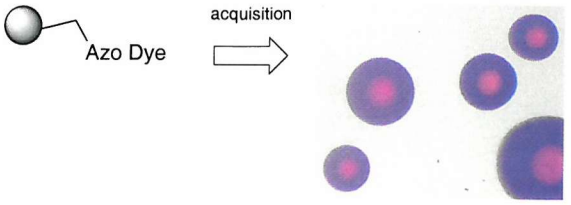

Bead	X	Y	R	G	B
1	110	18	255	11	228
2	98	34	254	11	229
3	35	49	255	12	229
4	115	89	255	11	230
5	21	90	223	12	228

Scheme 5.1: Proposed digital image analysis of supported azo-dyes.

However, before this can be achieved the image analysis system needs to be able to identify the beads within the image, separating them from the background and other artefacts present. This was attempted using a variety of imaging methods, and analysis using modern image analysis software to extract information on the bead structure.

5.3 Digital Image Analysis of Resin Beads

Digital images of resin beads were acquired using scanning electron microscopy (SEM), conventional optical microscopy and fluorescence optical microscopy. The images were obtained in such a manner as to maximise the contrast between the background and the beads, hence maximising the signal to noise ratio. The images were transferred to Image Pro Plus© (IPP) image analysis software,[210] converted to 8-bit greyscale and the pixels divided into two groups depending on their intensity (thresholding) (Figure 5.6).

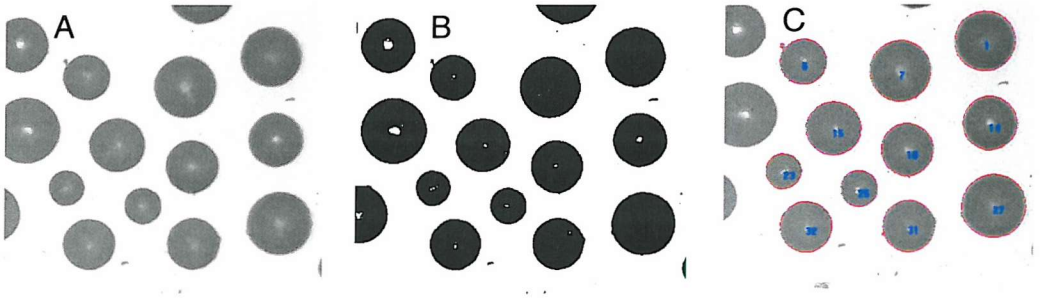

Figure 5.6: Thresholding of a digital image; a) 8-bit greyscale image, b) 1-bit image after thresholding, c) object recognition based on the 1-bit image.

Any pixel with intensity above a specified threshold-value was changed to white, and those lower were changed to black to give a 1-bit image (Figure 5.6b). The software

then 'found' all the black 'objects', calculated their area and assumed that all the 'objects' above a specified size were beads (Figure 5.6c). The high intensity 'holes' in the centre of each bead were included in this area calculation. This process required two parameters to be provided by the user: the threshold-value and the area above which 'objects' were recognised as beads. Once the beads were identified the data associated with them, including location, size, and shape, was exported to a spreadsheet.

5.4 Analysis of PS-DVB beads

Experiments were performed using amino methyl PS-*co*-DVB resin beads. Optical transmission microscope images (2.6 million pixels) showed that when swollen in DCM the beads showed a propensity to aggregate into groups (Figure 5.7a).

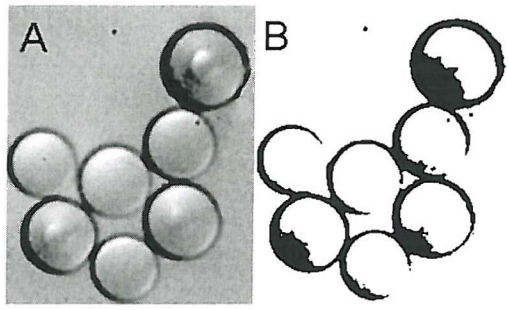

Figure 5.7: Aggregated PS-co-DVB beads in DCM; a) microscope image, b) after thresholding.

Analysis of the image was hampered by two factors. Firstly the difference in pixel-intensity between the background and the bead was low, which resulted in poor discrimination, as shown in Figure 5.7b. Secondly, the identification of beads within a cluster was not possible, as the software perceived the cluster as one object and was unable to ascertain either individual shape or size of the component beads.

In order to make the beads more identifiable in the image, fluorescein-stained PS-*co*-DVB beads were used. In order to prevent aggregation, the beads were repeatedly swollen in DCM and dried rapidly. This recurring swelling and contraction resulted in improved separation of the beads, and allowed effective image analysis (Figure 5.8).

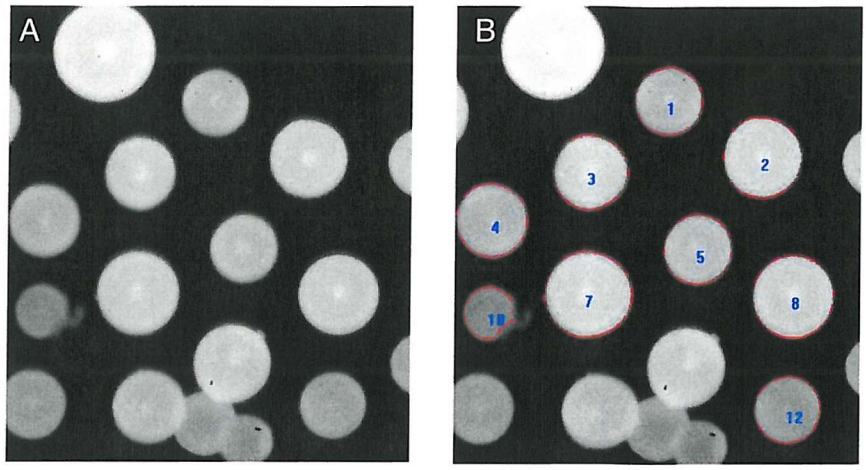

Figure 5.8: Fluorescein-tagged PS-co-DVB beads after DCM separation, a) before analysis, b) after analysis.

As this technique required functionalisation of the resin beads, this method of visualisation would be only applicable to beads with suitable functional groups. The presence of the fluorescein might also affect the bead size, distorting the apparent bead size.

Scanning electron microscopy (SEM) was also used to generate images for analysis (Figure 5.9). The images produced tended to be of good contrast, although the output resolution of the SEM was lower (0.3 million pixels) than that of the optical microscope.

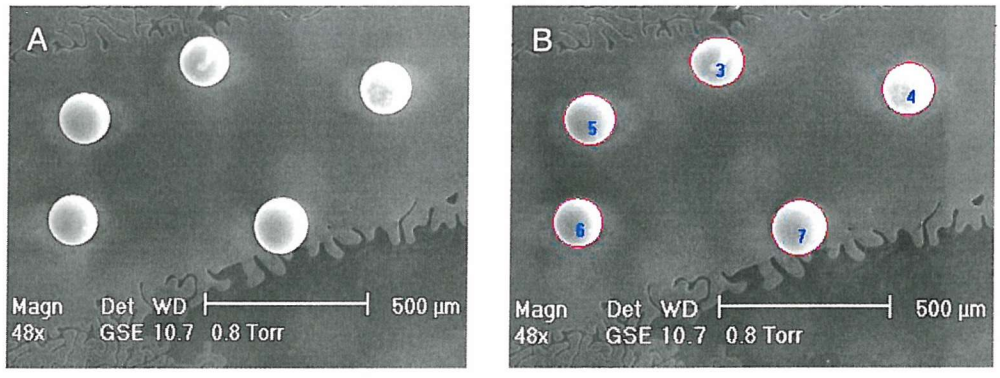

Figure 5.9: SEM images of PS-DVB beads; a) before analysis, b) after analysis.

5.5 Size Analysis of PS-*co*-DVB Beads

In order to compare the use of SEM and optical microscopy for image acquisition, images of a sample of PS-*co*-DVB were obtained using both techniques, and the bead size distribution was analysed using the methods described in section 5.4. The results were compared with data from laser-diffraction of the same sample. For comparable data

sets to be generated, spatial calibration was required. The SEM images contained an internal scale, but the optical microscope required the use of an external scale. An image of a graticule (microscope scale) was acquired and the ratio of pixels to microns was calculated allowing the calibration of subsequent images. High-throughput analysis was achieved by the use of macros, short programs which allowed a series of commands to be performed rapidly and automatically. Macros were written to perform all the image processing steps required to extract the necessary data.[i]

The results of these experiments are summarised in Table 5.1, and are shown plotted against the laser diffraction results in Graph 5.1.

Table 5.1: Results of bead size analysis experiments, using two different image acquisition techniques.

	Optical (fluorescent)	SEM	Laser Diffraction (in water)	Manufacturers Specifications
Number of beads	419	75	n/a	n/a
Mean size (μM)	117.6	119.1	115.2	75-150
Standard deviation (μM)	20.1	20.7	23.7	n.d.

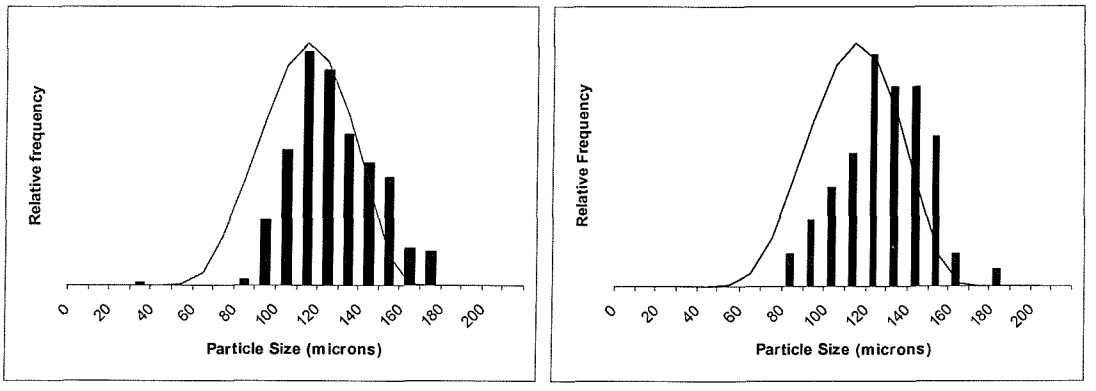

Graph 5.1: Distribution graphs comparing the DIA results of PS-co-DVB beads against laser diffraction measurements (continuous black line); a) data from images acquired by optical microscopy, b) data from images acquired by SEM.

The mean values of the DIA data showed a slightly higher result in both cases when compared to the laser diffraction data. The difference between the three averages (mean) was less than 4 μm (approximately 3% of the total diameter), which was well within experimental error.

[i] Macro-code can be found in section 6.6.3.

5.6 Conclusions

The accurate digital image analysis of PS-*co*-DVB beads to determine particle size has been demonstrated using both optical and SEM image acquisition. The contrast of the optical images was optimised by the use of fluorescent-dye functionalised beads. Following bead identification, data concerning the shape and size of the beads was extracted and used to analyse the bead sample.

5.7 Future Work on the DIA of Supported-dyes

Section 5.5 showed that DIA can be used to accurately determine the particle size distribution of bead samples. Accurate spatial calibration was required so that any data extracted could be compared with other techniques. For DIA to be used in the determination of pixel-intensity from colour images, intensity calibration is critical, so that the RGB values obtained are reproducible and comparable with images acquired using other techniques.

DIA is commonly applied to the extraction of intensity data from fluorescent assays, an example of which is provided by Henry.[211] During this study, images of cells containing GFP were analysed for colour intensity using only the green-colour channel. The intensity-value obtained was compared to a calibration curve of various concentrations of dyes in solution to ascertain the dye concentration in the cell.

If DIA methodology is to be applied to the analysis of different dyes, a method of calibrating the RGB values will be required so that the results are compatible with conventional spectrophotometric techniques. This could be achieved by the use of three colour 'standards', of known RGB-values, which could be used to calibrate each image. These dyes should be carefully chosen so that each one absorbs only in their respective regions of the electromagnetic spectrum, and hence are as close to the 'pure' colour as possible.

However, even with accurate calibration techniques the behaviour of the supported dyes may still not be representative of the dye in solution, or when printed on a page. The azo-hydrazo tautomerisation is affected by both the pH and the polarity of the dye environment (so called solvatochromism).[47] Supported dyes also have the added complication of the presence of the resin matrix affecting the colour of the dye. Hence the observed bead colour will be affected by the solvent used to swell the beads, the nature of the bead and the dye concentration within it.

Results and Discussion Summary

The immobilisation of various diazonium salts onto Amberlyst A-15 resin provided a powerful tool for the storage and handling of these reactive species. Treatment of this supported reagent with phenolic coupling agents at pH 9 allowed rapid synthesis of azo-dye products in variable yield and purity. However, the high rate of decomposition of the supported species at such a high pH required a large excess of supported reagent to be used, suggesting that this technique would probably be better suited to coupling reactions performed at lower pH.

This approach to dye synthesis was integrated with solid-phase extraction to allow rapid and parallel purification of the crude reaction mixture. A selection of H-acid derived azo-dyes prepared in this way was reacted with monochloro-triazines in an attempt to perform a convergent synthetic strategy. This unfavourable process was forced using high-temperature microwave synthesis, which gave the desired triazinylated azo-dyes in several cases.

Similar triazinylated azo-dyes were synthesised using the Marshal safety-catch linker. Although the solid-phase approach was unsuccessful, the solution-phase approach gave the final dye in good yield and high purity when used in conjunction with SPE, suggesting this technique could be used to synthesise large azo-dye libraries.

The accurate digital image analysis of PS-*co*-DVB beads has been demonstrated using both optical and SEM image acquisition. Successful bead identification and analysis suggests that this technique could be adapted for the analysis of supported azo-dyes to allow rapid parallel dye evaluation.

Chapter 6: Experimental

6.1 General Information

Melting points were obtained using an Electrothermal melting point apparatus, and are quoted uncorrected. Infrared (IR) spectra were obtained using either a Biorad FTS-135 or Thermo Mattson Satellite FT-IR spectrometer, fitted with a Golden Gate ATR sample holder. UV/Vis spectra were obtained using a Hewlett Packard HP8452A diode-array spectrometer. Microwave irradiation was achieved using a Smith Synthesiser (Personal Chemistry). Solid-phase extraction (SPE) was performed using 10 g/60 mL RP Supelclean SPE cartridges (Supelco, octadecyl, ~10% C, encapped), attached to a Flash-Master *Lite* (Jones Chromatography) solvent pump.

Polymer Supports Used

All solid-phase chemistry was performed on ArgoPoreNH_2, a macroporous amino methyl functionalised PS-*co*-DVB polymer (Argonaught, 16-140 mesh, 0.6-1.1 mmol/g).[212] Amberlyst A-26, a macroporous quaternary ammonium functionalised PS-*co*-DVB polymer (Rohm:Haas, 4.2 mmol/g, 250 Å average pore size) was used as a strong anion exchanger. Amberlyst A-15, a macroporous sulphonic acid functionalised PS-*co*-DVB polymer (Rohm:Haas, 4.7 mmol/g, 250 Å average pore size) was used as a strong cation exchanger.

Mass Spectrometry (MS)

Low resolution mass spectra were recorded using either a VG Platform quadrupole mass spectrometer, a Hewlett Packard 1100 series MSD, or a Waters ZMD quadrupole mass spectrometer, all using electrospray ionisation (ESI) sources. Low resolution gas chromatography mass spectra were recorded using a ThermoQuest TraceMS system with electrical ionisation (EI) source, and Optima Delta 3 column.

High resolution mass spectroscopy was performed using a Bruker Apex III, FT-ICR mass spectrometer, with electrospray ionisation (ESI) source.

Nuclear Magnetic Resonance (NMR)

300 MHz ^{1}H and 75 MHz ^{13}C-NMR spectra were obtained using a Bruker AC300 NMR spectrometer. 400 MHz ^{1}H and 100 MHz ^{13}C-NMR spectra were obtained using a Bruker DPX-400 NMR spectrometer. Chemical shifts (δ) were measured in parts per million (ppm) and coupling constants (J) in Hz. H-H couplings quoted were short range unless stated (e.g. $J_{6\text{-}8}$=2 Hz). Unless otherwise stated, spectra were obtained at 298 K.

Chromatography

Flash chromatography was performed according to the procedure outlined by Still,[213] using Sorbsil C_{60}, 40-60 mesh silica. Unless otherwise stated, thin-layer chromatography was performed on aluminium backed silica plates, coated with a 0.25 mm layer of silica gel 60, with fluorescent indicator Augram SIL G/UV_{254}. Unless otherwise stated, compounds were visualised with UV radiation at 254 nm. Analytical high-performance liquid chromatography (HPLC) was performed using an Hewlett Packard 1100 series HPLC system, using a combination of a variable wavelength detector, multiple wavelength detector and evaporative light scattering detector (Polymer Labs). Mobile phases were water (HPLC grade) containing 0.1% TFA and MeCN (HPLC grade) containing 0.042% TFA. The following gradients and columns were used:

Gradient code	Column	Gradients
STD254	Prodigy (Phenomenex) 150 mm x 2 mm, 5 μ, ODS(3)	0 –100 % MeCN in water over 10 minutes, isocratic for 5 minutes.
S5OD	Discovery (Supelco) 50 mm x 4.6 mm, 5 μ, ODS(2)	10 –90 % MeCN in water over 3 minutes, isocratic for 1 minute.
S15OD	Prodigy (Phenomenex) 150 mm x 2 mm, 5 μ, ODS(3)	10 –90 % MeCN in water over 10 minutes, isocratic for 5 minutes.
L5OD	Discovery (Supelco) 50 mm x 4.6 mm, 5 μ, ODS(2)	10 –90 % MeCN in water over 1 minute, isocratic for 8 minutes.

Qualitative ninhydrin test

Reagent A (6 drops) and reagent B (2 drops) were added to 1-5 mg of sample and the mixture was heated at 100°C for 10 minutes. Solution colouration was inspected visually. Reagents A and B were prepared in the following manner.

Reagent A;

Solution-1: Phenol (40 g) was dissolved in EtOH (10 mL) with heating, and was stirred over Amberlite mixed-bed resin (MB-3, 4 g) for 45 minutes, and filtered.

Soiution-2: KCN (65 mg) was dissolved in water (100 mL). 2 mL of this solution was diluted with pyridine (100 mL, freshly distilled from ninhydrin) and stirred over Amberlite mixed-bed resin (MB-3, 4 g). The solution was filtered and mixed with solution-1 to give reagent A.

Reagent B;

Ninhydrin (2.50 g) was dissolved in ethanol (50 mL).

6.2 Experimental to Chapter 2

6.2.1 Amberlyst A-26 (NO_2^- form), 108

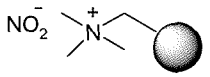

Amberlyst A-26 (Cl^- form, 200.0 g) was pre-swollen in water, and packed in to a column (70 mm diameter) and washed with water (200 mL). $NaNO_2$ (69 g, 1.0 mol) was dissolved in water (500 mL) and passed slowly (50 mL/min) through the column. Water was passed through the column, until eluent no longer tested positive for Cl^-, using $AgNO_3$. Once complete exchange was achieved, the column was washed with water (500 mL) and MeOH (500 mL) before being dried under vacuum at 45°C for 18 hours.

IR (υ, cm^{-1}) 1209 (N=O).

6.2.2 Amberlyst A-15 (Na^+ form), 113

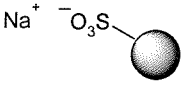

A-15 resin (H^+ form, 200.0 g) was treated with aq. NaOH (2 N, 500 mL) for 12 hours. The resin was washed with MeOH (2 x 200 mL), before treating with aq. HCl (2 N, 500 mL) for 12 hours. Aq. NaOH (2 N, 4 x 150 mL) was passed through the column, followed by MeOH (2 x 200 mL), before being dried under vacuum at 45°C for 18 hours.

IR (υ, cm^{-1}) 1035, 1163 (SO_2-O), 2921 (C-H), 3441 (O-H).

6.2.3a Synthesis of Supported Diazonium Salts 114/1-6

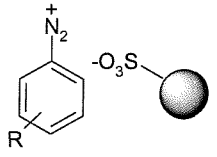

To a solution of the aniline component (Table 6.1, 40.0 mmol) in aq. HCl (12 M, 100 mL) cooled to 0°C was added A-26 (NO_2^- form, 71.0 g) and the reaction was shaken for 30 minutes at 0°C.The reaction mixture was filtered and the filtrate passed through a column (20 mm diameter, 10 mL/min) of A-15 (Na^+ form, 12.0 g) and the resin washed with water (2 x 50 mL), MeOH (2 x 50 mL), dried and stored at 0°C.

Table 6.1: Aniline derivatives used.

Code[a]	Product	Aniline derivative	Mass used
1	**115/1**	4-chloroaniline	4.70 g
2	**115/2**	4-bromoaniline	6.48 g
3	**115/3**	4-iodoaniline	8.36 g
4	**115/4**	4-nitroaniline	5.16 g
5	**115/5**	Aniline	3.32 g
6	**115/6**	4-sulphamic acid	6.48 g

a) Code for each derivative was used to describe following dye products.

6.2.3b Synthesis of Azo-Dye Library 116/a1-f6

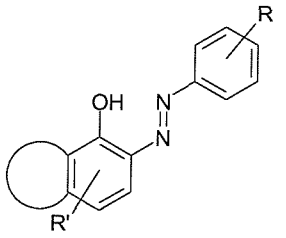

To a solution of the phenolic component (Table 6.2, 0.40 mmol) in aq. NH_4OH (2 N, 3 mL) was added A-15 (diazonium form, **114/1-6**, 2.0 g), and the reaction was shaken for 40 minutes. NH_4OH (aq.,18 N, 150 μL) was added to adjust the pH from 5 to 9. The reaction mixture was filtered and the resin washed with water (2 x 5 mL). The filtrate was concentrated *in vacuo* to 3 mL and freeze-dried, to give dyes **116/a1-f6** in variable yield and purity (Table 6.3).

*Table 6.2: Phenolic components used to form dyes **116/a1-f6**.*

Code [a]	Phenolic derivative	Mass used
a	4-amino-5-hydroxynaphthalene-2,7-disulphonic acid, mono Na^+	136 mg
b	Phenol	37 mg
c	4-hydroxybenzene sulphonic acid	69 mg
d	4-nitrophenol	55 mg
e	2-naphthol-3,6-disulphonic acid	139 mg
f	1-naphthol-4-sulphonic acid	98 mg

a) Code for each derivative was used to describe following dye products.

*Table 6.3: Yield (%) of Dyes **116/a1-f6.***

	a [a]	b	c	d	e	d
1	71 (69%)[b]	6.4 (99%)	37 (31%)	0 (0%)	32 (93%)	37 (74%)
2	57 (60%)	4.5 (89%)	35 (33%)	0 (0%)	48 (77%)	39 (48%)
3	52 (95%)	3.8 (57%)	34 (13%)	0 (0%)	45 (47%)	38 (47%)
4	67 (95%)	6.1 (84%)	41 (13%)	0 (0%)	39 (85%)	38 (61%)
5	90 (94%)	25 (94%)	35 (18%)	0 (0%)	84 (90%)	28 (90%)
6	57 (16%)	5 (86%)	36 (20%)	0 (0%)	51 (99%)	48 (41%)

a) First row contains codes for phenolic derivative used; first column contains codes for aniline derivative used: b) Purities in parenthesis (HPLC @ 254 nm).

*Table 6.4: Low resolution mass spectrometry of dyes **116/a1-f6**.*

	A	B	C	D	E	F
1	277.5 (100%)	231.0 (100%)	311.0 (100%)		443.0 (100%)	361.0 (100%)
2	250.4 (100%)	275.0 (100%)	356.9 (100%)		242.9 (100%)	406.9 (100%)
3	273.5 (100%)	323.0 (100%)	402.9 (100%)		265.9 (100%)	452.9 (100%)
4	233.6 (100%)	242.0 (100%)	322.0 (100%)		225.5 (100%)	372.0 (100%)
5	210.8 (100%)	197.0 (100%)	277.2 (100%)		203.0 (100%)	327.0 (100%)
6	250.4 (100%)	277.0 (100%)	178.0 (100%)		243.0 (93%)	203.0 (100%)

= $(M-H)^-$ and/or $(M-2H)^{2-}$ ions observed; = no molecular ion observed.

5-Amino-4-hydroxy-3-phenylazo-naphthalene-2,7-disulphonic acid di-ammonium salt, **116/a5** [216]

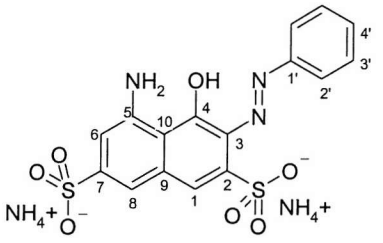

Mpt. >250°C: **TLC** (acetone/^{i}PrOH/NH_4OH; 1:1:1) R_f 0.83: **MS** (ESI, -ve, m/z) $[M-2NH_4]^{2-}$ 210.6 (100%): **^{1}H-NMR** (400 MHz, DMSO-d_6/H_2O-d_2) δ; 6.92 (1H, s, H8); 7.05 (1H, s, H6); 7.14 (1H, t, *J*=7 Hz, H4'); 7.32 (1H, s, H1); 7.40 (2H, t, *J*=8 Hz, H3'); 7.66 (2H, d, *J*=8 Hz, H2'): **^{13}C-NMR** (100 MHz, DMSO-d_6/H_2O-d_2) δ; 112.4 (C6); 112.7 (C10); 113.8 (C8); 116.9 (C2'); 123.1 (C1); 125.2 (C4'); 129.1 (C3); 129.9 (C3'); 136.8 (C9); 142.7 (C2); 143.0 (C1'); 152.9 (C7); 153.5 (C5); 181.7 (C4): **IR** (υ, cm^{-1}) 1167 (SO_2-O),

1493 (N=N), 3431 (O-H): **HPLC** (STD254) R_t 6.81 minutes (83%): **UV/Vis** (MeOH, nm) λ_{max} 530, ε 26579 $M^{-1}cm^{-1}$.

5-Amino-4-hydroxy-3-(4'-nitro-phenylazo)-naphthalene-2,7-disulphonic acid di-ammonium salt, **116/a4**

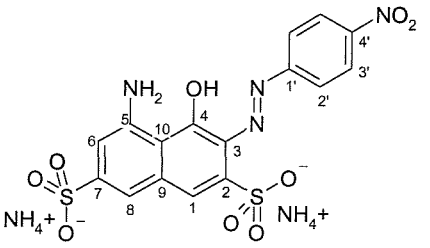

Mpt. >250°C; **TLC** (acetone/^{i}PrOH/NH_4OH; 1:1:1) R_f 0.63: **MS** (ESI, -ve, m/z) $[M-2NH_4]^{2-}$ 233.6 (100%): **HRMS** (ESI, -ve, m/z) $[M-2NH_4+H]^-$ calculated $C_{16}H_{11}N_4O_9S_2$, 466.9973; found 466.9980; error 1.6 ppm: **^{1}H-NMR** (300 MHz, MeOH-d_4) δ; 6.61 (1H, s, H8); 7.02 (1H, s, H6); 7.11 (1H, s, H1); 7.46 (2H, d, *J*=9 Hz, H2'); 7.61 (2H, d, *J*=9 Hz, H3'): **^{13}C-NMR** (75 MHz, d_4-MeOH) δ; 106.8 (C6); 107.5 (C10); 109.5 (C3); 115.2 (C2'); 116.8 (C8); 118.8 (C3'); 118.9 (C1); 122.1 (C9); 125.5 (C5); 137.4 (C7); 144.0 (C2); 144.8 (C4); 147.7 (C4'); 157.5 (C1'): **IR** (υ, cm^{-1}) 1326, 1585 (NO_2), 3354 (O-H): **HPLC** (STD254) R_t 7.47 minutes (95%): **UV/Vis** (MeOH, nm) λ_{max} 538, ε 25912 M^{-1} cm^{-1}.

3-(4'-Chloro-phenylazo)-4-hydroxy-naphthalene-1-sulfonic acid mono ammonium salt, **116/f1** [217]

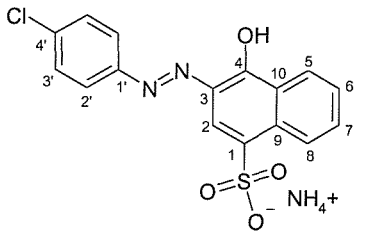

Mpt. >250°C (lit. 299°C); **TLC** (acetone/^{i}PrOH/NH_4OH; 1:1:1) R_f 0.71: **MS** (ESI, -ve, m/z) $[M-NH_4]^-$ 361.0 (100%): **HRMS** (ES, -ve, m/z) $[M-NH_4]^-$ calculated $C_{16}H_{10}N_2O_4SCl$, 361.0055; found 361.0059; error 0.9 ppm: **^{1}H-NMR** (300 MHz, DMSO-d_6) δ; 7.30 (8H, bs, NH_4^+); 7.59 (2H, d, *J*=8 Hz, H3'); 7.65 (1H, pst, *J*=7 Hz, H6); 7.82-7.90 (3H, m, H2'+H7); 7.98 (1H, d, *J*=7 Hz, H8); 8.30 (1H, s, H2); 8.49 (1H, d, *J*=8 Hz, H5): **^{13}C-NMR** (75 MHz, DMSO-d_6) δ; 110.2 (C2); 119.8 (C2'); 124.5 (C5); 124.9 (C6); 125.5 (C8); 126.6 (C10); 127.3 (C7); 129.5 (C3); 129.7 (C3'); 131.3 (C9); 138.7 (C1); 140.2 (C4'); 151.9 (C4); 170.7 (C1'): **IR** (υ, cm^{-1}) 1277, (SO_2-O), 1495 (N=N), 3345 (O-H): **HPLC** (STD254) R_t 7.82 minutes (74%): **UV/Vis** (MeOH, nm) λ_{max} 486, ε 5877 M^{-1} cm^{-1}.

4-(4'-Chloro-phenylazo)-phenol, **116/b1** [218]

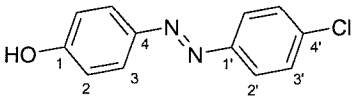

Mpt. 152-154°C (lit. 157-8°C): **TLC** (acetone/^{i}PrOH/NH_4OH; 1:1:1) R_f 0.91: **MS** (ESI, -ve, m/z) $[M\text{-}NH_4]^-$ 231.0 (100%): **HRMS** (ESI, -ve, m/z) $[M\text{-}H]^-$ calculated $C_{12}H_8N_2OCl$, 231.0031; found 231.0332; error 0.7 ppm; **^{1}H-NMR** (300 MHz, DMSO-d_6) δ; 6.23 (2H, d, *J*=8 Hz, H2); 6.74 (2H, d, *J*=9 Hz, H3'); 7.14 (2H, d, *J*=8 Hz, H3); 7.15 (2H, d, *J*=9 Hz, H2'): **^{13}C-NMR** (75 MHz, DMSO-d_6) δ; 116.7 (C2); 124.7 (C3); 126.0 (C2'); 130.2 (C3'); 136.8 (C4'); 147.3 (C4); 152.5 (C1'); 162.4 (C1); **IR** (υ, cm^{-1}) 3211 (O-H); **HPLC** (STD254) R_t 11.97 minutes (99%): **UV/Vis** (MeOH, nm) λ_{max} 354, ε 25151 M^{-1} cm^{-1}.

3-Hydroxy-4-phenylazo-naphthalene-2,7-disulfonic acid, di-ammonium salt, **116/e5**

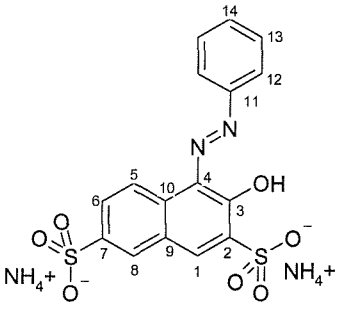

Mpt. >250°C; **TLC** (acetone/^{i}PrOH/NH_4OH; 1:1:1) R_f 0.73: **MS** (ESI, -ve, m/z) $[M\text{-}2NH_4]^{2-}$ 203.0 (100%): **HRMS** (ESI, -ve, m/z) $[M\text{-}2NH_4]^{2-}$ calculated $C_{16}H_{10}O_7N_2S_2$, 202.9970; found 202.9971; error 0.6 ppm: **^{1}H-NMR** (300 MHz, DMSO-d_6) δ; 7.30 (8H, bs, NH_4^+); 7.42 (1H, t, *J*=8 Hz, H14); 7.54 (2H, t, *J*=8 Hz, H13); 7.83 (1H, d, *J*=8 Hz, H12); 7.84 (2H, d, *J*=8 Hz, H5); 7.97 (1H, s, H8); 8.29 (1H, s, H1); 8.51 (1H, d, *J*=8 Hz, H6): **^{13}C-NMR** (75 MHz, DMSO-d_6) δ; 118.4 (C12); 121.0 (C1); 125.4 (C6); 126.6 (C8); 127.5 (C5); 127.7 (C9); 129.5 (C10); 129.9 (C13); 133.5 (C14); 138.4 (C4); 140.5 (C2); 143.4 (C7); 145.9 (C3); 170.4 (C11): **IR** (υ, cm^{-1}) 3421 (O-H); **HPLC** (STD254) R_t 7.02 minutes (90%): **UV/Vis** (MeOH, nm) λ_{max} 488, ε 16660 M^{-1} cm^{-1}.

4-Hydroxy-3-phenylazo-naphthalene-1-sulfonic acid mono ammonium salt, **116/f5**

219

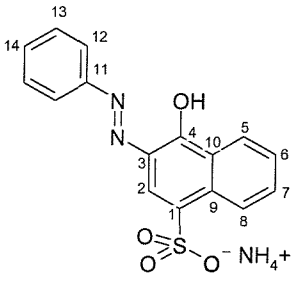

Mpt. >250°C (lit. 254°C); **TLC** (acetone/^{i}PrOH/NH_4OH; 1:1:1) R_f 0.86: **MS** (ESI, -ve, m/z) $[M-NH_4]^-$ 327.0 (100%): **HRMS** (ESI, -ve, m/z) $[M-NH_4]^-$ calculated $C_{16}H_{11}N_2O_4S$, 327.0445; found 327.0434; error 3.4 ppm: **^{1}H-NMR** (300 MHz, DMSO-d_6) δ; 6.77 (1H, d, *J*=8 Hz, H7); 7.45-7.55 (5H, m, H12+H13+H14); 7.74 (1H, t, *J*=8 Hz, H6); 7.92 (1H, d, *J*=8 Hz, H8); 8.23 (1H, d, *J*=8 Hz, H5); 8.71, 8.74 (1H, 2 s, H2): **^{13}C-NMR** (75 MHz, DMSO-d_6) δ; 107.4 (C2); 120.3 (C5); 124.2 (C12); 126.6 (C8); 126.7 (C6); 127.3 (C10); 128.2 (C3); 128.4 (C7); 128.6 (C13); 128.7 (C14); 129.8 (C9); 131.6 (C1); 132.5 (C4); 133.8 (C11): **IR** (υ, cm^{-1}) 3349 (O-H): **HPLC** (STD254) R_t 9.24 minutes (90%): **UV/Vis** (MeOH, nm) λ_{max} 486, ε 18315 M^{-1} cm^{-1}.

6.2.4 Stability study of Polymer Supported Benzene-Diazonium Salt.

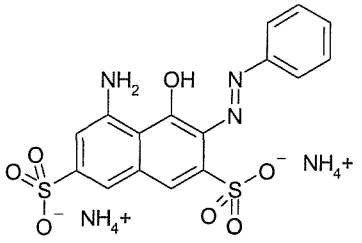

To a solution of aniline (3.72 g, 40.0 mmol) in aq. HCl (12 M, 100 mL) at 0°C was added **108** (71 g) and the reaction was shaken for 40 minutes at 0°C. The reaction mixture was filtered and the filtrate passed through a column (20 mm diameter) of **113** (12 g) and washed with water (2 x 50 mL) and MeOH (2 x 50 mL). The resin was stored in a refrigerator at 4°C, and an aliquot retrieved at a set time (Table 5, col. 1). The resin sample was allowed to warm to room temperature, and 20-30 mg was weighed in to a test tube. To this was added **50** (82 mg, 0.42 mmol) in aq. NH_4OH (18 N, 1 mL) and the reaction was shaken for 30 minutes. The reaction mixture was filtered in a 25 mL volumetric flask, and resin washed with water (2 x 5 mL). The volume was made up to 25 mL with water, and analysed by HPLC (Table 5.5), the result of which are discussed in section 2.4.

*Table 5.5: Results for stability test for resin **114/5**.*

Days	Loading (mmol/g)
0	0.145
1	0.140
2	0.130
4	0.137
8	0.121
90	0.030

6.3 Experimental to Chapter 3

6.3.1 Synthesis of Azo-Dyes 123/1-8

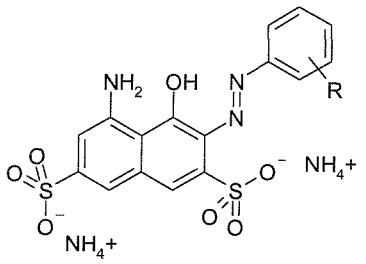

To a solution of aniline derivative (Table 6.6, 95.0 mmol) in MeOH (100 mL) was added aq. HCl (12 N, 10 mL). The solution was cooled to 0°C and **108** (71.0 g) was slowly added, and the reaction mixture was shaken for 40 minutes at 0°C. The reaction was filtered and filtrate was passed through a column (20 mm diameter, 20 mL/min) of **113** (Na^+ form, 12.0 g). A-15 resin was washed with cold MeOH (3 x 20 mL) to remove excess diazonium salt. **50** (425 mg, 1.24 mmol) was dissolved in an aq. NH_4OH (18 N, 30 mL) and A-15 (diazonium form, 12.0 g) was added. The reaction was shaken for 40 minutes. The reaction mixture was then filtered and the resin washed with water (2 x 20 mL). The combined washings and filtrate were concentrated *in vacuo* to 5 mL and applied onto a column of C-18 silica (Supelco Supelclean C-18, 10 g). The column was washed with water and the dye eluted with MeOH (20 mL). The solution was concentrated *in vacuo* and freeze-dried, to give dyes **123/1-8** as magenta solids in variable yields and purities (Table 6.7).

Table 6.6: Mass of anilines used.

Product	Aniline derivative	Mass used
123/1	2-methyl-6-ethylaniline	12.8 g
123/2	4-iodoaniline	19.6 g
123/3	4-bromoaniline	16.6 g
123/4	4-chloroaniline	11.6 g
123/5	4-^{t}butylaniline	14.2 g
123/6	2-fluoroaniline	10.5 g
123/7	2,4,6-trimethylaniline	12.8 g
123/8	aniline	8.8 g

*Table 6.7: Yields and purities of dyes **123/1-8.***

Dye	R	Yield (%)	Purity [a]
123/1	6-Ethyl-2-methyl-	29	95
123/2	4-Iodo-	32	95
123/3	4-Bromo-	64	87
123/4	4-Chloro-	68	75
123/5	4-^{t}Butyl-	64	95
123/6	2-Fluoro-	68	40
123/7	2,4,6-Trimethyl-	95	90
123/8	(H)	95	88

a) HPLC @ 254 nm, after C-18 purification.

5-Amino-4-hydroxy-3-(6'-ethyl-2'-methyl-phenylazo)-naphthalene-2,7-disulfonic acid, di-ammonium salt, **123/1**

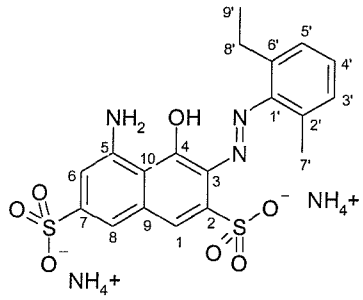

Mpt. >250°C: **TLC** (acetone/^{i}PrOH/NH_4OH; 1:1:1) R_f 0.79: **MS** (ESI, -ve, m/z) $[M-2NH_4]^{2-}$ 231.7 (100%): **HRMS** (ESI, -ve, m/z) $[M-2NH_4+H]^-$ calculated $C_{19}H_{18}N_3O_7S_2$, 464.0592; found 464.0600; error 1.7 ppm: **^{1}H-NMR** (400 MHz, DMSO-d_6/H_2O-d_2) δ; 1.12 (3H, t, *J*=7 Hz, H9'); 2.51 (3H, s, H7'); 2.86 (2H, q, *J*=7 Hz, H8'); 6.95 (1H, s, H8); 7.02 (1H, s, H6); 7.04-7.18 (3H, m, H3'+H4'+H5'); 7.35 (1H, s, H1): **^{13}C-NMR** (100 MHz, DMSO-d_6/H_2O-d_2) δ; 14.9 (C9'); 20.3 (C7'); 25.1 (C8'); 111.7 (C6); 113.3 (C10); 113.4 (C8); 122.4 (C1); 126.7 (C5'); 127.7 (C3'); 129.4 (C4'); 130.1 (C3); 131.1 (C2'); 136.0 (C6'); 136.8 (C9); 138.0 (C1'); 142.1 (C2); 151.9 (C7); 153.0 (C5); 181.0 (C4): **IR** (υ, cm^{-1}) 1178 (SO_2-O), 1490 (N=N), 3425 (O-H): **HPLC** (S5OD) R_t 2.78 minutes (95%); **UV/Vis** (MeOH, nm) λ_{max} 512, ε 42676 $M^{-1}cm^{-1}$

5-Amino-4-hydroxy-3-(4'-iodo-phenylazo)-naphthalene-2,7-disulfonic acid, di-ammonium salt, **123/2** [220]

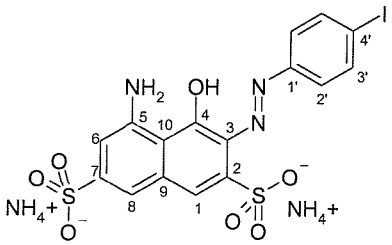

Mpt. >250°C (lit. 265°C): **TLC** (acetone/^{i}PrOH/NH_4OH; 1:1:1) R_f 0.79: **MS** (ESI, -ve, m/z) $[M-2NH_4]^{2-}$ 273.6 (100%): **HRMS** (ESI, -ve, m/z) $[M-2NH_4]^{2-}$ calculated $C_{16}H_{10}N_3O_7S_2I$, 273.4508, found 273.4512; error 1.6 ppm: ^{1}**H-NMR** (400 MHz, DMSO-d_6/H_2O-d_2) δ; 6.92 (1H, s, H8); 7.04 (1H, d, $J_{6\text{-}8}$=2 Hz, H6); 7.31 (1H, s, H1); 7.41, 7.47 (1H, 2 d, J=12 Hz, H2'); 7.67, 7.70 (1H, 2 d, J=12 Hz, H3'): ^{13}**C-NMR** (100 MHz, DMSO-d_6/H_2O-d_2) δ; 88.7 (C4'); 112.6 (C6); 113.5 (C10); 114.0 (C8); 119.0 (C2'); 123.8 (C1); 129.7 (C3); 136.7 (C9); 138.4 (C3'); 138.6 (C1'); 142.3 (C2); 152.7 (C7), 153.4 (C5); 181.9 (C4): **IR** (υ, cm^{-1}) 1175 (SO_2-O), 1493 (N=N), 3420 (O-H): **HPLC** (S5OD) R_t 2.28 minutes (95%): **UV/Vis** (MeOH, nm) λ_{max} 532, ε 24923 $M^{-1}cm^{-1}$.

5-Amino-4-hydroxy-3-(4'-bromo-phenylazo)-naphthalene-2,7-disulfonic acid, di-ammonium salt, **123/3** [221]

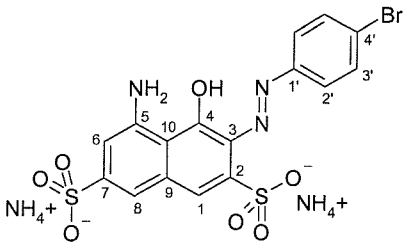

Mpt. >250°C (lit. 273-4°C): **TLC** (acetone/^{i}PrOH/NH_4OH; 1:1:1) R_f 0.81: **MS** (ESI, -ve, m/z) $[M-2NH_4]^{2-}$ 249.0 (50%): **HRMS** (ESI, -ve, m/z) $[M-2NH_4+H]^{-}$ calculated $C_{16}H_{11}O_7N_3S_2Br$, 499.9229 and 501.9207; found 499.9224 and 501.9209; errors 0.7 and 0.4 ppm: ^{1}**H-NMR** (400 MHz, DMSO-d_6/H_2O-d_2) δ; 6.92 (1H, d, $J_{8\text{-}6}$=2 Hz, H8); 7.03 (1H, d, $J_{6\text{-}8}$=2 Hz, H6); 7.24, 7.52 (2H, 2 d, J=12 Hz, H2'); 7.30 (1H, s, H1); 7.59 (2H, d, J=12 Hz, H3'): ^{13}**C-NMR** (100 MHz, DMSO-d_6/H_2O-d_2) δ; 110.9 (C10); 112.5 (C6); 113.9 (C8); 116.9 (C4'); 118.7 (C3'); 123.8 (C1); 129.2 (C3); 132.6 (C2'); 132.9 (C1'); 136.7 (C9); 139.7 (C2); 152.6 (C7); 153.3 (C5); 181.9 (C4): **IR** (υ, cm^{-1}) 1164 (SO_2-O), 1493 (N=N), 3423 (O-H): **HPLC** (S5OD) R_t 2.68 minutes (87%): **UV/Vis** (MeOH, nm) λ_{max} 354, ε 28420 $M^{-1}cm^{-1}$

5-Amino-4-hydroxy-3-(4'-chloro-phenylazo)-naphthalene-2,7-disulfonic acid, di-ammonium salt, **123/4** [222]

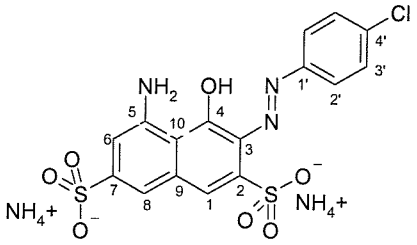

Mpt. >250°C (lit. 281-2°C): **TLC** (acetone/^{i}PrOH/NH_4OH; 1:1:1) R_f 0.83: **MS** (ESI, -ve, m/z) $[M-2NH_4]^{2-}$ 227.5 (100%): **HRMS** (ESI, -ve, m/z) $[M-2NH_4]^{2-}$ calculated $C_{16}H_{10}N_3O_7S_2Cl$, 227.4830; found 227.4826; error 1.6 ppm: **^{1}H-NMR** (400 MHz, DMSO-d_6/H_2O-d_2) δ; 6.93 (1H, d, $J_{6\text{-}8}$=2 Hz, H6); 7.05 (1H, d, $J_{8\text{-}6}$=2 Hz, H8); 7.28, 7.40 (2H, 2 d, J=12 Hz, H2'); 7.31 (1H, s, H1); 7.64 (2H, d, J=12 Hz, H3'): **^{13}C-NMR** (100 MHz, DMSO-d_6/H_2O-d_2) δ; 112.6 (C10); 112.5 (C6); 113.9 (C8); 116.1 (C4'); 118.4 (C3'); 125.0 (C1); 129.1 (C1'); 129.7 (C2'); 130.0 (C3); 136.7 (C9); 142.0 (C2); 152.3 (C7); 153.3 (C5); 181.8 (C4): **IR** (υ, cm^{-1}) 1163 (SO_2-O), 1492 (N=N), 3424 (O-H): **HPLC** (S5OD) R_t 2.62 minutes (75%): **UV/Vis** (MeOH, nm) λ_{max} 530, ε 28558 $M^{-1}cm^{-1}$.

5-Amino-4-hydroxy-3-(4'-[^{t}butyl]-phenylazo)-naphthalene-2,7-disulfonic acid, di-ammonium salt, **123/5**

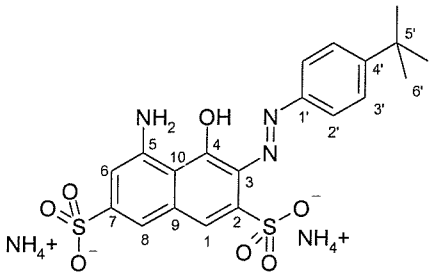

Mpt. >250°C: **TLC** (acetone/^{i}PrOH/NH_4OH; 1:1:1) R_f 0.81: **MS** (ESI, -ve, m/z) $[M-2NH_4]^{2-}$ 238.5 (100%): **HRMS** (ESI, -ve, m/z) $[M-2NH_4+H]^{-}$ calculated $C_{20}H_{20}N_3O_7S_2$, 478.0748; found 478.0761; error 2.7 ppm: **^{1}H-NMR** (400 MHz, DMSO-d_6/H_2O-d_2) δ; 1.35 (9H, s, H6'); 7.04 (1H, d, $J_{8\text{-}6}$=2 Hz, H8); 7.11 (1H, d, $J_{6\text{-}8}$=2 Hz, H6); 7.42 (1H, s, H1); 7.51 (2H, d, J=12 Hz, H3'); 7.68 (2H, d, J=12 Hz, H2'): **^{13}C-NMR** (100 MHz, DMSO-d_6/H_2O-d_2) δ; 29.7 (C6'); 32.9 (C5'); 110.2 (C6); 111.4 (C10); 111.9 (C8); 115.0 (C2'); 121.1 (C1); 124.9 (C3'); 126.7 (C3); 135.1 (C9); 138.4 (C1'); 140.3 (C2); 146.7 (C4'); 150.1 (C7); 151.3 (C5); 179.6 (C4): **IR** (υ, cm^{-1}) 1180 (SO_2-O), 1493 (N=N), 3424 (O-H): **HPLC** (S5OD) R_t 3.10 minutes (95%): **UV/Vis** (MeOH, nm) λ_{max} 534, ε 25248 $M^{-1}cm^{-1}$.

5-Amino-4-hydroxy-3-(2'-fluoro-phenylazo)-naphthalene-2,7-disulfonic acid, di-ammonium salt, **123/6**

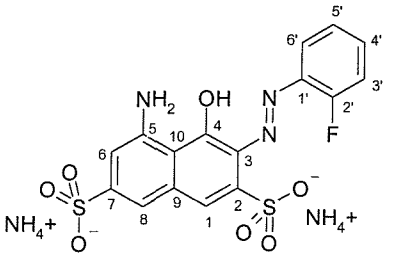

Mpt. >250°C: **TLC** (acetone/^{i}PrOH/NH_4OH; 1:1:1) R_f 0.82: **MS** (ESI, -ve, m/z) $[M-2NH_4]^{2-}$ 219.5 (100%): **HRMS** (ESI, -ve, m/z) $[M-2NH_4]^{2-}$ calculated $C_{16}H_{10}N_3O_7S_2F$, 219.4978; found 219.4975; error 1.2 ppm: **^{1}H-NMR** (400 MHz, DMSO-d_6/H_2O-d_2) δ; 6.99 (1H, d, $J_{8\text{-}6}$=2 Hz, H8); 7.08 (1H, d, $J_{6\text{-}8}$=2 Hz, H6); 7.10-7.34 (4H, m, H3'+H4'+H5'+H6'); 7.38 (1H, s, H1): **^{13}C-NMR** (100 MHz, DMSO-d_6/H_2O-d_2) δ; 109.3 (C6); 111.2 (C10); 112.8 (C8); 113.0 (C5'); 123.9 (C1); 124.6 (C6'); 126.3 (C3'); 130.4 (C3); 136.9 (C4'); 140.6 (C1'); 141.8 (C9); 145.2 (C2); 151.2 (2 peaks, C2'); 152.4 (C7); 153.6 (C5'); 182.3 (C4): **IR** (υ, cm^{-1}) 1182 (SO_2-O), 1506 (N=N), 3437 (O-H): **HPLC** (S5OD) R_t 2.42 minutes (40%): **UV/Vis** (MeOH, nm) λ_{max} 530, ε 16251 $M^{-1}cm^{-1}$.

5-Amino-4-hydroxy-3-(2',4',6'-trimethyl-phenylazo)-naphthalene-2,7-disulfonic acid, di-ammonium salt, **123/7**

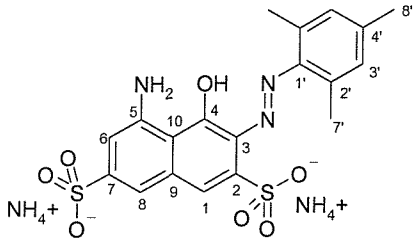

Mpt. >250°C: **TLC** (acetone/^{i}PrOH/NH_4OH; 1:1:1) R_f 0.84: **MS** (ESI, -ve, m/z) $[M-2NH_4]^{2-}$ 231.5 (100%): **HRMS** (ESI, -ve, m/z) $[M-2NH_4+H]^{-}$ calculated $C_{19}H_{18}N_3O_7S_2$, 464.0592; found 464.0598; error 1.3 ppm: **^{1}H-NMR** (400 MHz, DMSO-d_6/H_2O-d_2) δ; 2.33 (3H, s, H8'); 2.58 (6H, s, H7'); 7.03-7.05 (3H, m, H8+H3'); 7.12 (1H, d, $J_{6\text{-}8}$=2 Hz, H6); 7.45 (1H, s, H1): **^{13}C-NMR** (100 MHz, DMSO-d_6/H_2O-d_2) δ; 20.0 (C7'); 20.8 (C8'); 111.5 (C6); 113.3 (C8); 112.0 (C1); 129.0 (C3); 129.8 (C2'); 130.4 (C3'); 135.5 (C4'); 136.3 (C1'); 136.8 (C9); 142.4 (C2); 146.2 (C10); 152.2 (C7); 153.0 (C5); 180.7 (C4): **IR** (υ, cm^{-1}) 1166 (SO_2-O), 1489 (N=N), 3411 (O-H): **HPLC** (S5OD) R_t 2.81 minutes (90%): **UV/Vis** (MeOH, nm) λ_{max} 530, ε 20062 $M^{-1}cm^{-1}$.

5-Amino-4-hydroxy-3-phenylazo-naphthalene-2,7-disulfonic acid di-ammonium salt, **123/8** [216]

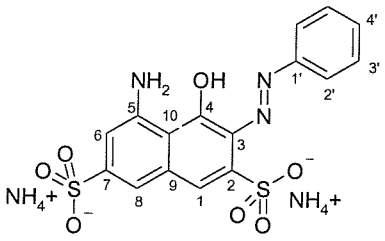

Mpt. >250°C: **TLC** (acetone/^{i}PrOH/NH_4OH; 1:1:1) R_f 0.82: **MS** (ESI, -ve, m/z) $[M-2NH_4]^{2-}$ 210.5 (100%): **HRMS** (ESI, -ve, m/z) $[M-2NH_4]^{2-}$ calculated $C_{16}H_{11}N_3O_7S_2$, 210.5025; found 210.5022; error 1.5 ppm: **^{1}H-NMR** (400 MHz, DMSO-d_6/H_2O-d_2) δ; 6.97 (1H, d, $J_{8\text{-}6}$=2 Hz, H8); 7.02 (1H, d, $J_{6\text{-}8}$=2 Hz, H6); 7.15 (1H, t, J=8 Hz, H4'); 7.33 (1H, s, H1); 7.39 (2H, t, J=8 Hz, H3'); 7.61 (2H, d, J=8 Hz, H2'): **^{13}C-NMR** (100 MHz, DMSO-d_6/H_2O-d_2) δ; 110.4 (C6); 110.5 (C10); 111.7 (C8); 114.8 (C2'); 121.0 (C1); 123.0 (C4'); 127.2 (C3); 127.8 (C3'); 134.8 (C9); 141.0 (C2); 141.1 (C1'); 151.5 (C7); 151.5 (C5); 179.8 (C4): **IR** (υ, cm^{-1}) 1161 (SO_2-O), 1491 (N=N), 3423 (O-H): **HPLC** (S5OD) R_t 2.35 minutes (88%): **UV/Vis** (MeOH, nm) λ_{max} 528, ε 31919 $M^{-1}cm^{-1}$.

6.3.2 Synthesis of Symmetrical Monochloro-Triazines 124/aa-ee

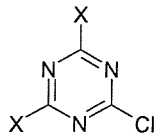

To a solution of cyanuric chloride (276 mg, 1.5 mmol) in acetone (3 mL) was added a solution of alkyl amine (Table 6.8, 6.0 mmol) dissolved in water (10 mL). The reaction was shaken for 1 hour, followed by centrifugation. The supernatant was decanted, and water (10 mL) was added. The reaction mixture was shaken and centrifuged, and the washing process repeated once. Finally the supernatant was decanted and water (10 mL) was added, before the sample was freeze-dried, to give symmetrical monochloro-triazines **124/aa-ee** in variable yields and purities (Table 6.9).

*Table 6.8: Masses of alkyl amines used in the synthesis of symmetrical monochloro-triazine **124/aa-ee.***

Product	Amines	Mass Used
124/aa	Benzylamine	642 mg
124/bb	Cyclohexylamine	595 mg
124/cc	*N,N*-dibutylamine	774 mg
124/dd	Ethanolamine	366 mg
124/ee	Furfurylamine	774 mg

*Table 6.9: Yields and purities of symmetrical monochloro-triazines **124/aa-ee.***

Product	Yield (%)	Purity [a]
124/aa	68%	95
124/bb	50%	95
124/cc	38%	95
124/dd	95%	95
124/ee	63%	87

a) HPLC @ 254 nm.

N,N'-Dibenzyl-6-chloro-[1,3,5]triazine-2,4-diamine, **124/aa** [223]

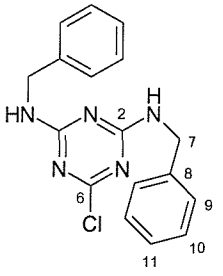

Mpt. 237-9°C: **TLC** (acetone) R_f 0.68: **MS** (ESI, +ve, m/z) $[M+H]^+$ 326.0 (100%): **HRMS** (ESI, +ve , m/z) $[M+H]^+$ calculated $C_{17}H_{17}N_5Cl$, 326.1167; found 326.1164; error 0.9 ppm: **^{1}H-NMR** (300 MHz, DMSO-d_6) δ; 4.53 (4H, d, *J*=6 Hz, H7); 7.27-7.46 (10H, m, H9+H10+H11): **^{13}C-NMR** (75 MHz, DMSO-d_6) δ: 44.06 (C7); 127.2 (C11); 127.8 (C9); 128.7 (C10); 138.7 (C8); 165.9 (C2); 168.3 (C6): **IR** (υ, cm^{-1}) 796 (C-Cl), 1404 (N-H), 1546 (C=N), 2946 (C-H): **HPLC** (L5OD) R_t 2.78 minutes (95%).

6-Chloro-*N,N'*-dicyclohexyl-[1,3,5]triazine-2,4-diamine, **124/bb** [162]

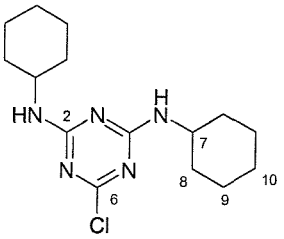

Mpt. 179-82°C (lit. 188-9°C): **TLC** (isohexane/EtOAc/AcOH; 20:20:1) R_f 0.69: **MS** (ESI, +ve, m/z) $[M+H]^+$ 310.2 (100%): **HRMS** (ESI, +ve, m/z) $[M+H]^+$ calculated $C_{15}H_{25}N_5Cl$, 310.1793; found 310.1792; 0.12 ppm error: ^{1}**H-NMR** (300 MHz, DMSO-d_6) δ; 0.99-1.42 (10H, m, H_{ax}); 1.43-1.96 (10H, m, H_{eq}); 3.51-3.79 (2H, m, H7): ^{13}**C-NMR** (75 MHz, DMSO-d_6) δ: 24.8 (C10); 25.0 (C9); 31.9 (C8); 49.8 (C7); 164.4 (C2); 167.5 (C6): **IR** (υ, cm^{-1}) 796 (C-Cl), 1407 (N-H), 1536 (C=N), 2853 (C-H): **HPLC** (L5OD) R_t 3.25 minutes (95%).

N,N,N',N'-Tetrabutyl-6-chloro-[1,3,5]triazine-2,4-diamine, **124/cc** [168]

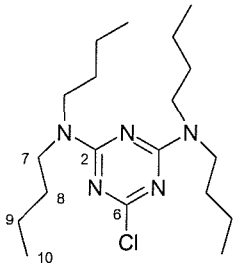

Mpt. Oil (lit. oil): **TLC** (isohexane/AcOH; 20:1) R_f 0.75: **MS** (ESI, +ve, m/z) $[M+H]^+$ 370.3 (100%): **HRMS** (ESI, +ve , m/z) $[M+H]^+$ calculated $C_{19}H_{37}N_5Cl$, 370.2732; found 370.2727; error 1.3 ppm: ^{1}**H-NMR** (300 MHz, DMSO-d_6) δ; 0.88-0.98 (12H, m, H10); 1.25-1.39 (8H, m, H9); 1.48-1.63 (8H, m, C8); 3.40-3.56 (8H, m, H7): ^{13}**C-NMR** (75 MHz, DMSO-d_6) δ: 14.1 (C10); 20.1 (C9); 29.4 (C8); 46.9 (C7); 164.6 (C2); 189.9 (C6): **IR** (υ, cm^{-1}) 756 (C-Cl), 1449 (N-H), 1555 (C=N), 2924 (C-H): **HPLC** (L5OD) R_t 3.59 minutes (95%).

2-[4'-Chloro-6'-(2''-hydroxy-ethylamino)-[1',3',5']triazin-2'-ylamino]-ethanol, **124/dd** [162]

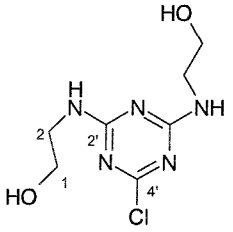

Mpt. 166-9°C (lit. 172-4°C): **TLC** (acetone) R_f 0.44: **MS** (ESI, +ve, m/z) $[M+H]^+$ 234.0 (100%): **HRMS** (ESI, +ve , m/z) $[M+H]^+$ calculated $C_7H_{13}N_5O_2Cl$, 234.0752; found 234.0750; error 1.1 ppm: **^{1}H-NMR** (300 MHz, DMSO-d_6) δ; 3.16-3.35 (4H, m, H2); 3.36-3.54 (4H, m, H1): **^{13}C-NMR** (75 MHz, DMSO-d_6) δ: 43.1 (C2); 59.3 (C1); 165.5 (C2'); 168.2 (C4'): **IR** (υ, cm^{-1}) 798 (C-Cl), 1402 (N-H), 1548 (C=N), 2941 (C-H) 3248 (br, O-H): **HPLC** (S5OD) R_t 0.70 minutes (95%).

6-Chloro-*N,N'*-bis-furan-2'-ylmethyl-[1,3,5]triazine-2,4-diamine, **124/ee** [224]

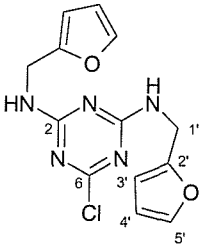

Mpt. (decomposed) (lit. 243°C): **TLC** (isohexane/EtOAc/AcOH; 20:20:1) R_f 0.52: **MS** (ESI, +ve, m/z) $[M+H]^+$ 306.0 (100%): **HRMS** (ESI, +ve , m/z) calculated $C_{13}H_{13}N_5O_2Cl$, 306.0753; found 306.0751; error 0.6 ppm: **^{1}H-NMR** (300 MHz, DMSO-d_6) δ; 4.32-4.51 (4H, m, H1'); 6.20 (2H, d, *J*=3 Hz, H3'); 6.35 (2H, t, *J*=3 Hz, H4'); 7.54 (2H, d, *J*=3 Hz, H5'): **^{13}C-NMR** (75 MHz, DMSO-d_6) δ: 37.1 (C1'); 107.1 (C3'); 110.5 (C4'); 142.1 (C5'); 152.1 (C2'); 165.2 (C2); 168.0 (C6): **IR** (υ, cm^{-1}) 796 (C-Cl), 1408 (N-H), 1543 (C=N), 2954 (C-H): **HPLC** (S5OD) R_t 3.76 minutes (87%).

6.3.3 Synthesis of Unsymmetrical Monochloro-Triazines 124/ab-de

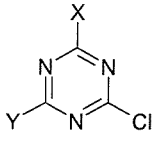

To a solution of cyanuric chloride (278 mg, 1.5 mmol) in acetone (3 mL) at 0°C was added water (7 mL) at 0°C, resulting in precipitation of the cyanuric chloride as a fine suspension. A solution of amine X (Table 6.10, col. 2, 3.0 mmol) in water (3 mL) was added dropwise to the cyanuric chloride suspension and the reaction was stirred for 20 minutes at 0°C. The reaction mixture was then filtered and the solid was washed with water (2 x 10 mL), and redissolved in acetone (3 mL). A solution of amine Y (Table 10, col. 3, 3.0 mmol) in water (7 mL) was added and the reaction mixture was shaken for 20 minutes, followed by centrifugation. The supernatant was decanted and acetone/water (1:3, 10 mL) was added. The mixture was shaken, centrifuged, and the supernatant was

decanted. Water (5 mL) was added and the sample was freeze dried, to give the monochloro-triazines **124/ab-de** in variable yields and purities (Table 6.11).

*Table 6.10: Masses of amines used for the synthesis of unsymmetrical monochloro-triazines **124/ab-de**.*

Product	Amine X	Mass used	Amine Y	Mass used
124/ab	Benzylamine	321 mg	Cyclohexylamine	297 mg
124/ac	Benzylamine	321 mg	*N,N*-dibutylamine	398 mg
124/ad	Benzylamine	321 mg	Ethanolamine	183 mg
124/ae	Benzylamine	321 mg	Furfurylamine	398 mg
124/be	Furfurylamine	398 mg	Cyclohexylamine	297 mg
124/ce	Furfurylamine	398 mg	*N,N*-dibutylamine	398 mg
124/de	Furfurylamine	398 mg	Ethanolamine	183 mg

*Table 6.11: Yields and purities of unsymmetrical monochloro-triazines **124/ab-de.***

Product	Yield (%)	Purity [a]
124/ab	73	87
124/ac	67	88
124/ad	58	84
124/ae	56	64
124/be	73	75
124/ce	67	94
124/de	58	78

a) HPLC @ 254 nm.

N-Benzyl-6-chloro-*N'*-cyclohexylmethyl-[1,3,5]triazine-2,4-diamine, **124/ab**

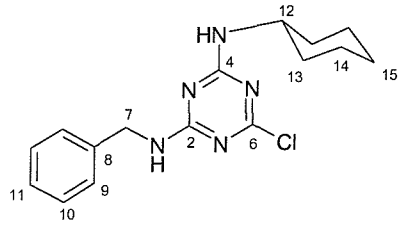

Mpt. 138-41°C: **TLC** (isohexane/EtOAc/AcOH; 20:20:1) R_f 0.74: **MS** (ESI, +ve, m/z) $[M+H]^+$ 318.2 (100%): **HRMS** (ESI, +ve, m/z) $[M+H]^+$ calculated $C_{16}H_{21}N_5Cl$, 318.1480; found 318.1476; error 1.1 ppm: **^{1}H-NMR** (300 MHz, DMSO-d_6) δ; 1.02-1.31 (H5, m, H_{ax}); 1.49-1.85 (5H, m, H_{eq}); 3.63 (1H, m, H12); 4.38 (2H, d, *J*=6 Hz, H7); 7.12-7.40 (5H, m, H9+H10+H11): **^{13}C-NMR** (75 MHz, DMSO-d_6) δ; 24.8 (C15); 25.3 (C14); 32.0 (C13); 44.0 (C7); 49.4 (C12); 126.8 (C11); 127.5 (C9); 128.2 (C10); 139.6 (C8);

164.4 (C4); 165.5 (C2); 167.7 (C6): **IR** (υ, cm^{-1}) 801 (C-Cl), 1404 (N-H), 1538 (C=N), 2933 (C-H): **HPLC** (L5OD) R_t 2.97 minutes (87%).

N-Benzyl-*N'*,*N'*-dibutyl-6-chloro-[1,3,5]triazine-2,4-diamine, **124/ac**

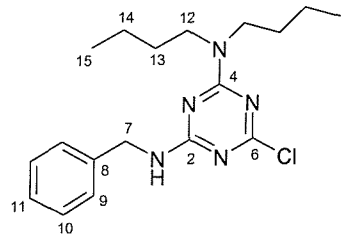

Mpt. 86-7°C: **TLC** (isohexane/EtOAc/AcOH; 20:20:1) R_f 0.83: **MS** (ESI, +ve, m/z) $[M+H]^+$ 348.2 (100%): **HRMS** (ESI, +ve, m/z) $[M+H]^+$ calculated $C_{18}H_{27}N_5Cl$, 348.1950; found 348.1946; error 1.1 ppm: **^{1}H-NMR** (300 MHz, DMSO-d_6) δ; 0.57-0.95 (6H, m, H15); 1.08-1.32 (4H, m, H14); 1.33-1.54 (4H, m, H13); 3.30-3.51 (4H, m, H12); 4.42 (2H, d, *J*=6 Hz, H7); 7.15-7.38 (5H, m, H9+H10+H11): **^{13}C-NMR** (75 MHz, DMSO-d_6) δ; 13.8 (C15); 19.5 (C14); 29.6 (C13); 43.7 (C7); 46.2 (C12); 126.7 (C11); 127.0 (C9); 128.3 (C10); 139.5 (C8); 164.1 (C4); 165.2 (C2); 168.1 (C6): **IR** (υ, cm^{-1}) 798 (C-Cl), 1403 (N-H), 1537 (C=N), 2929 (C-H): **HPLC** (L5OD) R_t 3.79 minutes (88%).

2-(4'-Benzylamino-6'-chloro-[1',3',5']triazin-2'-ylamino)-ethanol, **124/ad**

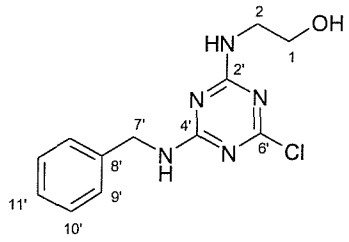

Mpt. 106-108°C: **TLC** (DCM/EtOAc/AcOH; 1:1:0.05) R_f 0.72: **MS** (ESI, +ve, m/z) $[M+H]^+$ 280.1 (82%): **HRMS** (ESI, +ve, m/z) $[M+H]^+$ calculated $C_{12}H_{15}N_5O_1Cl$, 280.0960; found 280.0958; error 0.47 ppm: **^{1}H-NMR** (300 MHz, DMSO-d_6) δ; 3.31-3.49 (2H, m, H2), 3.50-3.60 (2H, m, H1); 4.48 (2H, s, H7'); 7.32-7.45 (3H, m, H9'+H1'+H11'): **^{13}C-NMR** (75 MHz, DMSO-d_6) δ; 43.0 (C7'); 44.0 (C2); 59.5 (C1); 127.2 (C11'); 128.0 (C9'); 129.4 (C10'); 139.9 (C8'); 165.3 (C2'); 165.5 (C4'); 168.0 (C6'): **IR** (υ, cm^{-1}) 798 (C-Cl), 1406 (N-H), 1545 (C=N), 2945 (C-H), 3249 (br, O-H): **HPLC** (S5OD) R_t 3.15 minutes (84%).

N-Benzyl-6-chloro-*N'*-furan-2'-ylmethyl-[1,3,5]triazine-2,4-diamine, **124/ae** [224]

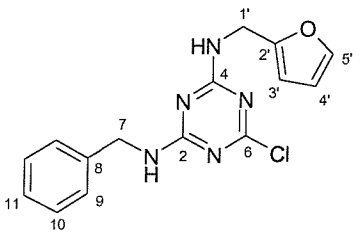

Mpt. 126-8°C (lit. 133°C): **TLC** (DCM/EtOAc/AcOH; 1:1:0.05) R_f 0.87: **MS** (ESI, +ve, m/z) $[M+H]^+$ 316.1 (30%): **HRMS** (ESI, +ve, m/z) $[M+H]^+$ calculated $C_{15}H_{15}N_5OCl$, 316.0960: found 316.0957; 0.77 ppm error: **^{1}H-NMR** (300 MHz, DMSO-d_6) δ; 4.37-4.47 (2H, m, H1'+H7); 6.07-6.41 (2H, m, H3'+H4'); 7.18-7.38 (5H, m, H9+H10+H11); 7.52 (1H, d, *J*=7 Hz, H5'): **^{13}C-NMR** (75 MHz, DMSO-d_6) δ; 37.0 (C1); 43.7 (C7); 107.0 (C3'); 110.5 (C4'); 126.9 (C11); 127.5 (C9); 128.4 (C10); 139.4 (C8'); 142.1 (C5'); 152.1 (C2'); 165.3 (C2); 165.4 (C4); 164.0 (C6): **IR** (υ, cm^{-1}) 797 (C-Cl), 1406 (N-H), 1544 (C=N), 2952 (C-H): **HPLC** (S5OD) R_t 3.94 minutes (64%).

6-Chloro-*N*-cyclohexyl-*N'*-furan-2'-ylmethyl-[1,3,5]triazine-2,4-diamine, **124/be** [224]

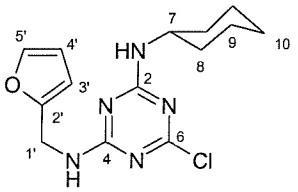

Mpt. 117-119°C (lit. 128°C): **TLC** (isohexane/AcOH; 20:1) R_f 0.36: **MS** (ESI, +ve, m/z) $[M+H]^+$ 308.2 (100%): **HRMS** (ESI, +ve, m/z) $[M+H]^+$ calculated $C_{14}H_{19}N_5OCl$, 308.1272; found 308.1269; error 1.1 ppm: **^{1}H-NMR** (300 MHz, DMSO-d_6) δ; 0.96-1.42 (5H, m, H_{ax}); 1.49-1.85 (5H, m, H_{eq}); 4.47 (2H, d, *J*=6 Hz, H1'); 6.17 (1H, d, *J*=3 Hz, H3'); 6.32-6.43 (1H, m, H4'); 7.59 (1H, bs, H5'): **^{13}C-NMR** (75 MHz, DMSO-d_6) δ; 24.7 (C10); 25.2 (C9); 32.0 (C8); 37.4 (C1'); 49.4 (C7); 106.8 (C3'); 110.6 (C4'); 142.1 (C5'); 152.3 (C2'); 164.4 (C4); 165.4 (C2); 168.0 (C6): **IR** (υ, cm^{-1}) 797 (C-Cl), 1408 (N-H), 1538 (C=N), 2934 (C-H): **HPLC** (L5OD) R_t 2.84 minutes (75%).

N,N-Dibutyl-6-chloro-*N'*-furan-2'-ylmethyl-[1,3,5]triazine-2,4-diamine, **124/ce**

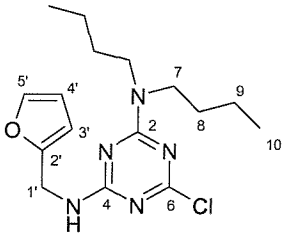

Mpt. 68-9°C: **TLC** (isohexane/AcOH; 20:1) R_f 0.20: **MS** (ESI, +ve, m/z) $[M+H]^+$ 338.2 (100%): **HRMS** (ESI, +ve, m/z) $[M+H]^+$ calculated $C_{16}H_{25}ON_5Cl$, 338.1742; found

388.1735; error 2.0 ppm: **^{1}H-NMR** (300 MHz, DMSO-d_6) δ; 0.88 (6H, d, *J*=7 Hz, H10); 1.14-1.32 (4H, m, H9); 1.40-1.59 (4H, m, H8); 3.42 (4H, t, *J*= 7 Hz, H7); 4.38 (2H, d, *J*=7 Hz, H1'); 6.18 (1H, d, *J*=3 Hz, H3'); 6.37 (1H, t, *J*=3 Hz, H4'); 7.55 (1H, bs, H5'): **^{13}C-NMR** (75 MHz, DMSO-d_6) δ; 13.8 (C10); 19.5 (C9); 29.6 (C8); 37.2 (C1'); 46.2 (C7); 106.6 (C3'); 110.4 (C4'); 142.1 (C5'); 152.4 (C2'); 164.1 (C2); 165.1 (C4); 168.1 (C6): **IR** (υ, cm^{-1}) 797 (C-Cl), 1405 (N-H), 1536 (C=N), 2956 (C-H): **HPLC** (L5OD) R_t 3.50 minutes (94%).

2-{4'-Chloro-6'-[(furan-2"-ylmethyl)-amino]-[1',3',5']triazin-2'-ylamino}-ethanol, **124/de**

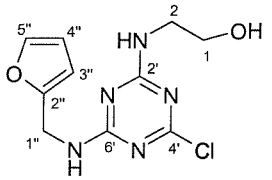

Mpt. 162-3°C: **TLC** (EtOAc/DCM/AcOH; 20:20:1) R_f 0.55: **MS** (ESI, +ve, m/z) $[M+H]^+$ 370.1 (100%): **HRMS** (ESI, +ve, m/z) $[M+H]^+$ calculated $C_{10}H_{13}N_5O_2Cl$, 270.0753; found 270.0752; error 0.6 ppm: **^{1}H-NMR** (300 MHz, DMSO-d_6) δ; 3.23-3.40 (4H, m, H1+H2); 4.41 (2H, d, *J*=7 Hz, H1"); 6.26 (1H, d, *J*=3 Hz, H3"); 6.38 (1H, t, *J*=3 Hz, H4"); 7.54 (1H, bs, H5"): **^{13}C-NMR** (75 MHz, DMSO-d_6) δ; 37.0 (C1"); 43.1 (C2); 59.3 (C1); 107.2 (C3"); 110.6 (C4"); 142.1 (C5"); 152.1 (C2"); 165.4 (C6'); 165.6 (C2'); 168.0 (C4'): **IR** (υ, cm^{-1}) 797 (C-Cl), 1407 (N-H), 1545 (C=N), 2951 (C-H), 3248 (br, O-H): **HPLC** (S5OD) R_t 2.90 minutes (78%).

6.3.4 Synthesis of Monochloro-Triazines 124/bc, 124/bd and 124/dc.

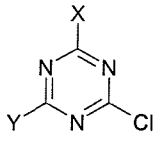

To a solution of cyanuric chloride (556 mg, 3.0 mmol) in acetone (2 mL) at 0°C, a solution of amine X (Table 6.12, col. 2, 6 mmol) in water (20 mL) was, resulting in precipitation of the cyanuric chloride as a fine suspension. The reaction was stirred for 30 minutes at 0°C. The reaction mixture was concentrated *in vacuo* to about 15 mL, and extracted with EtOAc (3 x 30 mL). The extractions were combined, dried over anhydrous $MgSO_4$ and concentrated to dryness *in vacuo*, to yield an oil which was redissolved in acetone (2 mL). A solution of amine Y (Table 6.12, col. 3, 6.0 mmol) in water (25 mL) was added dropwise to the acetone solution over 5 minutes, resulting in precipitation of the

dichloro-triazine as a fine suspension. The reaction was shaken for 30 minutes, concentrated *in vacuo* to about 20 mL, and extracted with EtOAc (3 x 30 mL). The extractions were combined, dried over anhydrous $MgSO_4$ and concentrated *in vacuo*, to yield monochloro-triazines in variable yields and purities (Table 6.13).

Table 6.12: Masses of amines used.

Product	Amine X	Mass Used	Amine Y	Mass Used
124/bc	*N,N*-dibutylamine	790 mg	Cyclohexylamine	590 mg
124/bd	Ethanolamine	270 mg	Cyclohexylamine	590 mg
124/cd	*N,N*-dibutylamine	790 mg	Ethanolamine	270 mg

*Table 6.13: Yields of **124/bc, 124/bd** and **124/dc.***

Product	Yield (%)	Purity [a]
124/bc	77%	88%
124/bd	41%	95%
124/cd	51%	87%

a) HPLC @ 254 nm.

N,N-Dibutyl-6-chloro-*N'*-cyclohexyl-[1,3,5]triazine-2,4-diamine, **124/bc**

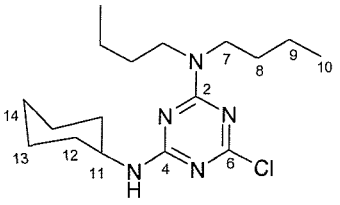

Mpt. oil: **TLC** (isohexane/AcOH; 20:1) R_f 0.47: **MS** (ESI, +ve, m/z) $[M+H]^+$ 340.3 (100%): **HRMS** (ESI, +ve, m/z) $[M+H]^+$ calculated $C_{17}H_{31}N_5Cl$, 340.2263; found 340.2259: error 1.1 ppm: **^{1}H-NMR** (300 MHz, DMSO-d_6) δ; 0.87 (6H, t, *J*=8 Hz, H10); 1.02-1.34 (9H, m, H9 + H_{ax}); 1.38-1.62 (5H, m, H_{eq}); 1.62-5.85 (4H, m, H8); 3.38 (4H, t, *J*=8 Hz, H7); 3.52-3.65 (1H, m, H11): **^{13}C-NMR** (75 MHz, DMSO-d_6) δ; 13.8 (C10); 19.5 (C9); 19.8 (C14); 24.8 (C13); 29.2 (C8); 32.0 (C12); 46.8 (C7); 49.6 (C11); 164.1 (C2); 164.2 (C4); 168.0 (C6): **IR** (υ, cm^{-1}) 800 (C-Cl), 1429 (N-H), 1564 (C=N), 2930 (C-H): **HPLC** (L5OD) R_t 4.69 minutes (88%).

2-(4'-Chloro-6'-cyclohexylamino-[1',3',5']triazin-2'-ylamino)-ethanol, **124/bd**

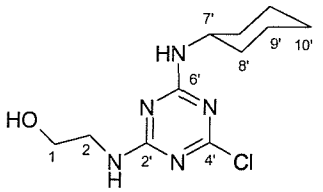

Mpt. 119-121°C: **TLC** (DCM/EtOAc/AcOH; 1:1:0.05) R_f 0.66: **MS** (ESI, +ve, m/z) $[M+H]^+$ 272.1 (100%): **HRMS** (ESI, +ve, m/z) $[M+H]^+$ calculated $C_{11}H_{19}ON_5Cl$, 272.1273; found 272.1270; error 1.0 ppm: **^{1}H-NMR** (300 MHz, DMSO-d_6) δ; 0.99-1.42 (5H, m, H_{ax}); 1.48-1.92 (5H, m, H_{eq}); 3.19-3.31 (2H, m, H1); 3.34-3.52 (2H, m, H2); 5.53-5.72 (1H, m, H7'): **^{13}C-NMR** (75 MHz, DMSO-d_6) δ; 24.7 (C10'); 25.2 (C9'); 32.0 (C8'); 43.2 (C2); 49.3 (C7'); 59.3 (C1); 164.5 (C2'); 165.8 (C6'); 167.7 (C4'): **IR** (υ, cm^{-1}) 797 (C-Cl), 1407 (N-H), 1539 (C=N), 2930 (C-H), 3252 (br, O-H): **HPLC** (S5OD) R_t 3.34 minutes (95%).

2-(4'-Chloro-6'-dibutylamino-[1',3',5']triazin-2'-ylamino)-ethanol, **124/cd**

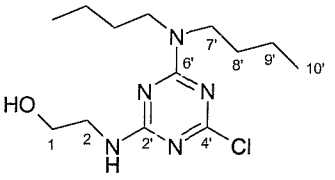

Mpt. 33-5°C: **TLC** (dichloromethane/ethyl acetate/acetic acid; 1:1:0.05) R_f 0.32: **MS** (ESI, +ve, m/z) $[M+H]^+$ 302.2 (55%): **HRMS** (ESI, +ve, m/z) $[M+H]^+$ calculated $C_{13}H_{25}ON_5Cl$, 302.1742; found 302.1743; error 0.4 ppm: **^{1}H-NMR** (300 MHz, DMSO-d_6) δ; 0.87 (6H, d, *J*=7 Hz, H10'); 1.17-1.39 (4H, m, H9'); 1.40-1.66 (4H, m, H8'); 2.80-2.86 (2H, m, H1); 3.25-3.29 (2H, m, H2); 3.40-3.52 (4H, m, H7'): **^{13}C-NMR** (75 MHz, DMSO-d_6) δ; 13.9 (C10'); 19.5 (C9'); 30.1 (C8'); 42.9 (C2); 46.5 (C7'); 60.4 (C1); 164.5 (C6'); 165.7 (C2'); 168.0 (C4'): **IR** (υ, cm^{-1}) 798 (C-Cl), 1400 (N-H), 1547 (C=N), 2944 (C-H), 3250 (br, O-H): **HPLC** (L5OD) R_t 3.07 minutes (87%).

6.3.5 4-(4'-Cyclohexylamino-6'-dibutylamino-[1',3',5']triazin-2'-ylamino)-5-hydroxy-naphthalene-2,7-disulfonic acid, mono sodium salt, 130/bc

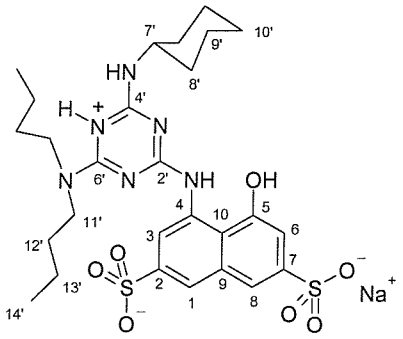

To a solution of 4-amino-5-hydroxynaphthalene-2,7-disulphonic acid, mono sodium salt (**50**) (50 mg, 0.147 mmol) in hot water (2 mL) was added a solution of **130/bc** (25 mg, 0. 073 mmol) in MeCN (1 mL). The reaction was stirred at 130°C for 10 minutes in a microwave cavity. The reaction mixture was directly applied onto a column of C-18 silica (Supelco Supelclean C-18, 10 g). The column was washed with water and the desired product eluted with MeOH (20 mL). The solution was concentrated *in vacuo* to give triazine **130/bc** as a brown solid (7 mg, 0.011 mmol, 15% yield).

Mpt. >250°C: **TLC** (acetone/^{i}PrOH/NH_4OH; 1:1:1) R_f 0.53: **MS** (ESI, -ve, m/z) $[M-2NH_4]^{2-}$ 310.4 (100%): **HRMS** (ESI, +ve, m/z) $[M-Na-H]^{2-}$ calculated $C_{27}H_{37}N_6O_7S_2$, 310.1049; found 310.1060; error 3.5 ppm: **^{1}H-NMR** (400 MHz, DMSO-d_6/H_2O-d_2) δ; 0.91 (6H, t, *J*=8 Hz, H14'); 1.14-1.35 (9H, m, H13'+H_{ax}); 1.49-1.62 (5H, m, H_{eq}); 1.63-1.93 (4H, m, H12'); 3.40-3.48 (4H, m, H11'); 3.55-3.64 (1H, m, H7'); 7.18 (1H, s, H6); 7.59 (1H, s, H3); 7.82 (1H, s, H1); 8.25 (1H, s, H8): **^{13}C-NMR** (100 MHz, DMSO-d_6) δ; 15.0 (C14'); 20.7 (C13'); 21.1 (C10'); 26.0 (C9'); 30.5 (C12'); 33.3 (C8'); 47.5 (C11'); 50.9 (C7'); 110.3 (C6); 117.7 (C3); 118.7 (C10); 120.4 (C8); 125.9 (C1); 129.2 (C4); 136.1 (C9); 146.8 (C2); 148.8 (C7); 154.2 (C5); 165.1 (C6'); 165.5 (C4'); 169.2 (C2'): **IR** (υ, cm^{-1}) 1035, 1170 (SO_2-O), 1393 (N-H), 1525 (C=N), 2934 (C-H), 3364 (br, O-H): **HPLC** (S5OD) R_t 3.73 minutes (82%).

6.3.6 Synthesis of Triazinyl Azo-Dyes 125/bc

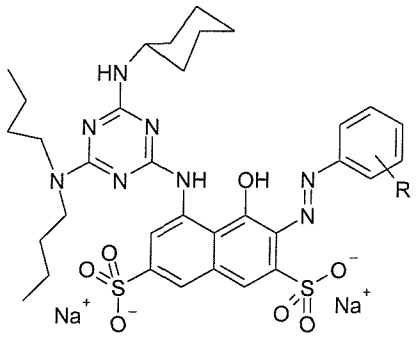

Dye **123** (Table 6.14, 95 μmol) was dissolved in MeCN/water (3:1, 2 mL) and passed twice in succession through a column (9 mm diameter, 0.5 mL/min) containing A-15 (Na^+ form, 1.0 g, 4.0 mmol). Triazine **124/bc** (16 mg, 0.47 mmol) was added and the reaction was heated at 160°C for 10 minutes in a microwave cavity. The reaction mixture was applied onto a column of C-18 silica (Supelco Supelclean C-18, 10 g). The column was washed with 40% MeOH in water, and the dye was eluted with MeOH (20 mL). The solution was concentrated *in vacuo* to yield dye **125/bc** as a magenta solid (Table 6.15).

*Table 6.14: Masses of dye **123** used.*

Azo-dye	R	Mass
123/1	2-Ethyl-6-methyl	44 mg
123/2	4-Iodo	52 mg
123/3	4-Bromo	47 mg
123/8	H	40 mg

*Table 6.15: Yields and purities of dyes **125/1bc-4bc**.*

Product	R	Yield (%)	Purity [a,b]
125/bc1	2-Ethyl-6-methyl	67	82
125/bc2	4-Iodo	20	48
125/bc3	4-Bromo	12	47
125/bc4	4-Chloro	51	70

a)After RP-SPE purification; b) HPLC @ 254 nm.

5-(4'-Cyclohexylamino-6'-dibutylamino-[1',3',5']triazin-2'-ylamino)-4-hydroxy-3-(2''-methyl-6''-ethyl-phenylazo)-naphthalene-2,7-disulfonic acid, di-sodium salt, **125/bc1**

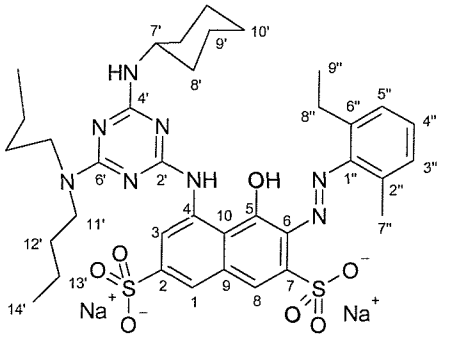

Mpt. >250°C: **TLC** (acetone/^{i}PrOH/NH_4OH; 1:1:1) R_f 0.89: **MS** (ESI, +ve, m/z) $[M-2NH_4+3H]^+$ 769.4 (20%): **HRMS** (ESI, +ve, m/z) $[M-2Na]^{2-}$ calculated $C_{36}H_{46}N_8O_7S_2$, 383.1471; found 383.1463; error 1.9 ppm: **^{1}H-NMR** (300 MHz, DMSO-d_6/H_2O-d_2) δ; 0.70-0.91 (6H, m, H14'); 0.92-1.32 (12H, m, H9''+H13'+H_{ax}); 132-1.62 (5H, m, H_{eq}); 1.63-1.91 (4H, m, H12'); 2.27 (1H, s, H7''); 2.91-3.02 (1H, m, H8''); 3.25-3.52 (5H, m, H11'+H7'); 6.79-7.02 (4H, m, H1+H3''+H4''+H5''); 7.31 (1H, s, H3); 7.41 (2H, s, H8): **^{13}C-NMR** (100 MHz, DMSO-d_6/H_2O-d_2) δ; 13.6 (C14'); 14.6 (C9''); 19.4 (13'); 19.7 (C10'); 20.1 (C7''); 24.4 (C9'); 24.8 (C8''); 31.5 (C8''); 31.9 (C12'); 46.8 (C11'); 50.0 (C7'); 111.4 (C6); 112.8 (C10); 113.1 (C8); 122.0 (C1); 126.1 (C5''); 127.3 (C3''); 129.2 (C4''); 129.7 (C3); 130.7 (C2''); 135.5 (C6''); 136.4 (C9); 137.8 (C1''); 142.0 (C2); 152.1 (C7); 152.7 (C5); 164.0 (C6'); 167.9 (C4'); 169.6 (C2'); 180.7 (C4): **IR** (υ, cm^{-1}) 1228 (SO_2-O), 1558 (C=N), 2929 (C-H), 3428 (br, OH): **HPLC** (S5OD) R_t 4.48 minutes (82%): **UV/Vis** (MeOH, nm) λ_{max} 526, ε 40028 $M^{-1}cm^{-1}$.

5-(4'-Cyclohexylamino-6'-dibutylamino-[1',3',5']triazin-2'-ylamino)-4-hydroxy-3-(4''-iodo-phenylazo)-naphthalene-2,7-disulfonic acid, di-sodium salt, **125/bc2**

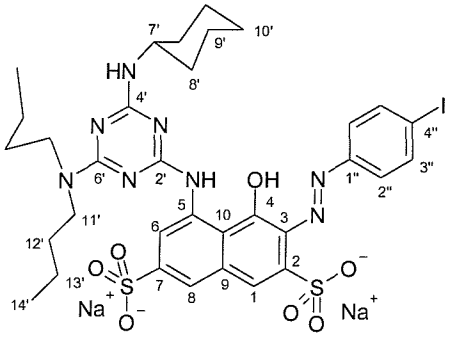

Mpt. >250°C: **TLC** (acetone/^{i}PrOH/NH_4OH; 1:1:1) R_f 0.92: **MS** (ESI, +ve, m/z) $[M-2NH_4+3H]^+$ 853.4 (100%): **HRMS** (ESI, -ve, m/z) $[M-2Na]^{2-}$ calculated $C_{33}H_{39}N_8O_7S_2I$, 425.0719; found 425.0714; error 1.2 ppm: **^{1}H-NMR** (300 MHz, DMSO-d_6/H_2O-d_2) δ; 0.62-0.83 (6H, m, H14'), 0.93-1.29 (9H, m, H_{ax}+H13'); 1.30-1.52 (5H, m, H_{eq}); 1.53-1.78 (4H, m, H12'); 2.95 (4H, t, *J*=8 Hz, H11'); 3.28-3.47 (1H, m, H7'); 7.06 (1H, s, H8); 7.31 (1H, s, H6); 7.36 (2H, d, *J*=8 Hz, H2''); 7.06 (1H, s, H1); 7.65 (2H, d, *J*=8 Hz, H3''): **^{13}C-NMR** (100 MHz, DMSO-d_6/H_2O-d_2) δ; 15.9 (C14'); 18.7 (C13'); 18.9 (C10'); 23.6 (C9'); 28.4 (C12'); 30.7 (C8'); 46.1 (C11'); 49.2 (C7'); 87.5 (C4''); 111.4 (C6); 112.5 (C10); 112.8 (C8); 117.9 (C2''); 122.6 (C1); 128.6 (C3); 135.6 (C9); 137.2 (C3''); 137.5 (C1'); 141.1 (C2); 151.5 (C7); 152.1 (C5); 163.4 (C6'); 167.8 (C4'); 168.8 (C2'); 180.9 (C4): **IR** (υ, cm^{-1}) 1227 (SO_2-O), 1401 (N-H), 1439 (N=N), 1562 (C=N), 2847 (C-H), 3253 (br, O-H): **HPLC** (S15OD) R_t 11.97 minutes (48%): **UV/Vis** (MeOH, nm) λ_{max} 538, ε 26523 $M^{-1}cm^{-1}$.

5-(4'-Cyclohexylamino-6'-dibutylamino-[1',3',5']triazin-2'-ylamino)-4-hydroxy-3-(4''-bromo-phenylazo)-naphthalene-2,7-disulfonic acid, di-sodium salt, **125/bc3**

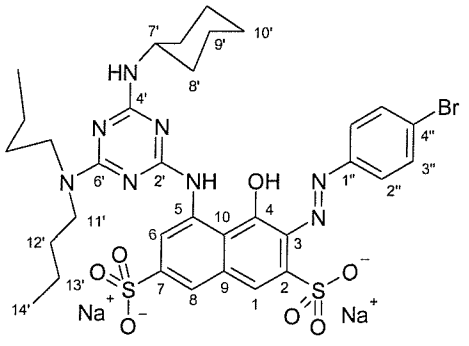

Mpt. >250°C: **TLC** (acetone/^{i}PrOH/NH_4OH; 1:1:1) R_f 0.87: **MS** (ESI, -ve, m/z) $[M-2NH_4]^{2-}$ 402.2 (15%): **HRMS** (ESI, -ve, m/z) $[M-2Na]^{2-}$ $C_{33}H_{39}N_8O_7S_2Br$, 401.0789 and 402.0779; found 401.0791 and 402.0778; error 0.6 and 0.1 ppm: **^{1}H-NMR** (300 MHz,

DMSO-d_6/H_2O-d_2) δ; 0.81-0.99 (6H, m, H14'); 1.14-1.47 (9H, m, H_{ax}+H13'); 1.49-1.67 (5H, m, H_{eq}); 1.68-1.99 (4H, m, H12'); 3.11 (4H, t, *J*=8 Hz, H11'); 3.51 (1H, m, H7'); 7.04 (1H, s, H8); 7.51 (1H, s, H6); 7.57 (1H, s, H1); 7.60-7.74 (4H, m, H2''+H3''): **^{13}C-NMR** (100 MHz, DMSO-d_6/H_2O-d_2) δ; 14.5 (C14'); 20.1 (C13'); 21.7 (C10'); 25.2 (C9'); 29.5 (C12'); 32.2 (C8'); 48.0 (C11'); 50.8 (C7'); 113.0 (C10); 113.3 (C6); 114.3 (C8); 116.7 (C4''); 118.8 (C3''); 124.2 (C1); 129.4 (C3); 130.2 (C2''); 130.5 (C1''); 137.2 (C9); 142.1 (C2); 152.3 (C7); 153.6 (C5); 164.9 (C6'); 169.4 (C4'); 170.3 (C2'); 182.2 (C4): **IR** (υ, cm^{-1}) 1216 (SO_2-O), 1366 (N-H), 1454 (N=N), 1571 (C=N), 2947 (C-H), 3462 (br, O-H): **HPLC** (S5OD) R_t 4.30 minutes (47%): **UV/Vis** (MeOH, nm) λ_{max} 548, ε 24517 $M^{-1}cm^{-1}$.

5-(4'-Cyclohexylamino-6'-dibutylamino-[1',3',5']triazin-2'-ylamino)-4-hydroxy-3-phenylazo-naphthalene-2,7-disulfonic acid, di-sodium salt, **125/bc8**

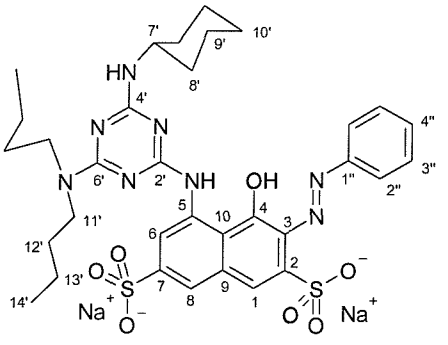

Mpt. >250°C: **TLC** (acetone/^{i}PrOH/NH_4OH; 1:1:1) R_f 0.89: **MS** (ESI, -ve, m/z) [M-NH_4]$^-$ 362.4 (70%): **HRMS** (ESI, +ve, m/z) [M-2Na+3H]$^+$ calculated $C_{33}H_{43}N_8O_7S_2$, 727.2691; found 727.2718; error 3.8 ppm: **^{1}H-NMR** (300 MHz, DMSO-d_6/H_2O-d_2) δ; 0.84-1.00 (6H, m, H14'); 1.01-1.46 (9H, m, H13'+H_{ax}); 1.47-1.67 (5H, m, H_{eq}); 1.68-1.99 (4H, m, H12'); 3.38-3.57 (5H, m, H7'+H11'); 7.29 (1H, s, H8); 7.45-7.53 (5H, m ,H2''+H3''+H4''); 7.73 (1H, s, H6); 7.75 (1H, s, H1): **^{13}C-NMR** (100 MHz, DMSO-d_6) δ; 11.9 (C14'); 17.7 (C13'); 18.1 (C10'); 23.1 (C9'); 28.8 (C12'); 30.3 (C8'); 44.5 (C11'); 47.9 (C7'); 110.4 (C6); 110.5 (C10); 111.7 (C8); 114.8 (C2''); 121.0 (C1); 122.8 (C4''); 127.2 (C3); 127.7 (C3''); 134.8 (C9); 141.0 (C2); 141.1 (C1''); 151.5 (C7); 151.6 (CC5); 162.1 (C6'); 162.6 (C4'); 166.2 (C2'); 179.8 (C4): **IR** (υ, cm^{-1}) 1066, 1216 (SO_2-O), 1420 (N-H), 1469 (N=N), 1567 (C=N), 2849 (C-H): **HPLC** (S5OD) R_t 4.02 minutes (70%): **UV/Vis** (MeOH, nm) λ_{max} 548, ε 32105 $M^{-1}cm^{-1}$.

6.4 Experimental to Chapter 4

6.4.1 (4-Hydroxy-phenylsulfanyl)-acetic acid, 161 [214]

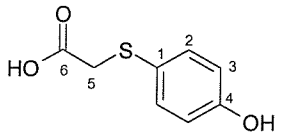

To a solution of 4-mercaptophenol (10.0 g, 79.3 mmol) in THF (200 mL) was added DIPEA (12.0 g, 118.8 mmol) dropwise over 2 minutes and the reaction was stirred for 20 minutes.

Bromoacetic acid (16.5 g, 118.8 mmol) was added portionwise over 3 minutes and the reaction stirred for 2 hours. The reaction mixture was concentrated to dryness *in vacuo* and redissolved in EtOAc (200 mL). The solution was washed with aq. HCl (2 N, 200 mL), and the aqueous washings were extracted with EtOAc (50 mL). The organics were combined and dried over anhydrous $MgSO_4$ and concentrated to dryness *in vacuo* to give an off-white solid, which was recrystallised from hot EtOAc to give **161** as a white solid (6.10 g, 33.1 mmol, 41%).

Mpt. 136-137°C: **TLC** (DCM/MeOH/AcOH; 9:1:0.05) R_f 0.36: **MS** (ESI, -ve, m/z) $[M-H]^-$ 183.0 (15%): **^{1}H-NMR** (300 MHz, DMSO-d_6) δ; 3.56 (2H, s, H5); 6.71 (2H, d, *J*=8 Hz, H3); 7.21 (2H, d, *J*=8 Hz, H2): **^{13}C-NMR** (75 MHz, DMSO-d_6) δ; 37.8 (C5); 116.2 (C3); 123.1 (C1); 133.0 (C2); 157.2 (C4); 171.0 (C6): **IR** (υ, cm^{-1}) 1683 (C=O), 3112 (br, CO_2H): **HPLC** (S5OD) R_t 2.71 minutes (95%).

6.4.2 *N*-Benzyl-2-(4'-hydroxy-phenylsulfanyl)-acetamide, 162 [193]

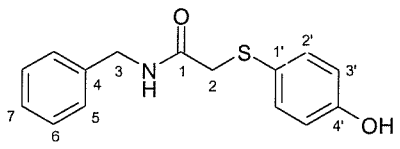

To a solution of **161** (2.0 g, 10.9 mmol) in THF (50 mL) was added HOBt (1.61 g, 12.0 mmol) and benzylamine (1.28 g, 12.0 mmol). The reaction was stirred for 10 minutes, before DIC (2.70 g, 13.0 mmol) was added. The reaction was stirred for 2 hours, during which time precipitation of a white solid (DCU) was observed. The reaction mixture was filtered, and concentrated to dryness *in vacuo*. The resulting solid was redissolved in DCM (200 mL) and washed with water (2 x 200 mL). The aqueous washings were extracted with DCM (2 x 100 mL) and the organics were combined and concentrated to

dryness *in vacuo*. The resulting white solid was purified by flash chromatography (silica; EtOAc/isohexane, 1:1) to yield amide **162** as a white solid (2.31 g, 8.46 mmol, 78%).

Mpt. 104-108°C: **TLC** (EtOAc/hexane; 1:1) R_f 0.29: **MS** (ESI, +ve, m/z) $[M+H]^+$ 274.0 (100%): **^{1}H-NMR** (300 MHz, DMSO-d_6) δ; 3.39 (2H, s, H2); 4.29 (2H, d, *J*=6 Hz, H3); 6.62 (2H, d, *J*=8 Hz, H3'); 7.11 (2H, d, *J*=8 Hz,H2'); 7.18-7.30 (5H, m, H7+H6+H5): **^{13}C-NMR** (75 MHz, DMSO-d_6) δ; 38.7 (C2); 42.4 (C3); 116.1 (C3'); 123.3 (C1'); 126.8 (C7); 127.2 (C5); 128.3 (C6); 133.1 (C2'); 139.2 (C4); 157.1 (C4'); 168.3 (C6): **IR** (υ, cm^{-1}) 1647 (C=O), 2928 (N-H), 3077 (br, O-H): **HPLC** (S5OD) R_t 3.25 minutes (95%).

6.4.3 *N*-Benzyl-2-[4'-(4'',6''-dichloro-[1'',3'',5'']triazin-2''-yloxy)-phenylsulfanyl]-acetamide, 163 [193]

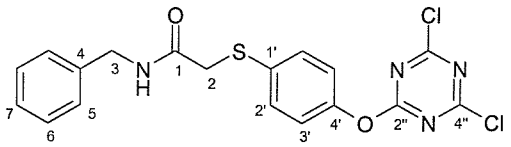

Cyanuric chloride (0.71 g, 3.84 mmol) was dissolved in THF (10 mL) and cooled to 0°C. Phenol **162** (1.0 g, 3.66 mmol) was dissolved in THF (5 mL) and added to the cyanuric chloride solution dropwise over 5 minutes. DIPEA (0.39 mmol, 3.84 mmol) was dissolved in THF (5 mL) and added to the reaction mixture over 5 minutes. The reaction was stirred at 0°C for 2 hours. The reaction mixture was concentrated to dryness *in vacuo*, and redissolved in DCM (100 mL). The solution was washed with water (3 x 100 mL) and the aqueous washings extracted with DCM (2 x 100 mL). The organics were combined, dried over anhydrous $MgSO_4$ and concentrated to dryness *in vacuo*, to yield **163** as a white solid (1.25 g, 2.97 mmol, 81%).

Mpt. 140-142°C: **TLC** (EtOAc/isohexane, 2:3), R_f 0.22: **MS** (ESI, +ve, m/z) $[M+H]^+$ 420.9 (100%): **^{1}H-NMR** (300 MHz, DMSO-d_6) δ; 3.74 (2H, s, H2); 4.25 (2H, d, *J*=6 Hz, H3); 7.09-7.38 (5H, m, H7+H6+H5+H3'); 7.45 (2H, d, *J*=8 Hz, H2'): **^{13}C-NMR** (75 MHz, DMSO-d_6) δ; 36.6 (C2); 42.5 (C3); 116.1 (C3'); 122.5 (C1'); 126.9 (C7); 127.2 (C5); 128.3 (C6); 129.3 (C4); 134.2 (C2'); 139.2 (C4'); 148.8 (C2''); 161.6 (C4''); 167.9 (C1): **IR** (υ, cm^{-1}) 1640 (C=O): **HPLC** (S15OD) R_t 8.06 minutes (90%).

6.4.4 5-{4'-[4''-(Benzylcarbamoyl-methylsulfanyl)-phenoxy]-6-chloro-[1',3',5']triazin-2'-ylamino}-4-hydroxy-3-(2''',4''',6'''-trimethyl-phenylazo)-naphthalene-2,7-disulfonic acid, di-sodium salt, 164

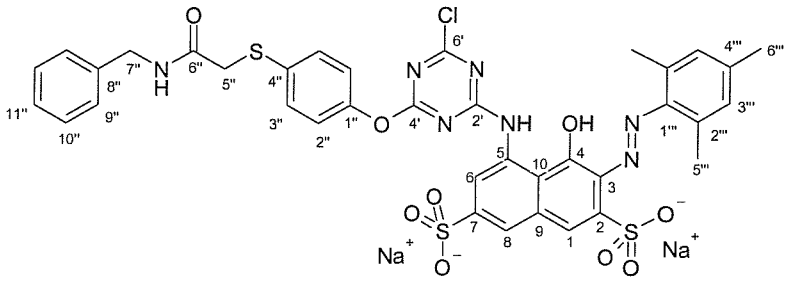

To a solution of **164** (0.54 g, 1.28 mmol) in THF (15 mL) was added a solution of **123/7** (312 mg, 0.64 mmol) in water (4 mL). DIPEA (64 mg, 0.64 mmol) dissolved into THF (3 mL) and added dropwise to the reaction mixture and the reaction was stirred for 18 hours. The reaction mixture was concentrated to dryness *in vacuo*, and water (200 mL) was added. The solution was washed with EtOAc (3 x 100 mL) and concentrated to about 10 mL *in vacuo*. The solution was applied onto a column of C-18 silica (Supelco Supelclean C-18, 10 g). The column was washed with 5% MeCN in water and the dye eluted with MeCN (20 mL). The solution was concentrated to dryness *in vacuo*, which yielded **164** as a dark solid (324 mg, 0.38 mmol, 59%).

Mpt. >250°C: **TLC** (acetone/^{i}PrOH/NH_4OH; 1:1:1) R_f 0.62: **MS** (ESI, -ve, m/z) $[M-2Na+H]^-$ 423.7 (33%): **HRMS** (ESI, -ve, m/z) $[M-2Na]^{2-}$ calculated $C_{37}H_{30}ClN_7O_9S_3$, 423.5483; found 423.5496; error 2.9 ppm: **^{1}H-NMR** (300 MHz, DMSO-d_6/H_2O-d_2) δ; 2.29 (3H, s, H6'''); 2.55 (6H, s, H5'''); 3.50 (2H, s, H5''); 4.26 (2H, d, *J*=6 Hz, H7''); 6.70 (2H, d, *J*=8 Hz, H2''); 6.99 (2H, s, H1); 7.01 (2H, s, H3'''); 7.08-7.32 (7H, m, H3''+H9''+10''+H11''); 7.45 (2H, d, *J*=9 Hz, H6); 7.53 (1H, s, H8): **^{13}C-NMR** (75 MHz, DMSO-d_6/H_2O-d_2) δ; 19.8 (C5'''); 20.8 (C6'''); 37.0 (C5''); 42.0 (C7''); 116.2 (C2''); 120.0 (C10); 122.3 (C8); 123.5 (C4''); 126.9 (C11''); 127.3 (C3); 127.3 (C9''); 128.4 (C1); 128.4 (C10''); 129.5 (C6); 129.7 (C2'''); 130.4 (C3'''); 133.1 (C3''); 135.7 (C6'); 136.0 (C4'''); 137.0 (C1'''); 139.2 (C9); 139.3 (C8''); 143.9 (C7); 149.9 (C4'); 152.6 (C2'); 157.2 (C1''); 168.1 (C6''); 168.4 (C4); 170.5 (C2); 176.9 (C5): **IR** (υ, cm^{-1}) 1223 (SO_2-O), 1558 (C=N), 1668 (C=O), 3432 (br, O-H): **HPLC** (S5OD) R_t 3.52 minutes (88%): **UV/Vis** (MeOH, nm) λ_{max} 526, ε 21384 $M^{-1}cm^{-1}$.

6.4.5 5-{4'-[4''-(Benzylcarbamoyl-methylsulfanyl)-phenoxy]-6'-cyclohexylamino-[1',3',5']triazin-2'-ylamino}-4-hydroxy-3-(2''',4''',6'''-trimethyl-phenylazo)-naphthalene-2,7-disulfonic acid, di-sodium salt, 170

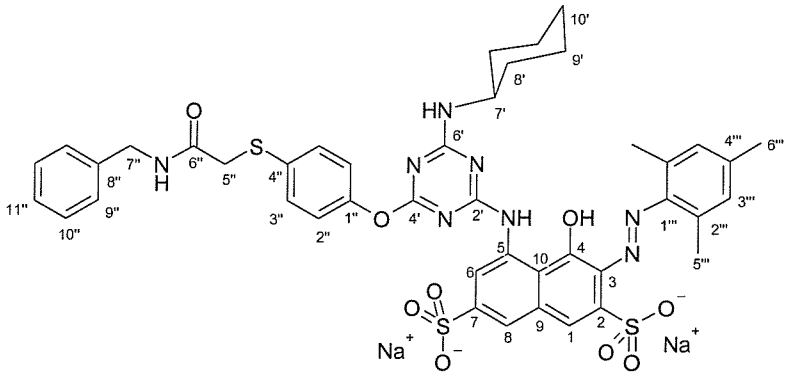

To a solution of cyclohexylamine (16 mg, 0.16 mmol) in MeOH (1 mL) was added a solution of **164** (36 mg, 0.042 mmol) in MeOH (1 mL) and the reaction was stirred for 1 hour. The reaction mixture was then concentrated to dryness *in vacuo*, redissolved in water (3 mL) and applied onto a column of C-18 silica (Supelco Supelclean C-18, 10 g). The column was washed with 40% MeOH in water and the dye eluted with MeOH (20 mL). The solution was concentrated to about 5 mL *in vacuo*, and freeze-dried, to give dye **165** as a dark solid (25 mg, 0.027 mmol, 64%).

Mpt. >250°C: **TLC** (acetone/^{i}PrOH/NH_4OH; 1:1:1) R_f 0.74: **MS** (ESI, -ve, m/z) $[M-2Na]^{2-}$ 455.4 (100%): **HRMS** (ESI, +ve, m/z) $[M-2Na+3H]^{+}$ calculated $C_{43}H_{45}N_8O_9S_3$, 913.2469; found 913.2439; error 3.3 ppm: **^{1}H-NMR** (300 MHz, DMSO-d_6/H_2O-d_2) δ; 0.95-1.39 (5H, m, H_{ax}); 1.50-1.25 (5H, m, H_{eq}); 2.26 (3H, s, H6'''); 2.53 (6H, s, H5'''); 3.52 (2H, s, H5''); 4.02 (1H, m, H7'); 4.24 (2H, d, *J*=9 Hz, H7''); 6.72 (2H, d, *J*=8 Hz, H2''); 6.98 (1H, s, H1); 7.04 (2H, s, H3'''); 7.05-7.33 (6H, m, H6+H3''+H9''+H11''); 7.55 (1H, s, H8); 7.50 (2H, m, H10''): **^{13}C-NMR** (100 MHz, DMSO-d_6/H_2O-d_2) δ; 21.0 (C5'''); 21.9 (C6'''); 25.0 (C10'); 25.8 (C9'); 31.5 (C8'); 33.4 (C5''); 43.6 (C7''); 50.6 (C7'); 117.4 (C2''); 122.0 (C10); 24.1 (C1); 24.5 (C4''); 128.2 (C11''); 128.2 (C9''); 128.4 (C8); 128.5 (C2'''); 129.1 (C10''); 129.3 (C6); 129.4 (C1'''); 129.6 (C4'); 129.7 (C2'); 130.4 (C3); 130.9 (C4'''); 131.5 (C3'''); 131.6 (C6'); 134.4 (C3''); 140.1 (C8''); 140.2 (C9); 158.2 (C1''); 169.5 (C6''); 170.1 (C5); 171.5 (C7); 171.6 (C2); 179.4 (C4): **IR** (υ, cm^{-1}) 1216 (SO_2-O), 1366 (N-H), 1457 (N=N),1738 (C=O), 3452 (br, O-H): **HPLC** (S15OD) R_t 9.23 minutes (95%): **UV/Vis** (MeOH, nm) λ_{max} 526, ε 20026 $M^{-1}cm^{-1}$.

6.4.6 5-(4'-Cyclohexylamino-6'-dibutylamino-[1',3',5']triazin-2-ylamino)-4-hydroxy-3-(2'',4'',6''-trimethyl-phenylazo)-naphthalene-2,7-disulfonic acid, di-sodium salt, 124/bc7

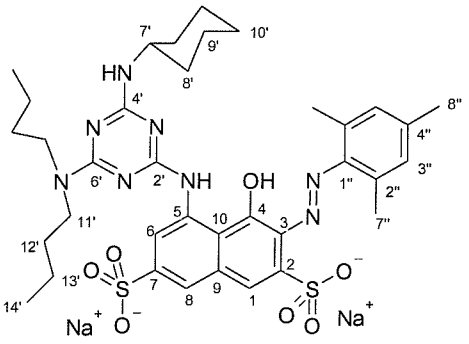

To a solution of **165** (18 mg, 0.02 mmol) in MeCN (1 mL) was added m-CPBA (70%, 5 mg, 0.022 mmol) and the reaction was stirred for 1 hour. *N,N*-dibutylamine (26 mg, 0.20 mmol) was added and the reaction was stirred for a further 18 hours. m-CPBA (5.0 mg, 0.020 mmol) was added and the reaction was stirred for a further 1 hour. The reaction was applied directly onto a column of C-18 silica (Supelco Supelclean C-18, 10 g). The column was washed with 40% MeOH in water and the dye eluted with MeOH (20 mL). The solution was concentrated to dryness *in vacuo* to yield dye **160/bc** as a dark solid (11 mg, 0.014 mmol, 70%).

Mpt. >250°C: **TLC** (acetone/^{i}PrOH/NH_4OH; 1:1:1) R_f 0.84: **MS** (ESI, +ve, m/z) $[M-2Na+3H]^+$ 769.3 (10%): **HRMS** (ESI, +ve, m/z) $[M+3H]^+$ calculated $C_{36}H_{49}N_8O_7S_2$, 769.3160; found 769.3155; error 0.72 ppm: **^{1}H-NMR** (300 MHz, DMSO-d_6/H_2O-d_2) δ; 0.81-0.96 (6H, m, H14'); 1.02-1.43 (9H, m, H13'+H_{ax}); 1.44-1.66 (5H, m, H_{eq}); 1.67-2.00 (4H, m, H12'); 2.28 (3H, s, H8''); 2.56 (6H, s, H7''); 2.87 (4H, t, *J*=8 Hz, H13'); 3.42-3.59 (5H, m, H11'+H7'); 6.99 (1H, s, H8); 7.02 (1H, s, H3''); 7.46 (1H, s, H6); 7.52 (1H, s, H1): **^{13}C-NMR** (75 MHz, DMSO-d_6/H_2O-d_6) δ; 13.8 (C14'); 19.4 (C10'); 19.5 (C5''); 19.8 (C13'); 20.5 (C6''); 24.8 (C9'); 2.9.7 (C12'); 32.0 (C8'); 46.2 (C11'); 49.6 (C7'); 111.3 (C6); 112.4 (C10); 112.9 (C8); 121.6 (C1); 129.2 (C3); 129.3 (C2''); 129.9 (C3''); 134.6 (C4''); 136.1 (C1''); 139.4 (C9); 142.3 (C2); 152.6 (C7); 152.9 (C5); 163.9 (C6'); 164.1 (C4'); 167.9 (C2'); 180.3 (C4): **IR** (υ, cm^{-1}) 1222 (SO_2-O),1455 (N=N), 1568 (C=N), 2923 (C-H), 3426 (O-H): **HPLC** (S15OD), R_t 9.66 minutes (68%): **UV/Vis** (MeOH, nm) λ_{max} 530, ε 21207 $M^{-1}cm^{-1}$.

6.4.7 {4-Hydroxy-phenylsulfanyl}-acetamido polystyrene, 168

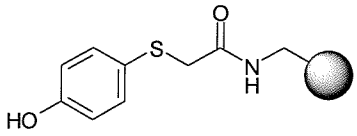

To a solution of **161** (257 mg, 1.4 mmol) in THF (3 mL) was added HOBt (202 mg, 1.5 mmol) and DIC (264 mg, 2.1 mmol) and the reaction was shaken for 10 minutes. The solution was added to amino methyl ArgoPore (1.0 g, 0.75 mmol) and the reaction was shaken for 18 hours. An aliquot of the reaction mixture was filtered, washed with THF (3 x 1 mL) and subjected to qualitative ninhydrin test (complete loss of free amine). The reaction mixture was filtered and the resin was washed with THF (3 x 20 mL) and Et_2O (3 x 20 mL) before being dried for 24 hours under vacuum.

IR (υ, cm^{-1}) 1114 (C-O), 1655 (C=O), 2921 (N-H), 3292 (br, O-H): **Elemental Analysis** (%w/w, ±0.3) C = 81.4%, H = 7.0%, N = 1.4%, S = 2.2%; Loading 0.65 $mmol.g^{-1}$ (based on S): Yield = 99%.

6.4.8 {4-(4',6'-dichloro-[1',3',5']triazin-2-yloxy)-phenylsulfanyl}-acetamido polystyrene, 156

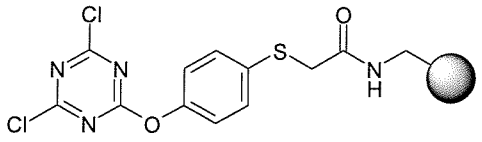

Resin **168** (1.0 g, 0.75 mmol) was mixed with THF (5 mL) and cooled to 0°C. Cyanuric chloride (413 mg, 2.20 mmol) was dissolved in THF (5 mL) and cooled to 0°C, before dropwise addition to the resin suspension over 5 minutes. DIPEA (112 mg, 1.11 mmol) was added to the reaction mixture dropwise over 5 minutes. The reaction was shaken at 0°C for 1 hour, before being shaken for 22 hours. The reaction mixture was filtered, and the resin was washed with THF (2 x 20 mL), DCM (2 x 20 mL) and Et_2O (2 x 20 mL). The resin was dried for 18 hours under vacuum.

IR (υ, cm^{-1}) 1667 (C=O), 2921 (N-H): **Elemental Analysis** (%w/w, ±0.3) C = 82.1%, H = 6.9%, N = 2.9%, S = 2.1%; Loading 0.43 $mmol.g^{-1}$ (based on N): Yield = 72%.

6.4.9 5-[4'-Chloro-6'-(4''-sulfanyl{acetamido-polystyrene}-phenoxy)-[1',3',5']triazin-2'-ylamino]-4-hydroxy-3-(2''',4''',6'''-trimethyl-phenylazo)-naphthalene-2,7-disulfonic acid, di-diisopropylethylammonium salt, 157

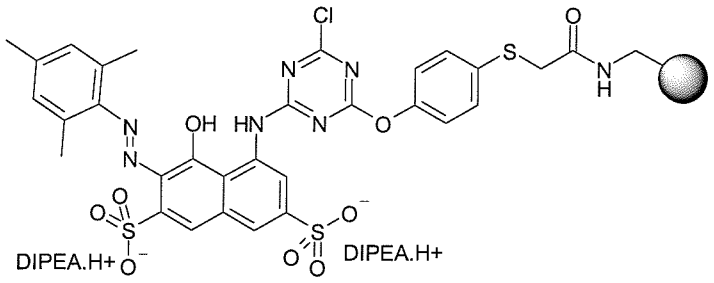

Dye **123/7** (0.20g, 0.40 mmol) was dissolved in MeOH (10 mL) and passed twice successively through a column (9 mm diameter, 5 mL/min) containing A-15 resin (Na^+ form, 1.5 g, 6.0 mmol). The solution was concentrated to dryness *in vacuo*, and redissolved in DMF (3 mL). DIPEA (40 mg, 0.40 mmol) was added, followed by resin **156** (285 mg, 0.10 mmol).

The reaction was heated to 100°C for 60 minutes in a microwave cavity. The reaction mixture was filtered and the resin washed with DMF (4 x 5 mL), THF (2 x 5 mL) and Et_2O (2 x 5 mL), before being dried under vacuum at 45°C for 12 hours.

IR (υ, cm^{-1}) 1210, 1369 (SO_2-O), 1653 (C=O), 2925 (N-H): **Elemental Analysis** (%w/w, ±0.3) C = 81.0%, H = 7.5%, N = 3.7%, S = 3.9%; Loading 0.41 $mmol.g^{-1}$ (based on S): Yield = 85%.

6.4.10 5-[4'-Cyclohexylamino-6'-(4''-sulfanyl{acetamido-polystyrene}-phenoxy)-[1',3',5']triazin-2'-ylamino]-4-hydroxy-3-(2''',4''',6'''-trimethyl-phenylazo)-naphthalene-2,7-disulfonic acid, di-diisopropylethylammonium salt, 158

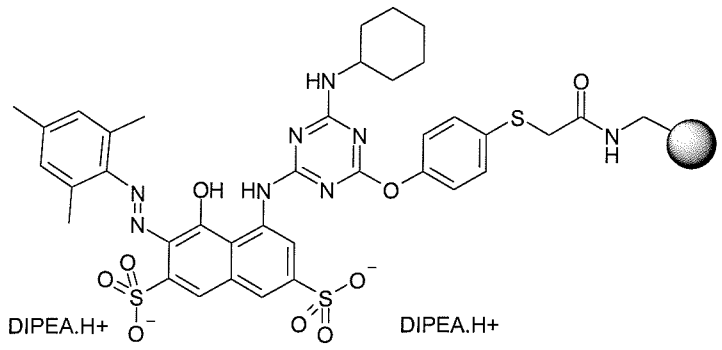

Cyclohexylamine (14 mg, 0.14 mmol) was dissolved in DMF (2 mL) and to this was added DIPEA (14 mg, 0.14 mmol). This solution was mixed with resin **157** (100 mg,

0.074 mmol) and the reaction was shaken for 1 hour. The reaction mixture was filtered and the resin washed with DMF (3 x 5 mL), THF (3 x 5 mL) and Et_2O (2 x 5 ml), and dried under vacuum for 12 hours at 45°C.

IR (υ, cm^{-1}) 1180 (SO_2-O), 1640 (C=O), 2877, 1408 (N-H): **Elemental Analysis** (%w/w, ±0.3) C = 81.4%, H = 7.6%, N = 4.2%, S = 3.8%; Loading 0.39 $mmol.g^{-1}$ (based on S): Yield = 85%.

6.5 Experimental to Chapter 5

Experiments were performed using amino methyl PS-*co*-DVB (NovaBiochem, 75-150 μm).

6.5.1 Image Acquisition

Optical images were obtained in a JPEG format from a Leica Leitz DM 1L inverted configuration microscope with a Nikon single-lens-reflex D1 digital camera attached, at a magnification of x40 and a resolution of 2.6 million pixels. SEM images in TIFF format were obtained from a Philips XL 30 scanning electron microscope, at a magnification of approximately x50 and a resolution of 0.34 million pixels. Laser scattering measurements were made with a Coulter LS 230 particle size analyser, with the beads suspended in water.

6.5.2 Image Analysis

All images were taken of dry beads, with care taken to minimise bead aggregation. The picture files were transferred to Image-Pro Plus © v4.5 (by Media Cybernetics, Silver Spring, Maryland) for processing. The scale (μm) of the optical microscope images was calibrated using a microscope graticule. The software automatically identified objects in the image, by difference in pixel-values (thresholding). The identified particles were electronically filtered to exclude any particles of an area less than 100 μm^2. A second filter of roundness was applied to exclude particles of a roundness index greater than 1.2 (Roundness index = $(\text{perimeter of object})^2 / (4\pi.\text{Area of object})$.

The selected beads were counted and the area and diameter calculated by the Image-Pro Plus software. The mean size values were also calculated by the software. This series of graphical manipulations was recorded as a "macro" which when executed, processed all the images automatically. The data was then exported to Excel 97®, by Microsoft.

6.5.3 Image Analysis Macros

These two macros, consisting of IPP functions, allowed the automatic image analysis of optical and SEM images respectively.

```
Sub flu_proc()
'F7
        ret = IpWsConvertImage(IMC_GRAY, CONV_SCALE, 0, 0, 0, 0)
        ret = IpFltShow(1)
```

```
        ret = IpFltMedian(3, 1)
        ret = IpFltShow(0)
        ret = IpBlbShow(1)
        ret = IpBlbSetFilterRange(BLBM_ROUNDNESS, 1.0, 1.200000048)
        ret = IpBlbCount()
        ret = IpBlbUpdate(0)
        ret = IpBlbSaveData("",  S_HEADER+S_Y_AXIS+S_DDE)
        ret = IpBlbShow(0)
        ret = IpDocClose()
        ret = IpAppSelectDoc(7)
End Sub
    ---------------------------------------------------------------------------------------
Sub SEM_proc()
'F8
        ret = IpAoiShow(FRAME_RECTANGLE)
        ret = IpDocMaximize()
        ret = IpDocSize(385, 290)
        ipRect.left = 0
        ipRect.top = 0
        ipRect.right = 708
        ipRect.bottom = 430
        ret = IpAoiCreateBox(ipRect)
        ipRect.left = 0
        ipRect.top = 0
        ipRect.right = 708
        ipRect.bottom = 416
        ret = IpAoiCreateBox(ipRect)
        ret = IpBlbShow(1)
        ret = IpBlbCount()
        ret = IpBlbUpdate(0)
        ret = IpBlbShow(0)
        ret = IpBlbSaveData("",  S_HEADER+S_Y_AXIS+S_DDE)
End Sub
```

7: References

1. Collis, M. *Marco Polo* (1959), Faber, London, pp. 67-71.
2. Kapr, A. *Johann Gutenberg* (1998), Scolar Press, pp. 153-187.
3. Reproduced with kind permission of CBBAG: http://www.cbbag.ca/callig2.html.
4. Reproduced with kind permission of Slippery Rock Universlty; http://www.sru.edu/depts/cisba/compsci/dailey/217students/sgm8660/Final/Flnalpages/gutenberg.html.
5. Gilmont, J-F. *The Reformation and the Book* (1990), Ashgate, pp. 1-9.
6. Williamson, H. *Methods of Book Design* (1956), Oxford University Press, pp. 252-3.
7. Whetton, H. *Practical Printing and Binding* (1948), Odhams, pp. 287-9.
8. Tarr, J.C. *Printing Today* (1945), Oxford University Press, pp. 11-13.
9. Information Transfer *The Print Book* (1985), NEC Cambridge, pp. 9-10.
10. Southward, J. *Modern Printing, vol. II* (1925), Rathby, Laurance and Co. Ltd, pp. 85-94.
11. Jacobi, C.T. *Printing* (1919), G. Bell and Sons Ltd, pp. 214-217.
12. Sain, M.M.; Daneault, C. *Polym. Degrad. Stabil.* (1996), **51**, 67-75.
13. Garfield, P. *Mauve* (2002), W. W. Norton and Co.
14. Caretto, A; De Santis, D; Moresi, M. *J. Sci. Food Agri.* (2002), **82**, 1189-1199.
15. a) Angellini, L. G.; Pistelli, L; Belloni, P.; Bertoli, A.; Panconesi, S. *Ind. Crops Prod.* (1997), **6**, 303-311: b) Mazzocchin, G.A.; Agnoli, F.; Mazzocchin, S. *Anal. Chim. Acta* (2003), **475**, 181-190.
16. a) Kokubun, T.; Edmonds, J.; John, P. *Phytochemistry* (1998), **49**, 79-87: b) Plowright, C.B. *J. Royal Hort. Soc.* (1901), **26**, 33-40: c) Maier, W.; Schumann, B.; Gröger, D. *Phytochemistry* (1990), **29**, 817-819.
17. Holt, D. *Robin Hood* (1982), Thames and Hudson, pp. 22-23.
18. Kahr, B.; Lovell, S.; Subramony, J.A. *Chirality* (1998), **10**, 66-77.
19. Nikzad, A. *Chem. Br.* (2003), **39**, 56-57.
20. Griess, P. *Ann. Chem.* (1858), **130**, 123-125.
21. Venkataraman, K. *The Chemistry of Synthetic Dyes, vol. I* (1952), Academic Press, pp. 3.
22. Kekule, F.A. *Ann. Chem.* (1865), **137**, 129-196.
23. Gordon, P.F.; Gregory, P. *Organic Chemistry in Colour* (1987), Springer-Verlag, Berlin, pp. 11-12.
24. Le, H.P. *J. Imag. Sci. Tech.*(1998), **42**, 49-62.
25. Rayleigh, Lord *Proc. London Math. Soc.* (1879), 71-97.

26. Sweet, R.G. *Rev. Sci. Instrum.* (1965), **36**, 131-136.
27. Kyser, E.L.; Sears, S.B. *US Patent* (1976), # 3,946,398.
28. a) Endo, .I; Sato Y.; Saito, S.; Nakagiri, T.; Ohno, S. *US Patent* (1988), # 4,723,129: b) Baker, J.P.; Johnson, D.A.; Joshi, V.; Nigro, S.J. *Hewlett-Packard J.* (1998), **39**, 6-15.
29. Croucher, M.D.; Hair, M.L. *Ind. Eng. Chem. Res.* (1989), **28**, 1712-1718.
30. Schultz, M.; v.-d. Waard, J. *US Patent* (2002), # 6,412,939.
31. Malhotra, S.L. *US Patent* (2002), # 20020137816.
32. Nakpathom, M.; Hinks, D.; Freeman, H.S. *Dyes Pigments* (2001), **48**, 93-106.
33. Kenyon, R.W. in *Printing and Imaging Systems* (1996), Ed. Gregory, P., Blackie Academic and Professional, pp. 122.
34. Kenyon, R.W. in *Printing and Imaging Systems* (1996), Ed. Gregory, P., Blackie Academic and Professional, pp. 123.
35. Jaeger, W.C. *EU Patent* (1991), # 91312100.
36. Gordon, P.F.; Gregory, P. *Organic Chemistry in Colour* (1987), Springer-Verlag, Berlin, pp. 9.
37. Solomons, G. *Organic Chemistry, 2nd edition* (1980), John Wiley and Sons, pp. 826-827.
38. Tedder, J.M. in *The Chemistry of Synthetic Dyes, vol. III* (1970), Ed. Venkataraman, K., Academic Press, pp. 229.
39. Friedman, L.; Chlebowski, J.F. *J. Org. Chem.* (1968), **33**, 1636-1638.
40. Clayden, J.; Greeves, N.; Warren, S.; Wothers, P. *Organic Chemistry* (2001), Oxford University Press, pp. 597-600.
41. Sidgwick, N.V. *The Organic Chemistry of Nitrogen* (1966), Oxford University Press, pp. 533-538.
42. Kuokkanen, T.; Palokanges, J.; Talvensaari, M. *J. Phys. Org. Chem.* (2000), **13**, 452-460.
43. March, J. *Advanced Organic Chemistry*, 4th Edition (1992), John Wiley and Sons, pp. 525-6.
44. Pandya, B.R.; Agrawal, Y.K. *Dyes Pigment* (2002), **52**, 161-168.
45. Statman, D.; Jánossy, I. *J. Chem. Phys.* (2003), **118**, 3222-3232.
46. Ashwell, M.A.; Solvibile, W.R.; Han, S.; Largis, E.; Mulvey, R.; Tillet, J. *Bioorg. Med. Chem. Lett.* (2001), **11**, 3123-3127.
47. a) Bekárek, V.; Rothschein, K.; Vetešik, P.; Večeřa, M. *Tetrahedron Lett.* (1968), **34**, 3711-3713: b) Arai, S.; Hida, M.; Yamagishi, T. *Dyes Pigments* (1995), **29**, 263-273.
48. Gordon, P.F.; Gregory, P. *Organic Chemistry in Colour* (1987), Springer-Verlag, Berlin, pp. 271.

49. Allen, R.L.M. *Colour Chemistry* (1971), Thomas Nelson and Sons, pp. 37-76.
50. Schwarz, W.M., *US Patent* (1994), 5,300,143.
51. Lakowicz, J.R. *Principles of Fluorescence Spectroscopy* (1999), Kluwer Academic/Plenum Publishers, pp. 10-11.
52. Gordon, P.F.; Gregory, P. *Organic Chemistry in Colour* (1987), Springer-Verlag, Berlin, pp. 288.
53. Ullman, D.; Wölcke, J. *Drug Discov. Today* (2001), **6**, 637-646.
54. Guttmann, A.; Khandurina, J. *Curr. Opin. Chem. Biol.* (2002), **6**, 359-366.
55. Maclean, D.; Baldwin, J.J.; Ivanov, V.T.; Kato, Y.; Shaw, A.; Schneider, P.; Gordon, E.M. *J. Comb. Chem.* (2000), **2**, 562-578.
56. Pirrung, M.C.; Chen, J. *J. Am. Chem. Soc.* (1995), **117**, 1240-1245.
57. Balkenhohl, F.; v.-d. Bussche-Hünnefeld, C.; Lansky, A.; Zechel, C. *Angew. Chem., Int. Ed. Engl.* (1996), **35**, 2288-2337.
58. Houghten, R.A.; Nefzi, A.; Ostresh, J.M. *Chem. Rev.* (1997), **97**, 449-472.
59. a) Furka, A.; Sebestyén, F.; Asgedom, M.; Dibó, G. *Int. J. Pept. Protein. Res.* (1991), **37**, 487-493: b) Houghten, R.A.; Dooley, C.T. *Bioorg. Med. Chem. Lett.* (1993), **3**, 415-412.
60. Dolle, R.E. *J. Comb. Chem.* (2000), **2**, 383-433.
61. Deeg, O.; Kirsch, P.; Pauluth, D.; Bauerle, P. *J. Chem. Soc., Chem. Commun.* (2002), 2762-2763.
62. Terrett, N.K.; Gardner, M.; Gordon, D.W.; Kobylecki, R.J.; Steele, J. *Tetrahedron* (1995), **51**, 8135-8173.
63. Frütchel, J.S.; Jung, G. *Angew. Chem., Int. Ed. Engl.* (1996), **35**, 17-42.
64. a) de Biasi, V.; Haskins, N.; Organ, A.; Bateman, R.; Giles, K.; Jarvis, S. *Rapid Commun. Mass Sp.* (1999), **13**, 1165-1168: b) Isabell, J.; Xu, R.; Cai, Z.; Kassel, D.B, *J. Comb. Chem.* (2002), **4**, 600-611: c) Fang, L.; Cournoyer, J.; Demee, M.; Zhao, J.; Tokushige, D.; Yan, B. *Rapid Commun. Mass Sp.* (2002), **16**, 1440-1447.
65. Merrifield, R.B. *J. Am. Chem. Soc.* (1963), **85**, 2149-2154.
66. Atherton, E.; Sheppard, R.C. *Solid-phase Peptide Synthesis* (1989), Oxford University Press, pp. 1-12.
67. a) Hermkens, P.H.H.; Ottenheijm, H.C.J.; Rees, D. *Tetrahedron* (1996), **52**, 4527-4554: b) Frechet, J.M.J. *Tetrahedron* (1981), **37**, 663-683.
68. Letsinger, R.L.; Mahadevan, V. *J. Am. Chem. Soc.* (1966), **88**, 5319-5324.
69. Frechet, J.M.J.; Schuerch, C. *J. Am. Chem. Soc.* (1971), **93**, 492-496.
70. Merrifield, R.B. *Angew. Chem., Int. Ed. Engl.* (1985), **24**, 799-892.
71. Pepper, K.W.; Paisley, H.M.; Young, M.A. *J. Org. Chem.* (1953), **18**, 4097-4105.

72. a) Sherrington, D.C. *J. Chem. Soc., Chem. Commun.* (1998), 2275-2286: b) Vaino, A.R.; Janda, K.D. *J. Comb. Chem.* (2000), **2**, 579-596.
73. Rana, S.; White, P.; Bradley, M. *J. Comb. Chem.* (2001), **3**, 9-15.
74. a) Arshady, R.; Ledwith, A. *React. Polym.* (1983), **1**, 159-174: b) Hori, M.; Gravert, D.J.; Wentworth, P.; Janda, K.D. *Bioorg. Med. Chem. Lett.* (1998), **8**, 2363-2368.
75. Rodinonov, I.L.; Baru, M.B.; Ivanov, V.T. *React. Polym.* (1992), **16**, 311-319.
76. Bardella, F.; Giralt, E.; Pedroso, E. *Tetrahedron Lett.* (1990), **31**, 6231-6234.
77. Wright, P.; Lloyd, D.; Rapp, W.; Andrus, A. *Tetrahedron Lett.* (1993), **34**, 3373-3376.
78. Meldal, M. *Tetrahedron Lett.* (1992), **33**, 3077-3080.
79. a) Meldal, M.; Auzanneau, F-I.; Hindsgaul, O.; Palcic, M.M. *J. Chem. Soc., Chem. Commun.* (1994), 1849-1850: b) Kress, J.; Zanaletti, R.; Amour, A.; Ladlow, M.; Frey, J.G.; Bradley, M. *Chem.-Eur. J.* (2002), **8**, 3769-3772: c) Schmitz, C.; Reetz, M.T. *Org. Lett.* (1999), **1**, 1729-1731.
80. Lorsbach, B.A.; Kurth, M.J. *Chem. Rev.* (1999), **99**, 1549-1581.
81. Gisin, B.F.; Merrifield, R. B. *J. Am. Chem. Soc.* (1972), **94**, 3102-3106.
82. Fodor, S.P.A.; Read, J. L.; Pirrung, M.C.; Stryer, L.; Lu, A.T.; Solas, D. *Science* (1991), **251**, 767-773.
83. Blackburn, C. *Biopolymers* (1998), **47**, 311-351.
84. Guillier, F.; Orain, D.; Bradley, M. *Chem. Rev.* (2000), **100**, 2091-2157.
85. Wang, S. *J. Am. Chem. Soc.* (1973), **95**, 1328-1333.
86. Mergler, M.; Nyfeler, R.; Gosteli, J. *Tetrahedron Lett.* (1989), **30**, 6741-6744.
87. Nugiel, D.A.; Wacker, D.A.; Nemeth, G.A. *Tetrahedron Lett.* (1997), **38**, 5789-5790.
88. Collini, M.D.; Ellingboe, J.W. *Tetrahedron Lett.* (1997), **38**, 7963-7966.
89. Hanessian, S.; Xia, F. *Tetrahedron Lett.* (1998), **39**, 733-736.
90. Cao, X.; Mjalli, A.M.M. *Tetrahedron Lett.* (1996), **37**, 6073-6076.
91. Zhang, C.; Mjalli, A.M.M. *Tetrahedron Lett.* (1996), **37**, 5457-5460.
92. Metcalf, C.A.; Vu, C.B.; Sundaramoorthi, R.; Jacobsen, V.A.; Laborde, E.A.; Green, J.; Green, Y.; Macek, K.J.; Merry, T.J.; Pradeepan, S.G.; Uesugi, M.; Varkhedkar, V.M.; Holt, D.A. *Tetrahedron Lett.* (1998), **39**, 3435-3438.
93. Ngu, K.; Patel, D.V. *Tetrahedron Lett.* (1997), **38**, 973-976.
94. Look, G.C.; Murphy, M.M.; Campbell, D.A.; Gallop, M.A. *Tetrahedron Lett.* (1995), **36**, 2937-2940.
95. Englebretsen, D.R.; Garnham, B.G.; Bergman, D.A.; Alewood, P.F. *Tetrahedron Lett.* (1995), **36**, 8871-8874.
96. Hanessian, S.; Ma, J.; Wang, W. *Tetrahedron Lett.* (1999), **40**, 4631-4634.

97. Mergler, M.; Nyfeler, R.; Tanner, R.; Gosteli, J.; Grogg, P. *Tetrahedron Lett.* (1988), **29**, 4009-4012.
98. Mitchell, A.R.; Erickson, B.W.; Ryabtsev, M.N.; Hodges, R.S.; Merrfield, R.B. *J. Am. Chem. Soc.* (1976), **98**, 7357-7362.
99. Rink, H. *Tetrahedron Lett.* (1987), **28**, 3787-3790.
100. Tam, J.P.; Dimarchi, R.D.; Merrifield, R.B. *Tetrahedron Lett.* (1981), **22**, 2851-2854.
101. Sieber, P. *Tetrahedron Lett.* (1987), **28**, 2107-3110.
102. Katti, S.B.; Misra, P.K.; Haq, W.; Mathur, K.B. *J. Chem. Soc., Chem. Commun.* (1992), 843-844.
103. Ramage, R.; Barron, C.A.; Bielecki, S.; Thomas, D.W. *Tetrahedron Lett.* (1987), **28**, 4105-4108.
104. Del Grado, W.F.; Kaiser, E.T. *J. Org. Chem.* (1980), **45**, 1295-1300.
105. Rich, D.H.; Gurwara, S.K. *J. Am. Chem. Soc.* (1975), **97**, 1572-1579.
106. Kenner, G.W.; McDermott, J.R.; Sheppard, R.C. *J. Chem. Soc., Chem. Commun.* (1971), 636-637.
107. Sarin, V.K.; Kent, S.B.H.; Tam, J.P.; Merrifield, R.B. *Anal. Biochem.* (1981), **117**, 147-157.
108. Jung, G.; Beck-Sickinger, A.G. *Angew. Chem., Int. Ed. Engl.* (1992), **31**, 367-383.
109. Caruthers, M.H. *Science* (1985), **230**, 281-285.
110. Schaefer, J. *Macromolecules* (1970), **3**, 110-112.
111. Schaefer, J.; Stejskal, E.O.; Buchdahl, R. *Macromolecules* (1976), **9**, 384-405.
112. a) Wells, N.J. *Investigations in Combinatorial and Solid Phase Chemistry* (2002), Southampton University Thesis, pp. 101-116: b) Jung, G. *Combinatorial Chemistry* (1999), Wiley-VCH, pp. 533-542.
113. Manatt, S.L. *Tetrahedron Lett.* (1980), **21**, 1397-1400.
114. Giralt, E.; Rizo, J.; Pedroso, E. *Tetrahedron* (1984), **40**, 4141-4152.
115. Look, G.C.; Holmes, C.P.; Chinn, J.P.; Gallop, M.A. *J. Org. Chem.* (1994), **59**, 7588-7590.
116. Fitch, W.L.; Detre, G.; Holmes, C.P. *J. Org. Chem.* (1994), **59**, 7955-7956.
117. Anderson, R.C.; Jarema, M.A.; Shapiro, M.J.; Stokes, J.P.; Ziliox, M. *J. Org. Chem.* (1995), **60**, 2650-2651.
118. a) Stones, D.; Miller, D.J.; Beaton, M.W.; Rutherford, T.J.; Gani, D. *Tetrahedron Lett.* (1998), **39**, 4875-4878: b) Hany, R.; Rentsch, D.; Dhanapal, B.; Obrecht, D. *J. Comb. Chem.* (2001), **3**, 85-89.
119. Egner, B.J.; Langley, G.J.; Bradley, M. *J. Org. Chem.* (1995), **60**, 2652-2653.

120. Fitzgerald, M.C.; Harris, K.; Shelvin, C.G.; Siuzdak, G. *Bioorg. Med. Chem. Lett.* (1996), **6**, 979-982.
121. Crowley, J.I.; Rapoport, H. *J. Org. Chem.* (1980), **45**, 3215-3227.
122. Yan, B.; Kumaravel, G. *Tetrahedron* (1996), **52**, 843-848.
123. a) Yan, B.; Kumaravel, G.; Anjaria, H.; Wu, A.; Petter, R.C.; Jewell, C.F.; Wareing, J.R. *J. Org. Chem.* (1995), **60**, 5736-5738: b) Yan, B.; Fell, J.B.; Kumaravel, G. *J. Org. Chem.* (1996), **61**, 7467-7472.
124. a) de Miguel, Y.R. *J. Chem. Soc., Perkin Trans. 1* (2000), 4213-4221: b) Shuttleworth, S.J.; Allin, S.M.; Wilson, R.D.; Nasturica, D. *Synthesis* (2000), 1035-1074: c) Thompson, L.A. *Curr. Opin. Chem. Biol.* (2000), **4**, 324-337: d) Bhattacharyya, S. *Comb. Chem. High T. Scr.* (2000), **3**, 65-92: e) Ley, S.V.; Baxendale, I.R.; Bream, R.N.; Jackson, P.S.; Leach, A.G.; Longbottom, D.A.; Nesi, M.; Scott, J.S.; Storer, R.I.; Taylor, S.J. *J. Chem. Soc., Perkin Trans. 1* (2000), 3815-4195.
125. Kulkarni, B.A.; Ganesan, A. *J. Chem. Soc., Chem. Commun.* (1998), 785-786.
126. Cainelli, G.; Contento, M.; Manescalchi, F.; Regnoli, R. *J. Chem. Soc., Perkin Trans. 1* (1980), 2516-2519.
127. a) Chesney, A. *Green Chem.* (1999), 209-219: b) Gayo, L.M.; Suto, M.J. *Tetrahedron Lett.* (1997), **38**, 513-516.
128. Kaldor, S.W.; Siegel, M.G.; Fritz, J.E.; Dressman, B.A.; Hahn, P.J. *Tetrahedron Lett.* (1996), **37**, 7193-7196.
129. Hodges, J.C. *Synlett* (1999), 152-158.
130. Nicewonger, R.B.; Ditto, L.; Varady, L. *Tetrahedron Lett.* (2000), **41**, 2323-2326.
131. Booth, R.J.; Hodges, J.C. *J. Am. Chem. Soc.* (1997), **119**, 4882-4886.
132. Dahman, S.; Bräse, S. *Angew. Chem., Int. Ed. Engl.* (2000), **39**, 3681-3683.
133. Bräse, S.; Dahman, S.; Popescu, C.; Schroen, M.; Wortmann, F-J. *Polym. Degrad. Stabil.* (2002), **75**, 329-335.
134. Bräse, S.; Dahman, S.; Pfefferkorn, M. *J. Comb. Chem.* (2000), **2**, 710-715.
135. Bräse, S.; Enders, D.; Köbberling, J.; Avemaria, F. *Angew. Chem., Int. Ed. Engl.* (1998), **37**, 3413-3415.
136. Brahman, S.; Bräse, S. *Org. Lett.* (2000), **2**, 3563-3565.
137. Bräse, S.; Köbberling, J.; Enders, D.; Lazny, R.; Wang, M. *Tetrahedron Lett.* (1999), **40**, 2105-2108.
138. Calderelli, M.; Baxendale, I.R.; Ley, S.V. *Green Chem.* (2000), 43-45.
139. Merrington, J.; James, M.; Bradley, M. *J. Chem. Soc., Chem. Commun.* (2002), 140-141.
140. Lui, Y-S.; Zhao, C.; Bergbreiter, D.E.; Romo, D. *J. Org. Chem.* (1998), **63**, 3471-3473.

141. Strenlow, F.W.E. *Anal. Chem.* (1984), **56**, 1053-1056.
142. Larhed, M.; Moberg, C.; Hallsberg, A. *Acc. Chem. Res.* (2002), **35**, 717-727.
143. Lew, A.; Krutzik, P.O.; Hart, M.E.; Chamberlin, A.R. *J. Comb. Chem.* (2002), **4**, 95-105.
144. Lindstrom, P.; Tierney, J.; Wathey, B.; Westman, J. *Tetrahedron* (2001), **57**, 9225-9283.
145. Gabriel, C.; Gabriel, S.; Grant, E.H.; Halstead, B.S.J.; Mingos, D.M.P. *Chem. Soc. Rev.* (1998), **27**, 213-223.
146. Gedye, R.; Smith, F.; Westaway, K.; Ali, H.; Baldisera, L.; Laberge, L.; Rousell, J. *Tetrahedron Lett.* (1986), **27**, 279-282.
147. Giguerre, R.J.; Bray, T.L.; Duncan, S.M.; Majetich, G. *Tetrahedron Lett.* (1986), **27**, 4945-4948.
148. Erdélyi, M.; Gogoll, A. *J. Org. Chem.* (2001), **66**, 4165-4169.
149. Tzschucke, C.C.; Markert, C.; Bannwarth, W.; Roller, S.; Hebel, A.; Haag, R. *Angew. Chem., Int. Ed. Engl.* (2002), **41**, 3964-4000.
150. Nilsson, U.J. *J. Chromatogr., A* (2000), **885**, 305-319.
151. Boger, D.L.; Goldberg, J.; Anderson, C-M. *J. Org. Chem.* (1999), **64**, 2422-2427.
152. Nilsson, U.J.; Fournier, E.J-L.; Hindsgaul, O. *Bioorg. Med. Chem.* (1998), **6**, 1563-1575.
153. Pipkorn, R.; Boenke, C.; Gehrke, M.; Hoffmann, R. *J. Pept. Res.* (2002), **59**, 105-114.
154. Ding, Y.; Labbe, J.; Kanie, O.; Hindsgaul, O. *Bioorg. Med. Chem. (*1996), **4**, 683-692.
155. Horváth, I. *Acc. Chem. Res.* (1998), **31**, 641-650.
156. Curran, D.P.; Hadida, S.; He, M. *J. Org. Chem.* (1997), **62**, 6714-6715.
157. Xia, Y.; Mirzai, B.; Chankalamannil, S.; Czarniecki, M.; Wang, S.; Clemmons, A.; Ahn, H-S.; Boykow, G.C. *Bioorg. Med. Chem. Lett.* (1996), **6**, 919-922.
158. Falorni, M.; Giacomelli, G.; Mameli, L.; Porcheddu, A. *Tetrahedron Lett.* (1998), **39**, 7607-7610.
159. Scharn, D.; Wenschuh, H.; Reineke, U.; Scheider-Mergener, J.; Germeroth, L. *J. Comb. Chem.* (2000), **2**, 361-369.
160. Grover, N.; Gupta, N.; Thorp, H.H. *J. Am. Chem. Soc.* (1992), **114**, 3390-3393.
161. Christy, C.; Vermant, S. *Desalination* (2002), **147**, 1-4.
162. Thurston, J.T.; Dudley, J.R.; Kaiser, D.W.; Hechenbleikner, I.; Schaefer, C.F.; Holm-Hansen, D. *J. Am. Chem. Soc.* (1951), **73**, 2981-2983.
163. Schmidt, M.; Klatte, C.; Kunz, K.; Lautner, J.; Ohlemacher, J.; Krimmer, H.P. *US Patent* (2001), # 6,252,073.

164. Katritzsky, A.R.; Ghiviriga, I.; Steel, P.J.; Oniciu, D.C. *J. Chem. Soc., Perkin Trans. 2* (1996), 443-447.

165. Brewer, S.A.; Burnell, H.T.; Holden, I.; Jones, B.G.; Willis, C.R. *J. Chem. Soc., Perkin Trans. 2* (1999), 1231-1234.

166. Birkett, H.E.; Harris, R.K.; Hodgkinson, P.; Carr, K.; Charlton, M.H.; Cherryman, J.C.; Chippendale, A.M.; Glover, R.P. *Magn. Reson. Chem.* (2000), **38**, 504-511.

167. Amm, M.; Platzer, N.; Guilhem, J.; Bouchet, J.P.; Volland, J.P. *Magn. Reson. Chem.* (1998), **36**, 587-596.

168. Katritzky, A.R.; Oniciu, D.C.; Ghiviriga, I.; Barcock, R.A. *J. Chem. Soc., Perkin Trans. 2* (1995), 785-792.

169. Joules, J.A.; Mills, K. *Heterocyclic Chemistry* (1972), Blackwells Science, pp. 80.

170. Walters, M.A.; Shay, J.J. *Tetrahedron Lett.* (1995), **36**, 7575-7578.

171. Attardi, M.E.; Falchi, A.; Taddei, M. *Tetrahedron Lett.* (2000), **41**, 7395-7399.

172. Moss,R.A.; Swarp, S. *J. Org. Chem.* (1988), **53**, 5860-5866.

173. Krchňák, V.; Vágner, J.; Šafář, P.; Lebl, M. *Collect. Czech. Chem. C.* (1988), **53**, 2542-2548.

174. Atterdi, M.A.; Procu, G.; Taddei, M. *Tetrahedron Lett.* (2000), **41**, 7391-7394.

175. Arienzo, R.; Kilburn, J.D. *Tetrahedron* (2002), **58**, 711-719.

176. Okiyama, N.; Santa, T.; Toriba, A.; Imai, K. *Anal. Chim. Acta* (2001), **429**, 293-300.

177. a) Qing, Z.; Yoon, H-S.; Parikh, P.B.; Chang, Y-T.; Yao, S.Q. *Tetrahedron Lett.* (2002), **43**, 5083-5086: b) Wurthner, F.; Sens, R.; Etzbach, K-H.; Seybold, G. *Angew. Chem., Int. Ed. Engl.* (1999), **48**, 1649-1652.

178. Isacsson, J.; Westman, G. *Tetrahedron Lett.* (2001), **42**, 3207-3210.

179. Mason, S.J.; Balasubramanian, S. *Org. Lett.* (2002), **4**, 4261-4264.

180. Bräse, S.; Dahman, S. *Chem.-Eur. J.* (2000), **6**, 1899-1905.

181. Blaney, P.; Grigg, R.; Sridharan, V. *Chem. Rev.* (2002), **102**, 2607-2624.

182. Obrecht, D.; Abrecht, C.; Grieder, A.; Villalgordo, J.M. *Helv. Chim. Acta* (1997), **80**, 65-72.

183. Breitenbucher, J.G.; Johnson, C.R.; Haight, M.; Phelan, J.C. *Tetrahedron Lett.* (1998), **39**, 1295-1298.

184. Kumar, A.; Sinha, S.; Chauhan, P.M.S. *Bioorg. Med. Chem. Lett.* (2002), **12**, 667-669.

185. Gayo, L.M.; Suto, M.J. *Tetrahedron Lett.* (1997), **38**, 211-214.

186. Marshall, D.L.; Liener, I.E. *J. Org. Chem.* (1970), **35**, 867-868.

187. Boldi, A.M.; Dener, J.M.; Hopkins, T.P. *J. Comb. Chem.* (2001), **3**, 367-373.

188. Dressman, B.A.; Singh, U.; Kaldor, S.W. *Tetrahedron Lett.* (1998), **39**, 3631-3634.
189. Fantauzzi, P.P.; Yager, K.M. *Tetrahedron Lett.* (1998), **39**, 1291-1294.
190. Breitenbucher, J.G.; Hui, H.C. *Tetrahedron Lett.* (1998), **39**, 8207-8210.
191. Stanková, M.; Lebl, M. *Mol. Diversity* (1996), **2**, 75-80.
192. a) Oakes, J.; Gratton, P. *J. Chem. Soc., Perkin Trans. 2* (1998), 1857-1864: b) Youssif, S. *ARKIVOC* (2001), 242-268.
193. Lebreton, S. *Immobilised dendrimers as high-loading solid-phase supports for synthesis and screening* (2002), Southampton University Thesis.
194. Patai, S.; Rapport, Z.; Stirling, C. *The Chemistry of Sulphones and Sulphoxides* (1988), John Wiley and Sons, pp. 235-242.
195. De Luca, L.; Giacomelli, G.; Porcheddu, A. *J. Org. Chem.* (2002), **67**, 5152-5155.
196. Paolesse, R.; Nardis, S.; Venanzi, M.; Mastroianni, M.; Russo, M.; Fronczek, F.R.; Vicente, M.G.H. *Chem.-Eur. J.* (2003), **9**, 1192-1197.
197. Johnson, C.R.; Phillips, W.G. *J. Org. Chem.* (1967), **32**, 1926-1931.
198. a) Allen, T. *Particle Size Measurement, 4th Edition* (1990), Chapman and Hall, pp. 483-502: b) Barth, H.G.; Flippen, R.B. *Anal. Chem.* (1990), **67**, 257R-272R.
199. Groth, T.; Grøtli, M.; Meldal, M. *J. Comb. Chem.* (2001), **3**, 461-468.
200. Miura, K. *Electrophoresis* (2001), **22**, 801-813.
201. Martinez, P.; Klotz, A. *A Practical Guide to CCD Astronomy* (1998), Cambridge University Press, pp. 1-22.
202. Gite, S.; Mamaev, S.; Olejnik, J.; Rothschild, K. *Anal. Biochem.* (2000), **279**, 218-225.
203. Zhou, C.H.; Yue, Z.Q.; Lee, C.F.; Zhu, B.Q.; Wang, Z.H. *Q. J. Eng. Geo. Hydro.* (2001), **34**, 325-332.
204. Tanaka, H.; Hayashi, T.; Nishi, T. *J. Appl. Phys.* (1986), **59**, 3627-3642.
205. Lahooti, S.; Yueh, H.K.; Neumann, A.W. *Colloid. Surface. B* (1995), **3**, 333-342.
206. Johnson, I.; Harman, M.; Forrow, D.; Norris, M. *Environ. Toxicol.* (2001), **16**, 68-77.
207. Schweitzer, B.; Kingsmore, S.F. *Curr. Opin. Biotech.* (2002), **13**, 14-19.
208. Chambers, G.; Lawrie, L.; Cash, P.; Murray, G.I. *J. Pathol.* (2000), **192**, 280-288.
209. Willis, R.C. *Mod. Drug Discov.* (2001), **4**, 63-64.
210. Reproduced with kind permission of Protagen: http://www.protagen.de/gel2.html.
211. Slice, D. *Q. Rev. Biol.* (1994), **69**, 143-144.
212. Furtando, A.; Henry, R. *Anal. Biochem.* (2002), **310**, 84-92.

213. Rice, K.D.; Nuss, J.M. *Bioorg. Med. Chem. Lett.* (2001), **11**, 753-755.
214. Still, W.C.; Kahn, M.; Mitra, A. *J. Org. Chem.* (1978), **43**, 2923-2925.
215. Zlatoidsky, P.; Mailar, T. *Eur. J. Med. Chem.* (1999), **34**, 1023-1034.
216. Commercially available in ~70% purity (Aldrich)
217. Ueda, I. *et al. Yakugaku Zasshi* (1952), **72**, 1354-1359.
218. Brode, A. *et al. J. Am. Chem. Soc.* (1908), **93**, 340-349.
219. Reeves, J.; Kaiser, L.. *J. Org. Chem.* (1970), **35**, 3670-3675.
220. Sedov, A.M.; Sergeeva, A.A.; Novikov, A. N. *USSR Izvestiya Tomoskogo Politekhnicheskogo Instituta* (1997), **238**, 141-142.
221. Neevel, J.G.; Van Beek, H.C.A.; Van de Graaf, B. *J. Soc. Dye Colour.* (1992), **108**, 489-492.
222. Gawlowski, A.; *Barwniki – Srodki Pomocnicze* (1978), **22**, 83-86.
223. Löwik, D.W.P.M.; Lowe, C. R. *Eur. J. Org. Chem.* (2001), 2825-2839.
224. S.E.R.T. *Ger. Pat.* (1970), number DE2012541.

8: Appendix

Permission note from:

1. CBBAG
2. Protagen

Date: Thu, 24 Apr 2003 07:09:31 -0400
From: "Susan V. Corrigan" <svcorr@istar.ca>
Subject: Re: Gutenberg Text...
To: James Merrington <J.MERRINGTON@soton.ac.uk>
Message-ID: <003e01c30a51$fb99df60$be630a40@d3n3q6>

Permission is granted, however, please use it without attribution.

----- Original Message -----
From: "James Merrington" <J.MERRINGTON@soton.ac.uk>
To: <admin@cbbag.ca>
Sent: Thursday, April 24, 2003 6:38 AM
Subject: Gutenberg Text...

> Dear Sir/Madam,
>
> I am currently writing up my PhD, which is on the synthesis of dyes for inkjet
> printers. In the introduction I would like to include a paragraph or two on
> Gutenberg's contribution to printing, including, with your permission, an image
> of his text found on your website:
> http://www.cbbag.ca/Callig2.html
>
> Is this OK?
>
> All the best.
>
> James
>
> James Merrington
> University of Southampton
> UK
> jm15@soton.ac.uk

Date: Wed, 16 Apr 2003 12:19:50 +0200
From: =?iso-8859-1?Q?Martin_Bl=FCggel?= <martin.blueggel@protagen.de>
Subject: AW: 2D Gel electrophoresis Image
To: James Merrington <J.MERRINGTON@soton.ac.uk>
Cc: =?iso-8859-1?Q?Christoph_H=FCls?= <christoph.huels@protagen.de>
In-Reply-To: <1050486709.3e9d27b5c7121@webmail.soton.ac.uk>
Message-ID: <OIEMKHPFDCCOPOBGFAOAIEFIDDAA.martin.blueggel@protagen.de>

Dear James,

thank you for asking. We agree to download http://www.protagen.de/gel2.html
for publication wihtin your PhD thesis.

By the way: What algorithm do you have developed ? Why do you see a chance
for this to be effective within this kind of data ?

Ciao
Martin

Visit our Webpage at http://www.protagen.de

Martin Blüggel
COO & Head of Bioinformatics

Protagen AG
Emil-Figge Str. 76A
44227 Dortmund
Germany

Phone +49 231 9742 890
FAX +49 231 9742 891

-----Ursprüngliche Nachricht-----
Von: James Merrington [mailto:J.MERRINGTON@soton.ac.uk]
Gesendet: Mittwoch, 16. April 2003 11:52
An: info@protagen.de
Betreff: 2D Gel electrophoresis Image

Dear Sir/Madam,

am currently writing up my PhD thesis (Chemistry) and need to include a
icture of a 2D-electrophoresis gel to illustrate potential Digital Image
nalysis applications. Is it possible that I can download and use the image
n
our web-site (http://www.protagen.de/gel2.html) for this?

ll the best,

ames

ames Merrington